GEOLOGICAL AND GEOMECHANICAL CHARACTERISTICS OF PROSPECTIVE CO_2 SINKS AND SEALS IN THE DESOTO CANYON SALT BASIN, EAST-CENTRAL GULF OF MEXICO

By
JINGYAO MENG
Bachelor of Engineering in Resource Exploration
Engineering (Oil and Gas)
Jilin University
Changchun, China
2012

Master of Science in Geology
Oklahoma State University
Stillwater, OK
2015

Submitted to the Faculty of the
Graduate College of the
Oklahoma State University
in partial fulfillment of
the requirements for
the Degree of
DOCTOR OF PHILOSOPHY
May, 2019

GEOLOGICAL AND GEOMECHANICAL CHARACTERISTICS OF PROSPECTIVE CO2 SINKS AND SEALS IN THE DESOTO CANYON SALT BASIN, EAST-CENTRAL GULF OF MEXICO

Dissertation Approved:

Dr. Jack C. Pashin

Dissertation Adviser

Dr. Daniel A. Laó Dávila

Dr. Ahmed Ismail

Dr. Runar Nygaard

Dr. Prem Bikkina

ACKNOWLEDGEMENTS

This research was funded by the National Energy Technology Laboratory of the U.S. Department of Energy under contract DE-FE0026086 as part of a project entitled, “Southeast Offshore Storage Resource Assessment”, and AAPG Grants-in-Aid Program.

My first and biggest thank goes to my dissertation advisor Dr. Jack Pashin, who has provided tremendous help in my research, teaching, and career development. From my masters to Ph.D., I am like a research infant growing to a mature investigator under your knowledge wings. Words cannot express my appreciation to you. You are the BEST advisor! I thank Drs. Daniel A. Laó Dávila, Runar Nygaard, Ahmed Ismail, and Prem Bikkina for serving on my dissertation committee and all their suggestions and feedback. I thank Dr. Mohamed Abdelsalam for all of his help and suggestions as graduate student coordinator. Drs. Brendan Hanger, Mary Hileman, Jim Puckette, and Tracy Quan provided opportunities for me as a teaching assistant for courses and outreach. Special thanks to Mr. Tim Sickbert for his technical support. I also thank Dr. Michael Grammer for providing me helpful career advice. Many thanks to my colleagues and project teammates, in particular, Sahar Mohammadi, Ibukun Bode Omoleye, Liang Xue, Mercy Achang, Babak Shabani, and Avinash Chandra. You have motivated me to work hard and supported me through my research. My friends within and outside the department, Xiaoyu, Yuan, Shuhao, Xitong, Mingying, Ruoshi, Pouyan, Esteffany, Fola, Seyi, Sara, and AY, thank you for always staying by my side. Thanks to all the faculty and staff of the Boone Pickens School of Geology who have made my life easier and brighter because of your help.

I would like to sincerely thank my family. My parents have encouraged me all the time to pursue higher education. Your infinite love will always be my strongest motivation. Thanks to my lovely husband Jian. It is like a fairy tale that we met here at OSU during the first semester and got married after the graduation ceremony. I believe there is a ‘happily ever after’ waiting for us. Last, but not least, thanks to my best friends back home in China. I am so lucky to have this many friends and all of your support.

谢谢！

Name: JINGYAO MENG

Date of Degree: MAY, 2019

Title of Study: GEOLOGICAL AND GEOMECHANICAL CHARACTERISTICS OF THE DESOTO CANYON SALT BASIN, EAST-CENTRAL GULF OF MEXICO

Major Field: GEOLOGY

Abstract: Subsurface geologic storage of CO_2 can play a major role in offsetting greenhouse gas emissions, and offshore storage in the DeSoto Canyon Salt Basin in the east-central Gulf of Mexico may be a viable solution due to large storage capacity (~150) Gt in Cretaceous-Cenozoic sandstone. The Cretaceous reservoirs are overlain by thick sections of tight mudrock, limestone, and chalk, which form regionally extensive seals. Understanding the structural styles and geomechanical properties of the associated reservoir rocks and seals is therefore essential for safe and effective CO_2 storage.

The structural framework in the Mississippi-Alabama-Florida shelf of the Gulf of Mexico includes the DeSoto Canyon Salt Basin, the Middle Ground Arch, and the Tampa Embayment. The Central DeSoto Canyon Salt Basin is structurally complex due to the presence of peripheral faults, salt pillows, salt rollers, and salt diapirs. Multiple faults associated with the peripheral faults and salt pillows displace the potential Cretaceous reservoirs and seal intervals. Elongation of borehole breakouts is aligned with the minimum horizontal compressive stress (Sh_{min}), which tends to be oriented northeast-southwest. Vertical reservoir stresses are influenced by rock and fluid density. Lithostatic and hydrostatic stress each have a power-law relationship to depth. The average lithostatic stress (Sv) gradient is ~21.4 kPa/m. Hydrostatic pressure gradient increases with brine density to a maximum of ~12.2 kPa/m. Geometric mean of the Sh_{min}-depth values corresponds to an effective Sh_{min}–effective Sv quotient of ~0.5. Reactivation tendency and seal analysis of the major faults shows that while the slip tendency is small, the dilation tendency and potential for cross-formational flow is relatively high, particularly where reservoir strata in the footwalls are juxtaposed with sealing strata in the hanging walls. Geomechanical analysis of reservoir and seal strata indicates that prospective reservoirs and associated seals are stable if injection pressure does not exceed fracture pressure.

Favorable CO_2 injection sites are available throughout the stable shelf areas of the DeSoto Canyon Salt Basin, where faults with high dilation tendency are absent above the Jurassic section. Future research should focus on further geomechanical, pressure, and flow simulation of the potential reservoirs and associated seals.

TABLE OF CONTENTS

Chapter Page

LIST OF TABLES

LIST OF FIGURES

Paper III: Geomechanical Characteristics of the Potential CO_2 Storage Reservoirs, DeSoto Canyon Salt Basin, Eastern Gulf of Mexico.

CHAPTER I

INTRODUCTION

1.1 Project Motivation

Subsurface geologic storage of CO_2 can play a major role in offsetting greenhouse gas emissions in a manner that is safe and efficient. Due to legal advantages and apparently vast resource capacity, offshore storage offers an attractive alternative to onshore storage. In a preliminary analysis of offshore Mississippi, Alabama and the western Florida Panhandle, a 28 Gt storage resource was identified in Cretaceous sandstone of the DeSoto Canyon Salt Basin (Chandra, 2018), 879 Gt in Cretaceous carbonate of the Sarasota Arch (Charbonneau, 2018), and 120 Gt in Cenozoic sand of the DeSoto Canyon Area (Pashin et al., 2018). According to the U.S. Environmental Protection Agency, about 40% of anthropogenic CO_2 emissions in the US are generated in the southeast part of the U.S. (SSEB, 2013). The lack of an offshore CO_2 assessment constitutes a major gap in understanding the regional storage resource and seal properties. This study is a product of the Southeast Offshore

Storage Resource Assessment (SOSRA), which is sponsored by the National Energy Technology Laboratory (NETL) of the U.S. Department of Energy (DOE) through the Southern States Energy Board. The SOSRA program aims to characterize and quantify the CO_2 storage resource in the eastern Gulf of Mexico shelf, and the Atlantic shelf and to provide advances in knowledge and technology that can facilitate commercialization of the offshore storage technology.

1.2 Significance

Ensuring safe, permanent storage of CO_2 is a central goal of the NETL initiative. An ideal CO_2 storage site selection should have little or no risk of gas migration of injected CO_2 beyond the boundaries of the storage complex. A previous study indicated that multiple sandstone formations in the DeSoto Canyon Salt Basin have commercially viable CO_2 storage capacity and are effectively sealed in the DeSoto Canyon Salt Basin (Chandra, 2018). Migration of injected CO_2 along preexisting structures, such as faults, is a widely acknowledged risk associated with CO_2 storage. In addition, storage capacity is limited by the overburden stress, hydraulic stress, and tectonic stress in each reservoir unit (Hawkes et al., 2005; Haug et al., 2007; Michael et al., 2009). Performing geological and geomechanical analyses of the potential storage unit can help reduce the risk of gas migration during and after the CO_2 injection events, which can help ensure that injection operations can be conducted in a safe, environmentally responsible manner that facilitates effective long-term storage of anthropogenic CO_2.

1.3 Knowledge Gap, Goal and Objectives

Unlike the western Gulf of Mexico, where the geologic framework has been defined by extensive oil and gas exploration, much less is known about the eastern Gulf of Mexico shelf due to a moratorium on drilling and production activities. To the author's knowledge, there has been very few comprehensive studies performed regarding the structural framework or geomechanical aspects in the DeSoto Canyon Salt Basin. Therefore, the primary goal of this study is to perform a comprehensive structural and geomechanical study of potential storage units to identify the favorable storage formations and sites that have minimal risk of injected CO_2 migrating out of the storage complex.

Accordingly, by using a variety of geologic techniques, including well log and seismic interpretation, structural mapping and modeling, fault analysis, and geomechanical assessment, this study achieved the following objectives:

1) Determined the in-situ stress and pressure information to illustrate the stress state of the DeSoto Canyon Salt Basin. This part of research provides a reference for maximum CO_2 injection pressure in the prospective reservoirs, and stress information for fault and geomechanical analysis in the other parts of the study.
2) Characterized the structural framework of the DeSoto Canyon Salt Basin; determined the reactivation tendency, as well as the seal property of the faults identified in the basin. This part of research evaluates the likelihood of gas migration along and across the fault

system, and suggests the favorable sites in the basin that have minimal risk of injected CO_2.

3) Estimated the rock mechanical properties of the reservoirs and seals of individual potential storage units. This part of the research determines the reservoir seal integrity for each potential reservoir unit and rank the reservoir formations according to stability to facilitate future development.

1.4 Dissertation Sections

This dissertation is structured in three sections. An outline of the dissertation is given below and introduces the three research objectives. The outline also presents the three manuscripts resulting from this dissertation that are in various stages of the publication process.

Paper I: Meng, J., Pashin, J. C., Nygaard, R., Chandra, A., 2018, Analysis of the stress field in the DeSoto Canyon Salt Basin for ensuring safe offshore carbon storage: International Journal of Greenhouse Gas Control, v. 79, p. 279-288.

Paper II: Meng, J., Pashin, J. C., Chandra, A., Xue, L., under revision, Structural Framework and Fault Analyses in the East-Central Gulf of Mexico Shelf: Implications for Offshore CO_2 Storage.

Paper III: Meng, J., Pashin, J. C., Chandra, A., Nygaard, R., in preparation, Geomechanical Characteristics of Potential CO_2 Storage Reservoirs, DeSoto Canyon Salt Basin, Eastern Gulf of Mexico.

References:

Chandra, A., 2018. Geological Characterization and CO_2 storage potential of Cretaceous sandstone in the DeSoto Canyon Salt Basin of the MAFLA shelf (thesis). Stillwater, Oklahoma, Oklahoma State University, 66p.

Charbonneau, P., 2018. Geologic framework for the assessment of offshore CO_2 storage resources: West Florida Platform (thesis). Stillwater, Oklahoma State University, 69 pp.

Hawkes, C.D., Bachu, S., Haug, K., Thompson, A.W., 2005. Analysis of in-situ stress regime in the Alberta Basin, Canada, for performance assessment of CO_2 geological sequestration sites. Fourth Annual Conference on Carbon Capture and Sequestration Pittsburgh, DOE-NETL, 1-22.

Haug, K., Nygaard, R., and Keith, D., 2007, Evaluation of stress and geomechanical characteristics of a potential site for CO_2 geological storage in central Alberta, Canada, in Proceedings 60th Canadian Geotechnical Conference and 8th Joint CGS/IAH-CNC Groundwater Conference, 21-24.

Michael, K., Bachu, S., Buschkuehle, B. E., Haug, K., and Talman, S., 2009, Comprehensive characterization of a potential site for CO_2 geological storage in central Alberta, Canada, 227-240.

Pashin, J. C., Meng, J., Hills, D. J., and Riestenberg, D., 2018, Eastern Gulf of Mexico, in Southern States Energy Board, eds., Southeast Offshore Storage Resource

Assessment, Prospective Storage Resource Assessment Results, U.S. Department of Energy Contract DE-FE0026086, 4-66.

CHAPTER II

PAPER I: ANALYSIS OF THE STRESS FIELD IN THE DESOTO CANYON SALT BASIN FOR ENSURING SAFE OFFSHORE CARBON STORAGE

2.1 Abstract

Offshore geologic CO_2 storage offers an attractive option to offset the greenhouse gas emissions. Vast CO_2 storage capacity exists in Cretaceous-Neogene sandstone in the DeSoto Canyon Salt Basin. Understanding the stress and pressure regimes in the basin can help evaluate the geomechanical integrity of the formations, thus minimizing the risk of CO_2 migrating out of the storage complex. Borehole breakouts were identified using four-arm dipmeter logs. Elongation of the breakouts is aligned with the minimum horizontal compressive stress (Sh_{min}), which tends to be oriented northeast-southwest. Vertical reservoir stresses are influenced by rock and fluid density. Lithostatic and hydrostatic stress each have a power-law relationship to depth. The average lithostatic stress (Sv) gradient is ~21.4 kPa/m. Hydrostatic pressure gradient increases with brine density to a maximum of ~12.2 kPa/m. Geometric mean of the Sh_{min}-depth values

correspond to an effective Sh_{min} - *effective Sv* quotient of ~0.5. Injection pressure can be maintained safely below the estimated effective minimum horizontal stress, thereby reducing the risk of cross-formational flow. Future study should focus on further constraint of geomechanical properties, reservoir integrity, and seal integrity.

2.2 Introduction

Subsurface geologic storage of CO_2 can play a critical role in offsetting greenhouse gas emissions in a manner that is safe, economical, and acceptable to the public. Due to uniform governmental ownership and an apparently vast storage resource, offshore CO_2 storage in the outer continental shelf (OCS) potentially offers an attractive alternative to onshore storage. Seal integrity is a critical issue that must be addressed to ensure safe long-term storage. Performing stress, pressure, and mechanical integrity analyses of potential storage units can help reduce risk, including the risk of leakage caused by injection.

This study is a product of the Southeast Offshore Storage Resource Assessment (SOSRA), which is sponsored by the National Energy Technology Laboratory (NETL) of the U.S. Department of Energy (DOE) though the Southern States Energy Board. The SOSRA program aims to characterize and quantify the CO_2 storage resource in the eastern Gulf of Mexico shelf and the Atlantic shelf and to provide advances in knowledge and technology that can facilitate commercialization of offshore storage technology. The SOSRA program is nearing completion, and volumetric estimates of the storage resource in the eastern Gulf of Mexico are becoming available (Chandra, 2018;

Charbonneau, 2018). A related project being conducted by the Southeastern Regional Carbon Sequestration Partnership (SECARB) called SECARB Offshore is beginning and will further assess the CO_2 storage potential and the potential for enhanced oil recovery in the central and eastern Gulf of Mexico.

This paper focuses on the DeSoto Canyon Salt Basin in the east-central Gulf of Mexico OCS (Figure 2.1). Recent studies indicate that vast storage capacity exists in Cretaceous through Neogene sandstone units in the salt basin (Pashin et al., 2016; Meng et al., 2017; Chandra, 2018) and in other continental shelf regions around the globe (e.g., Arts et al., 2009; Dai et al., 2018). The candidate sandstone units in the DeSoto Canyon Salt Basin are overlain by thick sections of shale, limestone and chalk, which form regionally extensive and proven seals for onshore hydrocarbon reservoirs; these seals define the top of the CO_2 storage complex. Based on geophysical well log data, the thickness of individual reservoirs is on the order of 10-120 m (30-360 ft) with porosity commonly exceeding 20%. To minimize the risk of injected CO_2 migrating out of the storage complex, stress and pressure information must be obtained to evaluate reservoir and seal integrity.

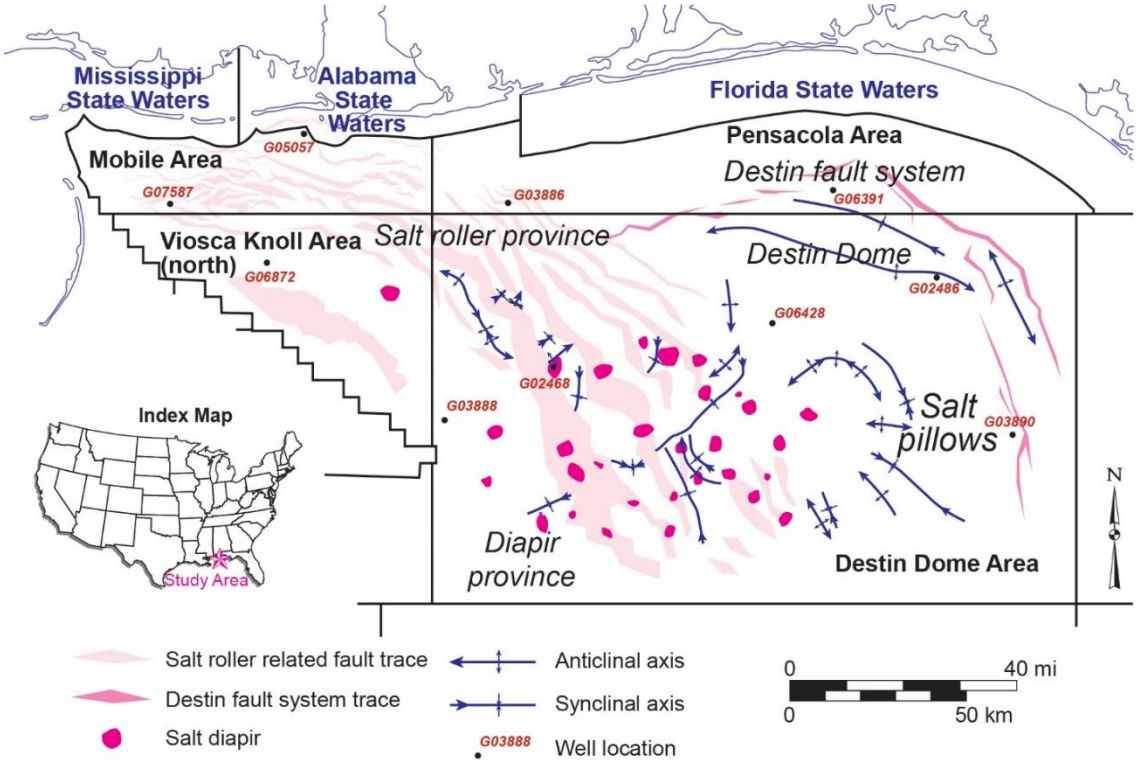

Figure 2.1. Map showing key structural elements in the DeSoto Canyon Salt Basin and the location of wells used to characterize stress in prospective reservoirs and seals (after Pashin et al., 2016).

Although several publications have discussed the stress field of the west-central Gulf of Mexico (Finkbeiner et al., 1996; Keaney et al., 2010; King et al., 2012; Moore et al., 2009; Yassir and Zerwer, 1997; Zerwer and Yassir, 1994; Zoback and Peska, 1995), a need remains to examine the stress field in the DeSoto Canyon Salt Basin and points east. To help fill this gap, this study analyzed the horizontal stress orientation, lithostatic stress, horizontal stress, and hydrostatic pore pressure in the DeSoto Canyon Salt Basin and adjacent areas. This research focused on obtaining stress and pressure information

using a broad range of geophysical and geochemical data. This analysis provides insight on the potential storage resource and risk profile of the candidate reservoirs in the basin, and also was used to help determine seal integrity for each potential reservoir unit, thus facilitating future development.

2.3 Geological Setting

The DeSoto Canyon Salt Basin is offshore of Mississippi, Alabama, and the western Florida Panhandle, and is a sub-basin of the Gulf of Mexico continental shelf (Figure 2.1). During Mesozoic to Cenozoic time, the Gulf of Mexico formed by rifting and drifting as a result of extension and isostatic adjustment of the crust as the Yucatan block rotated counterclockwise relative to North America (Pindell and Kennan, 2001; Sandwell et al., 2014). As defined by the U.S. Bureau of Ocean Energy Management (BOEM), the Desoto Canyon Salt Basin straddles the Central and Eastern Gulf of Mexico planning areas for development of oil and gas and mineral resources.

Mesozoic and Cenozoic strata in the Desoto Canyon Salt Basin include a thick succession of siliciclastic rocks, carbonate rocks, and evaporites, which constitute a sedimentary wedge that was deposited upon extended Paleozoic basement (Figures 2.1, 2.2) (Galloway, 2008; Pashin et al., 2016). The Middle Jurassic Louann Salt unconformably overlies the Paleozoic basement. Above the Louann Salt are the sandstone of the Norphlet Formation and the limestone and dolomite of the Smackover Formation. The Smackover Formation is overlain by the Haynesville Formation, which in

the DeSoto Canyon Salt Basin is dominated by limestone. The Cotton Valley Group spans the Jurassic-Cretaceous boundary and contains siliciclastic rocks capped by a carbonate unit called the Knowles Limestone. Lower Cretaceous strata consist mostly of terrigenous siliciclastic rocks and platform carbonate rocks. Upper Cretaceous sedimentation began with deposition of the siliciclastic strata of the Tuscaloosa Group and ended with deposition of the Selma Group, which represents a chalk-rich carbonate ramp that blanketed the Lower Cretaceous platform. Paleogene strata (Midway, Wilcox, and Claiborne groups) contain thick shale units and numerous sandstone intervals, and some chalky carbonate. Paleocene-Miocene strata of the Pensacola Clay constitute the bulk of the Neogene section and contain mudstone and poorly consolidated sandstone that was deposited in shelf and shoreline environments (Smith, 1991; Handford and Baria, 2003). Sandstone in the Paluxy Formation (Lower Creataceous), the Lower Tuscaloosa Group (Upper Cretaceous) and the Paleocene-Miocene section contain prospective targets for offshore CO_2 storage. Carbonate and shale in the Washita-Fredericksburg Interval (Lower Creataceous), the Marine shale of the Tuscaloosa Group (Upper Cretaceous), chalk of the Selma Group (Neogene), and Neogene-Quaternary mudrock successions contain widespread reservoir seals (Pashin et al., 2016; Meng et al, 2017; Chandra, 2018).

The Desoto Canyon Salt Basin contains four distinctive structural provinces that are related to salt tectonics (Figure 2.1) (Pashin et al., 2016): (1) the Destin fault system, which is an arcuate peripheral fault trend in the Destin Dome and Pensacola Areas that offsets Jurassic through Paleogene strata; (2) the salt pillow province, which is

basinward of the Destin fault system and contains broad, open anticlines in the Jurassic-Paleocene-Miocene section; (3) the salt diapir province, which contains diapiric bodies that in places rise more than 22,000 feet from basement into the Paleocene-Miocene section; and (4) the salt roller province, which includes an array of normal faults and salt-cored rollover structures that deform Jurassic and earliest Cretaceous strata.

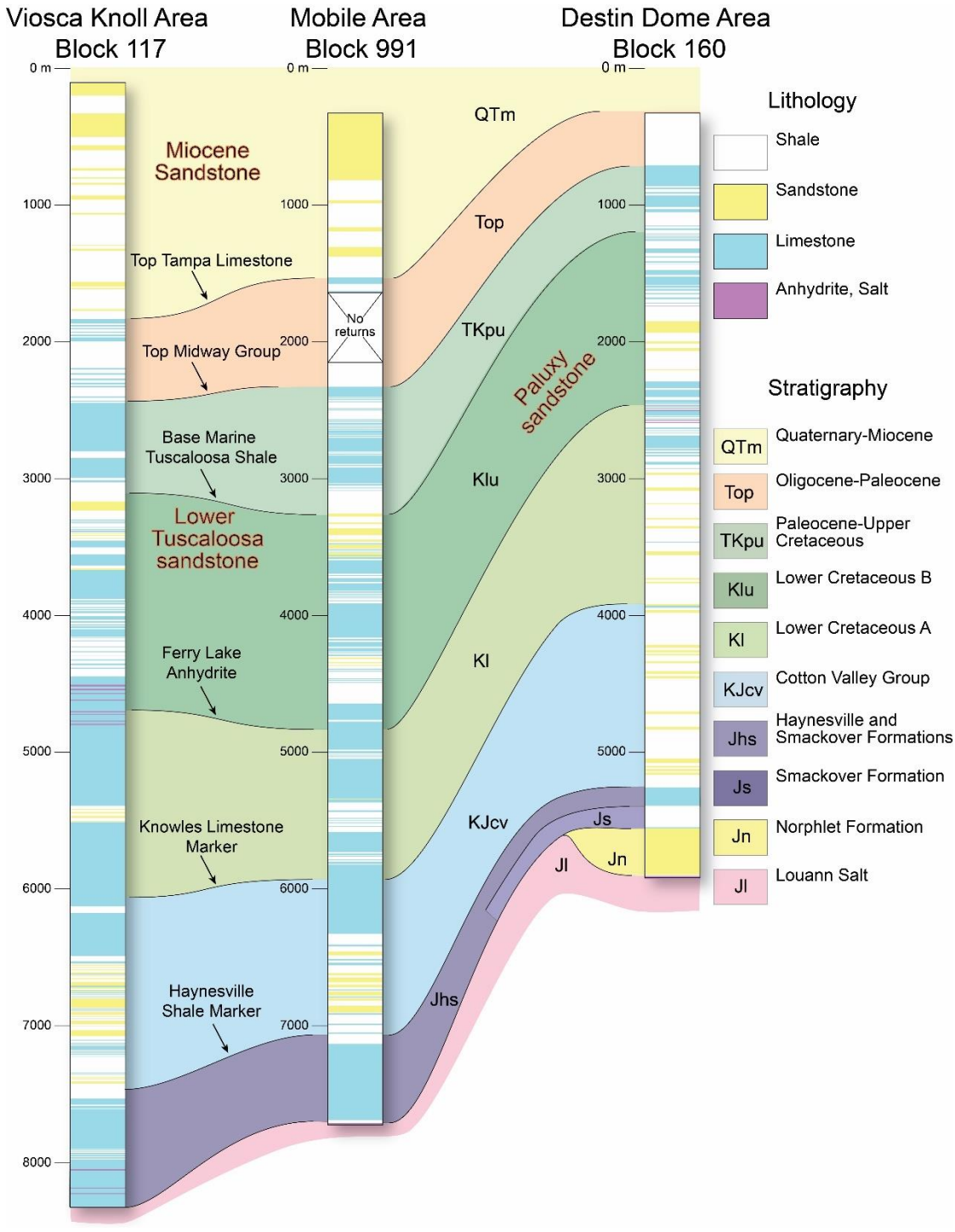

Figure 2.2. Stratigraphic columns showing rock types and major stratigraphic intervals of Desoto Canyon Salt Basin (after Pashin et al., 2016).

2.4 Methodology

Stress in the earth is defined by three mutually perpendicular principal stresses (σ1> σ2> σ3). When discussing a subsurface reservoir, these stresses typically can be assumed to be vertical stress (*Sv*), maximum horizontal stress (SH_{max}) and minimum horizontal stress (Sh_{min}). Another important stress parameter is hydrostatic pressure, or pore pressure (P_p), which is the pressure exerted by fluids within the pore space of the rock. This research analyzes the key in-situ stress parameters that were analyzed using geophysical well log data and geochemical data in the DeSoto Canyon Salt Basin and adjacent regions. The results of the stress field analysis were then used to generate a model of safe CO_2 injection pressure at reservoir conditions using Petrel software.

2.4.1 Stress Orientation

Horizontal stress orientation was analyzed on the basis of borehole breakouts. Borehole breakouts are stress-induced enlargements of the wellbore and form where the maximum circumferential stress (hoop stress) exceeds the compressive rock strength (Bell and Gough, 1979). For a vertical well, breakout of the wellbore wall is most likely to occur in the azimuth of Sh_{min} (Figure 2.3A; Zoback et al., 2003). Breakout zones were identified using four-arm caliper logs, which are typically associated with dipmeter logs. Caliper logs measure the size and shape of the boreholes and are used to identify breakout zones (Figure 2.3B). Characteristic four-arm caliper logs and the associated interpretations of borehole geometry are illustrated in Figure 2.3C. Azimuths

of the breakout elongations in each well have been recorded and plotted in rose diagrams to characterize Sh_{min}. The vector-mean orientation of SH_{max} (normal to Sh_{min}) was plotted on a well location map to illustrate the stress state of the Desoto Canyon Salt Basin. The orientation of SH_{max} for each well analyzed in this study has been ranked by quality by using the World Stress Map quality ranking system (Table 2.1), which is based on the number of breakouts in the well, the angular standard deviation of breakout orientation, and the total length of the observed borehole breakouts (Sperner et al., 2003).

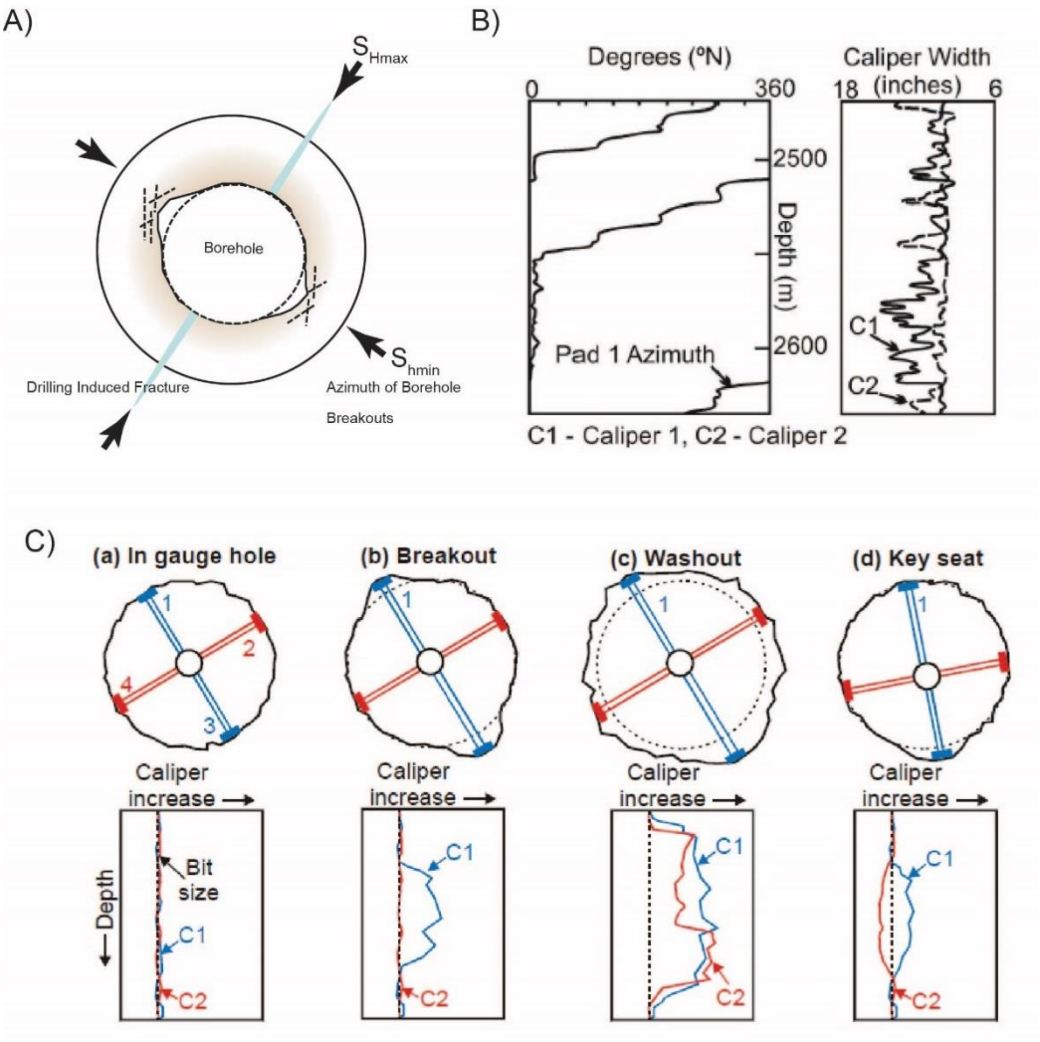

Figure 2.3. Interpreting in-situ horizontal stress using 4-arm caliper logs. A) Vertical view of a borehole breakout. SH_{max} and Sh_{min} refer to the orientations of maximum and minimum horizontal stress, respectively. B) Example of caliper log used to determine the orientation of horizontal stress (after Reynolds and Hillis, 2000). C) Examples of 4-arm caliper logs and common interpretations of borehole geometry. (a) In-gauge hole, (b) geometry resulting from stress-induced well bore breakouts, (c) minor washout with superimposed elongation, and (d) key seat where the sonde is not centered in the borehole (after Plumb and Hickman, 1985).

Table 2.1. Quality ranking scheme for four-arm dipmeter logs (Sperner et al., 2003).

Quality	No. of borehole breakouts	Total Length (m)	Standard Deviation (°)
A	≥10	≥300	≤12
B	≥6	≥100	≤20
C	≥4	≥30	≤25
D	<4	<30	≤40
E	-	-	>40

2.4.2 Lithostatic Stress (Vertical Stress Magnitude)

Subsea formations bear the weight of the overlying sea water and lithologic column. Therefore, the vertical lithostatic stress or overburden stress (*Sv*) for a given depth (*D*) is equivalent to the weight of the sea water and the overburden, with the stress derived from equation (2.1),

$$Sv = \int_0^{\mathrm{D}'} \rho(\mathrm{w})\mathrm{gd}(\mathrm{w}) + \int_0^{\mathrm{D}-\mathrm{D}'} \rho(\mathrm{z})\mathrm{gd}(\mathrm{z}) \qquad (2.1)$$

where D is depth of the strata; D’ is the depth of the seafloor; *ρ(w)* is the density of sea water (~1.03 g/cm^3 for seawater with brine concentration of 35,000 mg/L); *ρ(z)* is the bulk density of the fluid-saturated rock; *g* is the standard gravitational acceleration (9.80665 m/s^2); and *d(w)* and *d(z)* are depth increments. A lithostatic stress (*Sv*) profile was constructed using density log data recorded at 0.15 m (0.5 ft) intervals from ten wells in the Desoto Canyon Salt Basin (Figure 2.1). Nevertheless, density logs are rarely run in the shallow subsurface below the seafloor. So there are relatively few stress data

points from the seafloor to a depth of ~1 km (3,281 ft). Water depth at the ten wells used in this study ranges from 14 m (46 ft) to 185 m (607 ft).

2.4.3 Horizontal Stress Magnitude

The most common way to determine the magnitude of Sh_{min} is to use pressure test records obtained by direct gauging, micro- or mini-fracture tests, and pressure-buildup tests. This requires a large pool of pressure data at a broad range of depths to determine the fracture closure pressure that corresponds to Sh_{min} (Hawkes et al., 2005). However, it was difficult to apply this method because very few pressure measurements were recorded in the Desoto Canyon Salt Basin outside of the productive Jurassic and Paleocene-Miocene sandstone units. Indeed, no data are available for Cretaceous strata in the study area. Another method to estimate the magnitude of Sh_{min} employs an empirical approach. Assuming linear elastic rock behavior, the minimum stress state is given as equations (2.2) and (2.3),

$$Sh_{min} = \frac{\nu}{1-\nu}(Sv - P_p) + P_p \tag{2.2}$$

$$\nu = \frac{{V_p}^2 - 2{V_s}^2}{2{V_p}^2 - 2{V_s}^2} \tag{2.3}$$

where ν is Poisson's ratio, which describes the ratio of the proportional decrease in a lateral measurement to the proportional increase in length in a sample of material that is elastically stretched; V_p (m/μs) and V_s (m/μs) are the compressional wave velocity and

shear wave velocity derived from sonic logs (equivalently as Δt (μs/m)). Importantly, $S'h_{min}$ and $S'v$ are effective stresses that can be calculated by subtracting P_p from Sh_{min} and Sv, respectively (equations 2.4 and 2.5); SH_{max} cannot be obtained without fracture test information. In an extensional tectonic regime like the Gulf of Mexico, Sv is the maximum principal stress (Zoback, 2010). Therefore, the $Sv > SH_{max} > Sh_{min}$ stress state provides a range in which SH_{max} must fall.

$$S'v = Sv - P_p \quad (2.4)$$

$$S'h_{min} = Sh_{min} - P_p \quad (2.5)$$

2.4.4 Hydrostatic Pressure (Pore Pressure)

The normal hydrostatic gradient for fresh water is 9.792 MPa/km (0.433 psi/ft), and 10.516 MPa/km (0.465 psi/ft) for subsurface brine with 100,000 mg/L total dissolved solids (TDS). Normal marine water contains an average of 35,000 mg/L TDS. Gauged reservoir pressure data on file at the State Oil and Gas Board of Alabama from the Norphlet Formation in Alabama State Waters indicate that reservoirs in the study area are part of a brine-compensated hydrostatic system. Therefore, P_p can be estimated from the TDS information in geochemical databases. Due to a moratorium on drilling and production of oil and gas, the eastern part of the study area remains underexplored, and so brine chemistry data are not available in the DeSoto Canyon Salt Basin. Consequently, TDS data were obtained from a database that includes data from the interior salt basins of Mississippi, Alabama and Florida (Pashin and Payton, 2005), which are physically connected to the DeSoto Canyon Salt Basin. Primary data sources

include the NETL U.S. Brine Wells Database and the files of the State Oil and Gas Board of Alabama. These geochemical data were obtained from brine samples recovered from 785 oil and gas wells. Table 2.2 shows the geochemical information from three example wells that were used to estimate TDS and hydrostatic pressure.

Table 2.2. Typical geochemical record for estimating the hydrostatic pressure gradient using onshore Gulf Coast wells north of the study area.

Well name	P. C. RISHER #1-S	McMillan 12-11	ST REGIS 13-1
Latitude (deg)	31.8724	31.23837	30.9534
Longitude (deg)	-89.0012	-87.11732	-87.192
State	MS	AL	FL
County	Jasper	Escambia	Santa Rosa
Field	Heidelberg	Appleton	Jay
Formation/Group	Wilcox	Lower Tuscaloosa	Smackover
Lithology	Sandstone	Sandstone	Limestone, Dolomite
Depth (ft)	2,875	5,515	15,632
pH	7.7	7	5.6
Bicarbonate (mg/L)	240	305	346
Calcium (mg/L)	2,537	7,600	37,714
Magnesium (mg/L)	555	2,684	2,526
Sulfate (mg/L)	0	188	122
Sodium (mg/L)	18,309	33,011	72,044
Chloride (mg/L)	34,337	72,000	184,946
TDS (mg/L)	55,978	115,788	297,698
Pressure gradient (psi/ft)	0.451	0.470	0.528
Hydrostatic pressure (psi)	1,296	2,592	8,258
Data Source	NETL U.S. Brine Wells Database	AL State Oil and Gas Board files	NETL U.S. Brine Wells Database

2.5 Results

2.5.1 Stress orientation

Borehole breakouts were identified in 11 wells with four-arm dipmeter logs. These wells are located within the Mobile Area, the northern part of the Viosca Knoll Area, and the Pensacola Area. In total, 37 borehole breakouts were identified in the wells. Basic information about the wells and breakouts is given in Table 2.3. The vector-mean azimuth of SH_{max} is dominantly northwest-southeast (114°) in ten wells and northeast-southwest in the remaining well. The mean SH_{max} orientations from borehole breakouts were ranked by quality, with B-quality stress orientations identified in four wells, C-quality orientations in two wells, D-quality orientations in one well and E-quality orientations in the remaining four wells. All of the A-D quality well breakouts occur in strata deeper than 4,070 m (13,350 ft).

Table 2.3. Summary of basic well information and mean-maximum horizontal stress orientation as interpreted from borehole breakouts in the Desoto Canyon Salt Basin.

Lease Name	Water Depth (m)	Base of interval containing borehole breakouts (m)	Top of interval containing borehole breakouts (m)	No. of Breakouts	Total Length of Breakouts (m)	Vector Mean Azimuth of SH_{max} (°)	Standard Deviation (°)	Quality
G06391	50	5,799	5,482	6	137	128	6	B
G05062	18	6,024	5,793	8	143	136	9	B
G05056	15	5,488	4,561	5	183	94	26	C
G05760	15	941	300	1	27	135	-	E
G05057	14	6,433	4,146	3	247	10	18	B
G05056	16	6,637	6,546	2	24	131	-	D
G08774	34	943	506	1	30	120	-	E
G08778	37	1,206	524	1	18	135	-	E
G08763	27	5,104	4,680	4	73	116	7	C
G04921	38	5,710	5,520	2	15	124	-	E
G16536	37	4,488	4,299	4	174	104	7	B

Figure 2.4 is the stress orientation map showing a rose diagram with the vector-mean azimuth of SH_{max} in each well. The orientation of SH_{max} is highly consistent, save for one well in the Mobile Area. The map indicates that SH_{max} is oriented northwest-southeast with a vector mean azimuth of 114°, which is parallel to depositional strike. This consistency is remarkable, considering the broad range of data quality. Indeed, it is unclear whether anomalous orientations of some of the vectors in the northern Mobile Area reflect perturbations of the stress field or are artifacts of variable data quality. Anomalous orientations exist in three of the study wells, specifically wells G5057, G5056-1, and G4921. Well G5057 contains consistently oriented of anomalous breakouts in the Jurassic-Cretaceous section from 4,070-6,814 m (13,350-22,350 ft).

However, the anomalously oriented breakouts in wells G5056-1 and G4921 only appear in Jurassic strata deeper than 5,396 m (17,700 ft), where an array of normal faults exists within the salt roller province.

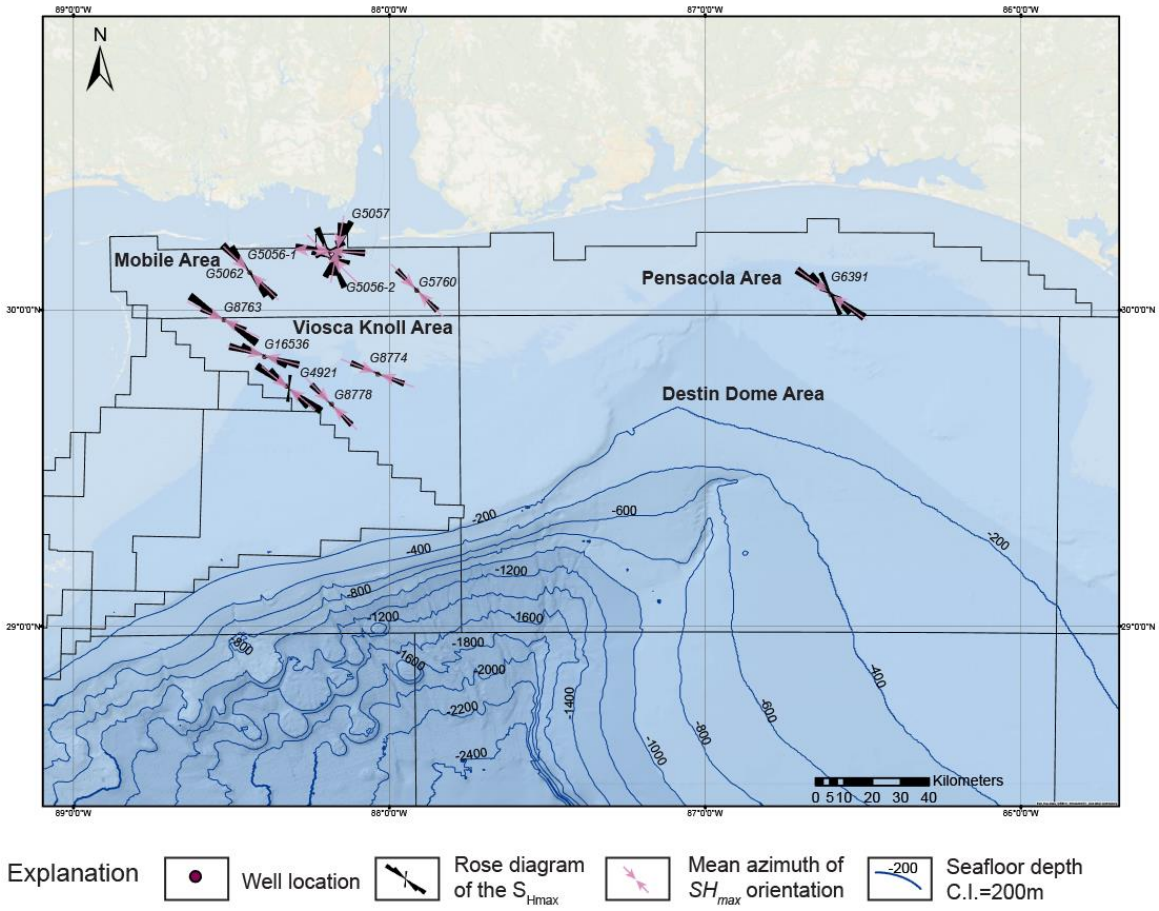

Figure 2.4. Map showing rose diagrams and vector mean azimuth of maximum horizontal stress in the Desoto Canyon Salt Basin. Base map source: ESRI; bathymetry source: GCOOS.

2.5.2 Lithostatic Stress

Figure 2.5 contains lithostatic stress (*Sv*) profiles derived from ten wells from the seafloor to a depth of 5,488 m (18,005 ft). The data are best fit with a power law curve, which has a coefficient of determination (R^2) of ~1.00. Lithostatic stress (*Sv*) increases with depth, and the average lithostatic gradient is 21.40 kPa/m (0. 944 psi/ft). The *Sv* profiles from individual wells are within 3 MPa (435 psi) of the best-fit curve in Figure 2.5, and thus have a high degree of consistency. The bulk density values used to derive *Sv* vary among rock types and tend to increase with depth. The density of carbonate rocks in the Smackover-Haynesville section ranges from 2.6-2.8 g/cm^3. The Ferry Lake Anhydrite (Lower Cretaceous) has a density of 2.9-3.0 g/cm^3, which is higher than the density of the other rock types analyzed. The density of sandstone in the Jurassic-Cretaceous section ranges from 2.2-2.7 g/cm^3, and the density of shale ranges from 2.2-2.7 g/cm^3. In the shallower section, chalk-rich carbonate in the Upper Cretaceous-Neogene section has a relatively low density of 2.3-2.5 g/cm^3. The density of sandstone in the Neogene-Quaternary section ranges from 2.2-2.4 g/cm^3, and the density of shale ranges from 1.9-2.1 g/cm^3. The *Sv* profile of individual wells varies slightly with bathymetry, reflecting the importance of accounting for water depth when calculating *Sv*. The standard deviation of *Sv* at depth ranges from 0.2-2.5 MPa (31-370 psi) and averages 1.4 MPa (205 psi).

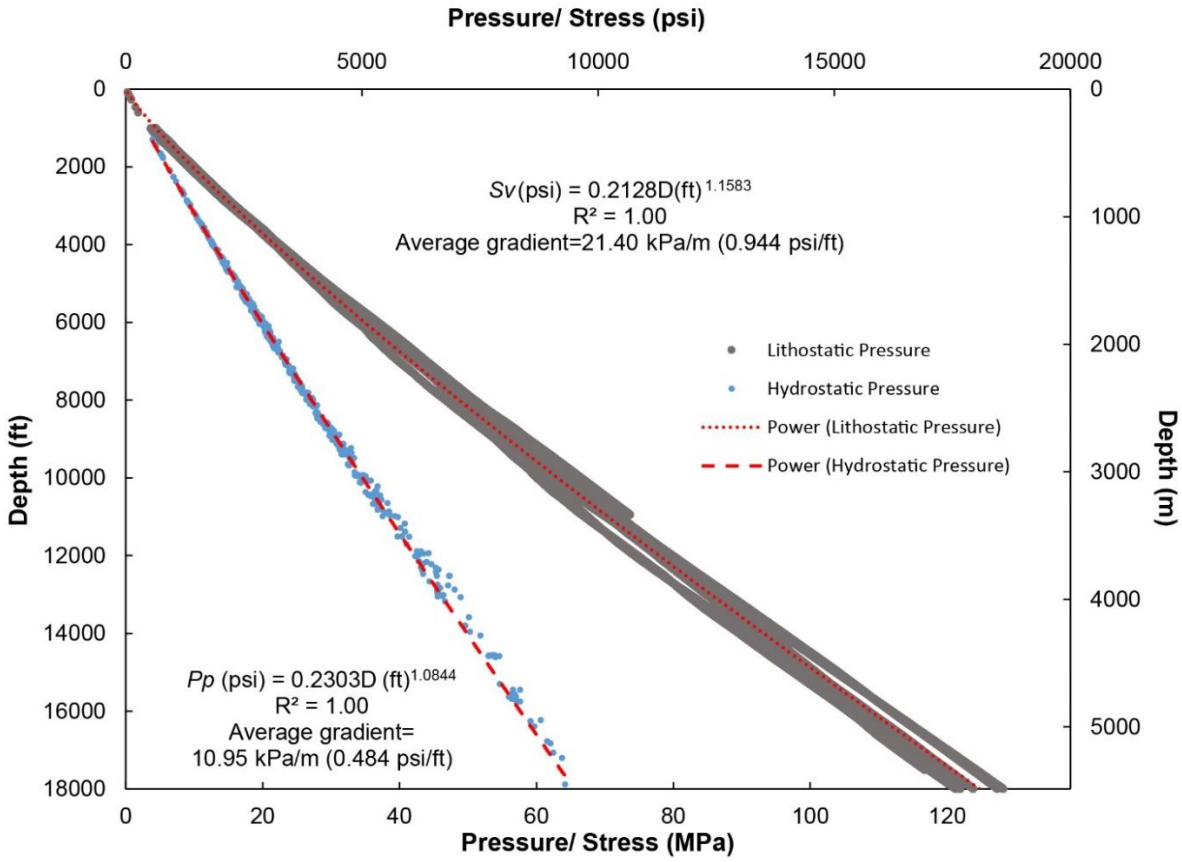

Figure 2.5. Plots showing variation of lithostatic stress (*Sv*) and pore pressure (P_p) with depth. Data for *Sv* were obtained from offshore wells in the Desoto Canyon Salt Basin, and data for P_p were obtained from wells in interior salt basins that are physically connected to the DeSoto Canyon Salt Basin.

2.5.3 Hydrostatic Pressure

Major geochemical components affecting TDS content include major ionic compounds, specifically chloride, sodium, calcium, magnesium, sulfate, and bicarbonate. The most abundant ionic compounds in formation water from the onshore

wells are Cl^-, Na^{2+}, and Ca^{2+} (Figure 2.6). The TDS data from the onshore wells ranges from ~24,000 mg/L to 360,000 mg/L and increases with depth. For a typical offshore area, TDS concentration has a minimum value equivalent to normal marine water (35,000 mg/L). Brine density, and hence the pore pressure gradient (P_p/depth), is influenced by the TDS content of the formation water, and so the P_p gradient increases with depth from a normal seawater gradient of 10.04 kPa/m (0.444 psi/ft) to a maximum of 12.40 kPa/m (0.548 psi/ft). The average gradient of P_p is 10.95 kPa/m (0.484 psi/ft). The hydrostatic pressure (P_p) profile from the seafloor to a depth of 5,488 m (18,000 ft) is shown in Figure 2.5. As in the *Sv*-depth plot, the P_p-depth plot follows a best-fit power law curve with a coefficient of determination (R^2) of 1.00.

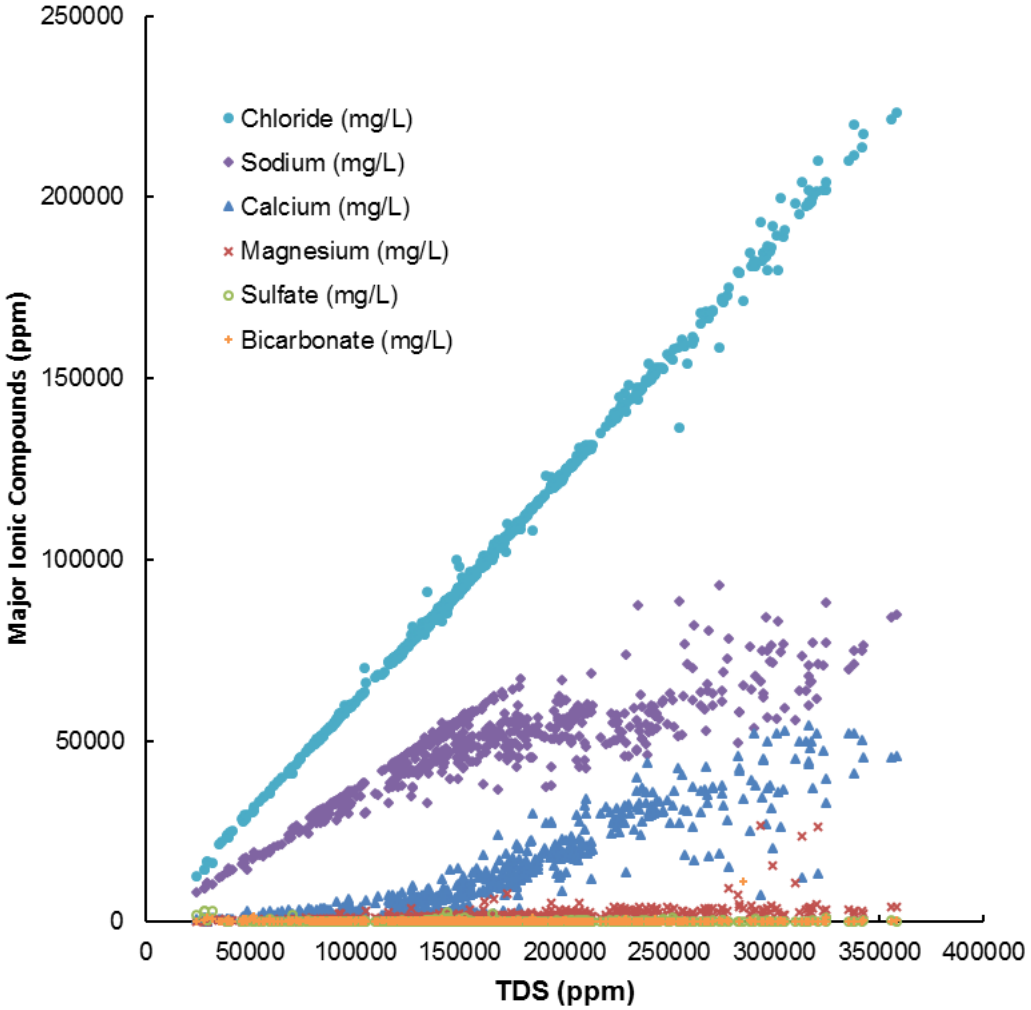

Figure 2.6. Plot of major ionic content versus TDS of formation water from wells north of the Desoto Canyon Salt Basin.

2.5.4 Horizontal Stress

Figure 2.7 shows the lithostatic and hydrostatic profiles from the previous sections, as well as a plot of Sh_{min} estimated from density and sonic logs in DeSoto Canyon Salt Basin. Plotting Sh_{min} with depth results in a highly scattered distribution and varies with

rock type. Figure 2.8 is a lithology-Sh_{min} correlation in one potential reservoir formation (Paluxy Formation), and the associated topseals (lower Washita-Fredericksburg shale and limestone). Gamma ray (GR), spontaneous potential (SP), and neutron-density logs provide guidance for identifying and correlating rock types with the estimated Sh_{min}. This graph shows that the Sh_{min} value in shale is distinctly higher than that in other rock types and demonstrates a highly scattered distribution of Sh_{min} with depth. A well-defined lower boundary for the data distribution exists in the Sh_{min}-depth plot. This lower boundary corresponds to an $S'h_{min}$-$S'v$ quotient of 0.28. The upper boundary of the effective stress distribution corresponds to an $S'h_{min}$-$S'v$ quotient of 0.90, which approaches the regional Sv gradient. However, most of the data points deeper than 2,750 m (9,000 ft) plot far below the regional Sv gradient. The minimum horizontal stress can be estimated base on geometric mean of the upper and lower bounds, and the result corresponds to an $S'h_{min}$-$S'v$ quotient of 0.50 (Figure 2.7). In the DeSoto Canyon Salt Basin, the SH_{max} ranges from Sh_{min} to Sv.

Based on the in-situ stress profiles in the DeSoto Canyon Salt Basin, an $S'h_{min}$ map was computed for the top of the Lower Tuscaloosa Group (Figure 2.9), which is the youngest of the three potential Cretaceous reservoir units in the study area (Meng et al., 2017; Chandra, 2018). This map shows the maximum injection pressure that can be applied safely based on the results of geomechanical analysis.

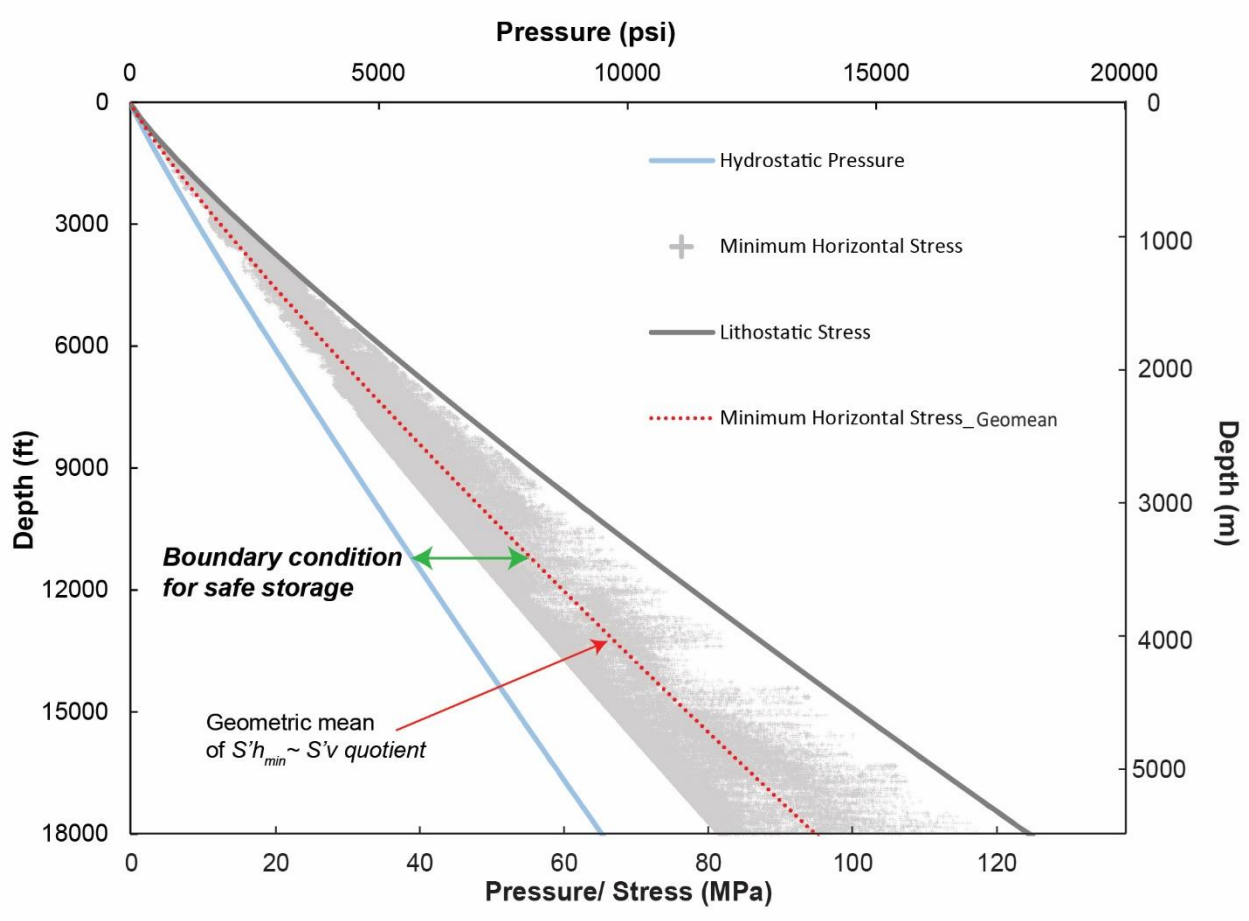

Figure 2.7. Depth profiles showing lithostatic stress (*Sv*), pore pressure (P_p) and minimum horizontal stress (Sh_{min}).

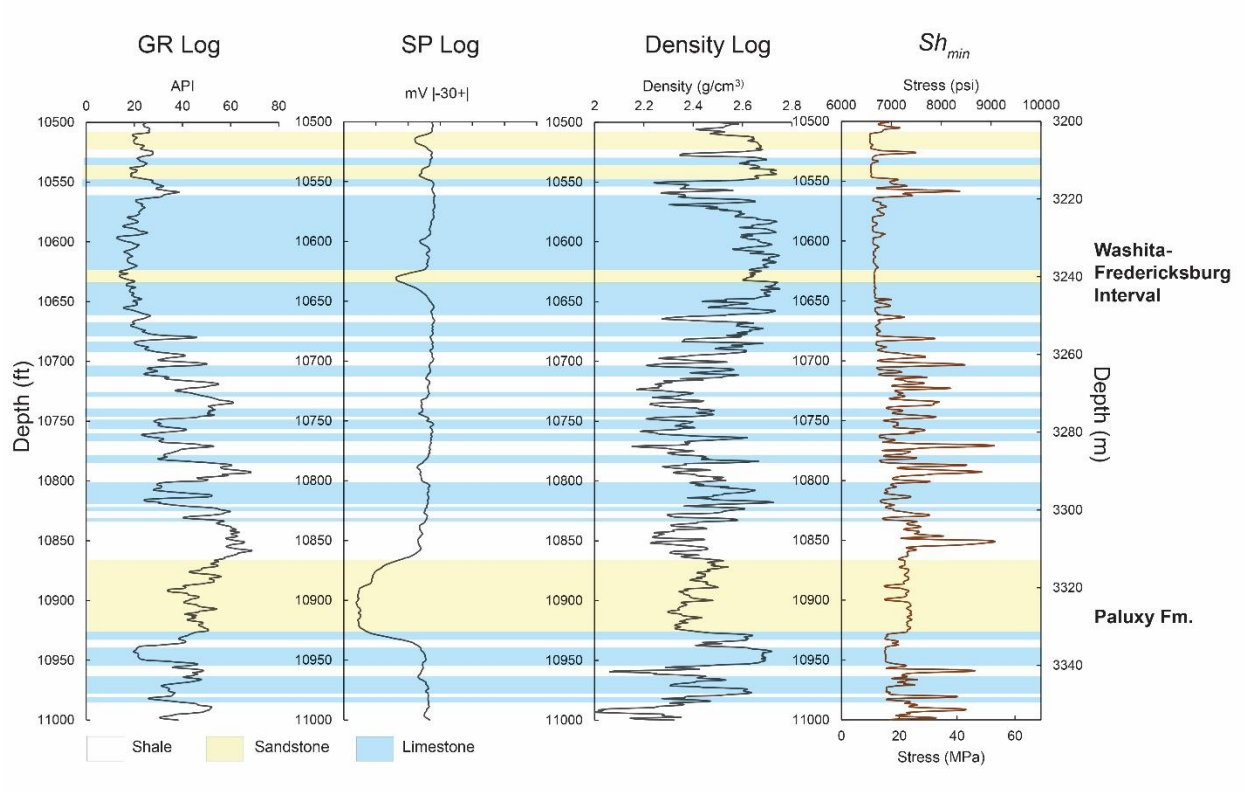

Figure 2.8. Geophysical well logs (from Well G02468) and Sh_{min} profiles showing that calculated Sh_{min} varies with rock type. Sandstone and limestone intervals have lower values of Sh_{min} than shale.

2.6 Discussion

2.6.1 Stress orientation

Nearly all of the stress orientation data are from exploration wells in the southwest-dipping Mobile-Viosca Knoll shelf. Regional structural dip in the salt basin is dominantly southwest, and faults in the Jurassic section generally parallel regional strike and record regional extension related to gravitational shelf spreading (Pashin et al., 2016).

Accordingly, the sediment wedge has been subjected to a northeast-southwest-directed extensional stress (Sh_{min}). Thus it follows that the maximum horizontal compressive stress (SH_{max}) would be parallel to regional strike, and this is confirmed by the analysis of borehole breakouts (Figure 2.4). Parallelism of vector-mean SH_{max} orientations with the depositional strike of the DeSoto Canyon Salt Basin is consistent with results from many of the stress orientation studies in the western and northern Gulf of Mexico (King et al., 2012; Yassir and Zerwer, 1997; Zerwer and Yassir, 1994). This type of stress orientation is likely to be a second-order stress trend that is independent of continental tectonic stress and is instead consistent with an interpretation of gravitational forces acting on accumulating sediment (Zoback, 1992).

Though the result of the study shows a dominant strike-parallel trend of SH_{max}, local stress deflections exist near faults and other salt-related structures in the Gulf of Mexico salt basins (Bell, 1996; King et al., 2012; Yassir and Zerwer, 1997). In wells G5056-1 and G4921, anomalous orientations (NW-SE) are developed only in faulted Jurassic strata in the salt roller province; the regional azimuth of SH_{max} prevails in the unfaulted strata above the roller-related structures. More information, such as that from dipole sonic and additional four-arm caliper logs, is needed to verify the relationship between the anomalous stress orientations and structure. In addition, no data are available to analyze the stress orientation in most of the Pensacola and Destin Dome Areas, but based on the studies cited above, similar deflections may occur in proximity to folds, faults, and salt diapirs at multiple scales. For example, numerous small-displacement normal faults are developed locally in the crestal regions of the salt pillow-cored

anticlines, whereas the peripheral faults of the Destin Fault System offset a thick stratigraphic section over a large area. According to the Andersonian theory of normal faulting (Anderson, 1951), SH_{max} is expected parallel to the normal fault strike. Faults with anomalous trends may cause or be a product of local deflection of SH_{max} (Yassir and Zerwer, 1997). Therefore, the Destin fault system, salt pillow province, and salt diapir province in the Desoto Canyon Salt Basin may contain significant perturbations of the regional stress field, whereas the large panel of southwest-dipping strata above the salt roller array hosts a uniform stress field that is driven by gravity. More data are needed from wells in structurally complex areas to verify the cause of the anomalous stress orientations.

2.6.2 Stress magnitude

Analysis of stresses in the Desoto Canyon Salt Basin indicates that lithostatic stress and hydrostatic pressure increase with depth and follow power-law curves. The Sh_{min} results are highly scattered and fall between a weakly defined upper bound in which maximum values approach Sv and a well-defined lower bound that is above P_p. An important reason for the variability of Sh_{min} is variation of rock type. Typically, shale has a higher Poisson's ratio than sandstone or limestone, which results in different ratios of $S'h_{min}$ to $S'v$. The lower bound of the Sh_{min}–depth plots represents the sandstone and limestone interval, and the upper bound represents shale. A number of pressure tests (e.g. leak-off tests, mini-fracture tests) are recommended to confirm Sh_{min} and SH_{max} at reservoir depth.

2.6.3 Implications for safe offshore CO_2 storage

These results provide valuable insight for evaluating CO_2 storage capacity and risk associated with these reservoirs. In the Paleocene-Miocene sandstone reservoirs, the pressure difference between the *Sv* and P_p profiles is smaller than that in the deeper Cretaceous reservoirs. Thus, those shallower reservoirs allow less pressure increase during injection. Stress magnitude, specifically that of Sh_{min}, controls the probability of leakage of injected CO_2 (Hawkes et al., 2005). During CO_2 injection, increasing pore pressure will change the stress state within the reservoir. If the stress magnitude exceeds the rock's shear strength or tensile strength, then shear or tensile fractures will develop during injection and may create leakage pathways through the caprock. Fracture breakdown pressures are greater than $S'h_{min}$, and so injection pressures exceeding $S'h_{min}$ may fracture the caprock. When injecting CO_2 into deep saline aquifers, the maximum bottom hole injection pressure is commonly set at 90% of the fracture pressure (Hawkers et al., 2005). During injection, an increase of P_p will increase the tendency of a pre-existing fault and associated fractures in the caprock to slip or open and form a potential migration pathway. The most critical orientation for reopening fractures and faults is in a plane normal to Sh_{min} (114°). Multiple faults associated with salt structures truncate and displace the prospective reservoir and seal intervals in the DeSoto Canyon Salt Basin. Accordingly, avoiding injection near seismically imaged faults in the study will help minimize risk. If subseismic faults and associated fractures are

present, then bottom-hole injection pressures higher than the minimum in-situ stress may open these structures. Consequently, it is essential to devise injection strategies that will maintain pressures below the estimated $S'h_{min}$. Simulation of the effective minimum horizontal stress in the basin (Figure 2.9) provides a reference for maximum CO_2 injection pressure in the prospective Cretaceous reservoirs, thereby reducing the risk of migration of injectate from the offshore CO_2 storage complex.

Further investigation should focus on the seal integrity of prospective reservoir caprocks. Geomechanical properties, such as the strength and elasticity of potential sealing strata, should be obtained to evaluate reservoir and seal integrity. Prospective reservoirs should be ranked according to their stability in order to facilitate initial CO_2 storage site selection and future development.

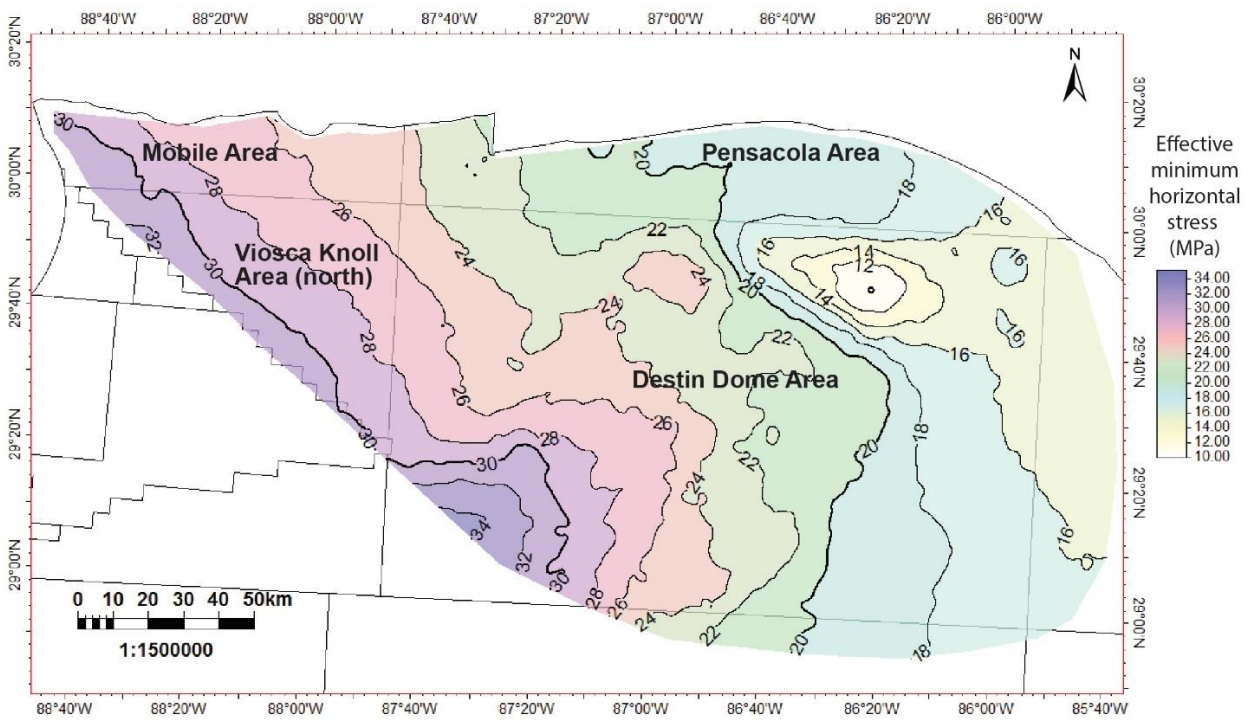

Figure 2.9. Simulation of fracture pressure ($S'h_{min}$) in the lower Tuscaloosa Group, DeSoto Canyon Salt Basin (Contour interval = 2 MPa). Injecting CO_2 at below fracture pressure will help minimize the risk of injectate migrating out of the target storage complex.

2.7 Conclusions

Ensuring safe, permanent storage of CO_2 is a central goal when planning and implementing geologic storage programs. Understanding the geomechanical integrity of potential storage objectives can help guide the selection of CO_2 storage sites and reduce the risk of CO_2 migrating out of the defined storage complex. Recent studies indicate that vast storage capacity exists in Cretaceous through Neogene sandstone in the

Desoto Canyon Salt Basin. These reservoirs are overlain by thick sections of shale and chalk, which form regionally extensive seals.

Horizontal stress orientations, lithostatic stress, and minimum horizontal stress were analyzed by using well log data in the study area. Hydrostatic pore pressure gradients were determined based on water chemistry in onshore wells north of the study area. Maximum horizontal stress orientations determined from borehole breakouts are highly consistent and parallel the dominant northwest strike of strata in the DeSoto Canyon Salt Basin. This orientation is locally deflected in faulted and folded Jurassic strata within the salt roller province, and similar deflections may occur near the other structures in the salt basin, which in places extend upward into the Neogene section. Lithostatic stress profiles follow power law curves from the seafloor to a depth of 5,480 m. Lithostatic stress increases with depth according to water column thickness, overburden thickness, and rock density, and has an average gradient of 21.4 kPa/m. The pore pressure profile, which is based on onshore water chemistry, also has a power-law relationship with depth. Brine density increases with depth in concert with increasing salinity, and pressure gradients range from 10.04 kPa/m to a maximum of 12.40 kPa/m. The magnitude of Sh_{min} has been estimated by assuming a linear elastic behavior of the strata, and the geometric mean $S'h_{min}$-$S'v$ quotient is 0.50.

Stress and pressure information is essential for determining the maximum allowable injection pressures for candidate injection zones, thus minimizing the risk of leakage. Based on analysis of the DeSoto Canyon Salt Basin, $S'h_{min}$ determines the critical stress

at which faults and fractures may open during injection, and tensile strength and shear strength control the pressures at which caprock integrity would be compromised. Additional investigation is needed to confirm stress orientation anomalies and measure the magnitude of the horizontal stresses. Further research should focus on more detailed analysis of reservoir and seal integrity to facilitate site selection and future development of CO_2 storage technology in the DeSoto Canyon Salt Basin.

References:

Anderson, E. M., 1951, The dynamics of faulting and dyke formation with applications to Britain. Oliver and Boyd, Edinburgh, UK, 206 pp.

Arts, R.J., Trani, M., Chadwick, R.A., Eiken, O., Dortland, S.L., and van der Meer, G.H., 2009. Acoustic and elastic modeling of seismic time-lapse data from the Sleipner CO_2 storage operation, *in* M. Grobe, J. C. Pashin, and R. L. Dodge, eds., Carbon dioxide sequestration in geological media—State of the science. AAPG Studies in Geology 59, 391–403.

Bell, J.S., 1996. In situ stresses in sedimentary rocks (part 2): applications of stress measurements. Geosci. Can. 23, 135–153.

Bell, J., and Gough, D., 1979. Northeast-southwest compressive stress in Alberta evidence from oil wells. Earth and Planet. Sci. Lett. 45, 475-482.

Chandra, A., 2018. Geological Characterization and CO_2 storage potential of Cretaceous sandstone in the DeSoto Canyon Salt Basin of the MAFLA shelf (thesis). Stillwater, Oklahoma, Oklahoma State University, 66 pp.

Charbonneau, P., 2018. Geologic framework for the assessment of offshore CO_2 storage resources: West Florida Platform (thesis). Stillwater, Oklahoma State University, 69 pp.

Dai, Z., Zhang, Y., Bielicki, J., Amooie, M.A., Zhang, M., Yang, C., Zou, Y., Ampomah, W., Xiao, T., Jia, W. and Middleton, R., 2018. Heterogeneity-assisted carbon dioxide storage in marine sediments. Applied Energy, 225, 876-883.

Finkbeiner, T., Stump, B., Zoback, M., Flemings, P., and Parker, R. A., 1996, Pressure (P), Overburden (Sv), and Minimum Horizontal Stress (Sh_{min}) in Eugene Island Block 330, Offshore Gulf of Mexico. Chicago, Gas Research Institute Final Report, Contract Number: 5095-260-3558, 30 pp.

Galloway, W. E., 2008. Depositional evolution of the Gulf of Mexico sedimentary basin, in Miall, A.D., ed., Sedimentary Basins of the World: Amsterdam, Elsevier, v. 5, 505-549.

Handford, C. R., and Baria, L. R., 2003. Exploration potential and high-resolution sequence stratigraphy of shelf-sand reservoirs, Miocene, south Mississippi. Gulf Coast Association of Geological Societies Transactions, 53, 304-312.

Hawkes, C.D., Bachu, S., Haug, K., Thompson, A.W., 2005. Analysis of in-situ stress regime in the Alberta Basin, Canada, for performance assessment of CO_2 geological sequestration sites. Fourth Annual Conference on Carbon Capture and Sequestration Pittsburgh, DOE-NETL, p. 22.

Keaney, G., Li, G., and Williams, K., 2010. Improved fracture gradient methodology-understanding the minimum stress in Gulf of Mexico, *in* Proceedings 44th US Rock Mechanics Symposium and 5th US-Canada Rock Mechanics Symposium, American Rock Mech. Assoc. ARMA-10-177.

King, R., Backé, G., Tingay, M., Hillis, R., and Mildren, S., 2012. Stress deflections around salt diapirs in the Gulf of Mexico. Geol. Soc. Lond. Spec. Publ. 367, 141–153.

Meng, J., Pashin, J. C., and Chandra, A., 2017, In-situ Stress in the DeSoto Canyon Salt Basin, Eastern Gulf of Mexico, Geological Society of America Abstracts with Programs, 49, doi: 10.1130/abs/2017AM-297935.

Moore, J. C., Iturrino, G. J., Flemings, P. B., and Sawyer, D. E., 2009, Data report: stress orientations from borehole breakouts, IODP Expedition 308, Ursa area, Mississippi Fan, Gulf of Mexico, in Gulf of Mexico Hydrogeology, Proc.Integr. Ocean Drill. Program, 308, doi:10.2204/iodp.proc.308.212.2009.

Pashin, J. C., Jin, G., and Hills, D. J., 2016, Mesozoic structure and petroleum systems in the DeSoto Canyon Salt Basin in the Mobile, Pensacola, Destin Dome, and Viosca Knoll Areas of the MAFLA Shelf, *in* Proceedings 35th Annual Gulf Coast Section SEPM (GCSSEPM) Foundation Bob F Perkins Research Conference, Houston, Texas. p. 315-340.

Pashin, J. C., and Payton, J. W., 2005. Geological sinks for carbon sequestration in Alabama, Mississippi, and the Florida panhandle: Alabama Geological Survey, Final Report to Southern States Energy Board, Subgrant SSEB-NT41980-997-GSA-2004-00, unpaginated CD-ROM.

Pindell, J.L., and Kennan, L., 2001. Kinematic evolution of the Gulf of Mexico and Caribbean, *in* Proceedings Petroleum Systems of Deepwater Basins: GCSSEPM 21st Annual Bob F. Perkins Research Conference Proceedings. 193-220.

Plumb, R. A., Hickman, S.H., 1985. Stress-induced borehole elongation: a comparison between the four-arm dipmeter and the borehole televiewer in the Auburn geothermal well. J. Geophys. Res. Solid Earth, 90, 5513–5521.

Reynolds, S.D., Hillis, R.R., 2000. The in situ stressfield of the Perth Basin, Australia. Geophys. Res. Lett. 27, 3421–3424.

Sandwell, D.T., Muller, R.D., Smith, W.H.F., Garcia, E., Francis, R., 2014. New global marinegravity model from CryoSat-2 and Jason-1 reveals buried tectonic structure. Science 346:65–67. https://doi.org/10.1126/science.1258213.

Smith, C. C., 1991, Foraminiferal biostratigraphic framework, paleoenvironments, rates of sedimentation, and geologic history of the subsurface Miocene of southern Alabama and adjacent state and federal waters. Geological Survey of Alabama Bull. 138, 1-223.

Sperner, B., Muller, B., Heidbach, O., Delvaux, D., Reinecker, J., Fuchs, K., 2003. Tectonic stress in the Earth's crust: advances in the World Stress Map project. Sp. Publ. Geol.Soc. Lond. 212, 101–116.

Yassir, N.A., Zerwer, A., 1997. Stress regimes in the Gulf Coast, offshore Louisiana; data from well-bore breakout analysis. AAPG Bull. 81, 293–307

Zerwer, A., and Yassir, N., 1994, Borehole breakoutinterpretation in the Gulf Coast, offshore Louisiana,in Rock Mechanics, edited by P. P. Nelson and S. E.Laubach, A. A. Rotterdam, Balkema. p. 225-232,

Zoback, M.D., Barton, C.A., Brudy, M., Castillo, D.A., Finkbeiner, T., Grollimund, B.R., Moos, D.B., Peska, P., Ward, C.D., Wiprut, D.J., 2003. Determination of stress orientation and magnitude in deep wells. Int. J. Rock Mech. Min. Sci. 40, 1049–1076.

Zoback, M. D., 2010, Reservoir geomechanics, first ed. Cambridge University Press, Cambridge

Zoback, M.D., Peska, P., 1995. In-situ stress and rock strength in the GBRN/DOEpathfinder well, South Eugene Island, Gulf of Mexico. J. Petrol. Technol. 582–585.https://doi.org/10.2118/29233-PA

Zoback, M.L., 1992. First- and second-order patterns of stress in the lithosphere: the worldstress map project. J. Geophys. Res. Solid Earth 97:11703–11728. https://doi.org/10.1029/92JB00132.23B.

CHAPTER III

PAPER II: STRUCTURAL FRAMEWORK AND FAULT ANALYSIS IN THE EAST-CENTRAL GULF OF MEXICO SHELF: IMPLICATIONS FOR OFFSHORE CO_2 STORAGE

3.1 Abstract

Ensuring safe, permanent storage of CO_2 is vital for the success of long-term offshore storage of carbon dioxide. Recent studies indicate that vast CO_2 storage capacity exists in Cretaceous through Neogene sandstone in the east-central Gulf of Mexico (Chandra, 2018; Charbonneau, 2018; Pashin et al., 2018). Understanding the structural styles, the likelihood of reactivation, and seal properties of the pre-existing faults is essential to provide safe carbon storage and minimize the risk of injected CO_2 migrating beyond the confines of the storage complex.

The structural framework in the study area includes a range of basement structures and salt-tectonic structures related to development of the DeSoto Canyon Salt Basin, the Middle Ground Arch, and the Tampa Embayment during the opening of

the Gulf of Mexico. The Central DeSoto Canyon Salt Basin is structurally complex due to the presence of peripheral faults, salt pillows, salt rollers, and salt diapirs. Multiple faults associated with the peripheral faults and salt pillows displace the potential Cretaceous reservoirs and seal intervals. Fault analysis shows that while the slip tendency is small, whereas the dilation tendency and potential for cross-formational flow is relatively high, particularly where reservoir strata in the footwalls are juxtaposed with sealing strata in the hanging walls.

Favorable CO_2 injection sites are available throughout the stable shelf areas of the DeSoto Canyon Salt Basin where faults with high dilation tendency are absent above the Jurassic section. Future research should focus on further geomechanical, pressure, and flow simulation of the potential reservoirs and associated seals.

3.2 Introduction

Annual anthropogenic CO_2 emissions in the U.S. were estimated at about 6.5 million metric tons in 2015 according to the U.S. Environmental Protection Agency (EPA). About 40% of the anthropogenic CO_2 in the US is emitted in the southeast (Southern States Energy Board, 2013). Subsurface geologic storage of CO_2 can play a major role in offsetting these emissions, and offshore storage may be a viable solution due to legal advantages and apparently vast storage capacity. The study area for this research encompasses the continental shelf offshore of Mississippi, Alabama, and Florida and is part of Central and Eastern Gulf of Mexico planning areas of the U.S.

Bureau of Ocean Energy Management (BOEM). Recent studies indicate that vast storage capacity exists in Cretaceous through Neogene sandstone (Hills and Pashin, 2010; Chandra, 2018). The sandstone units are thought to provide a storage resource greater than 20 Gt; these reservoirs are overlain by thick sections of tight mudrock, limestone, and chalk, which are thought to form regionally extensive seals (Pashin et al., 2000, 2016; Chandra, 2018).

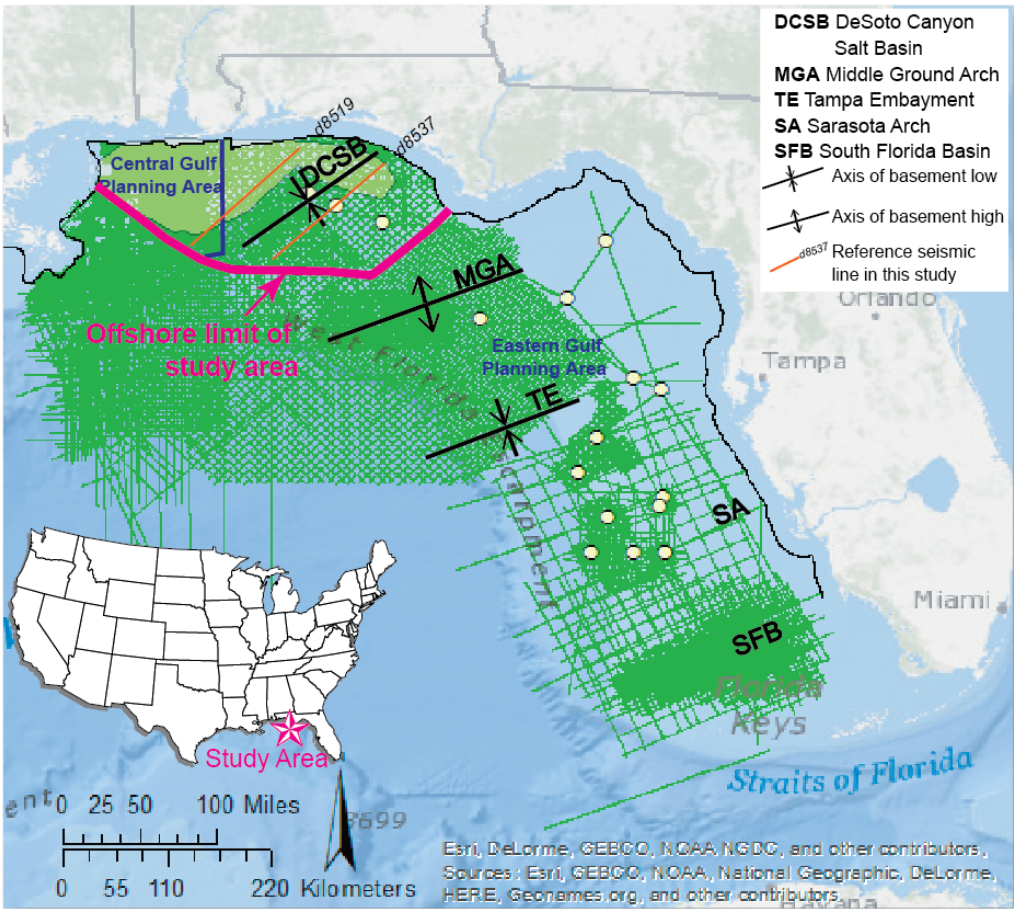

Figure 3.1. Map showing the location, seismic coverage, and well control of the study area. Green lines show reflection seismic control, white dots and shaded area show well control.

Ensuring safe, permanent subsurface storage of CO_2 is a central goal of research sponsored by the National Energy Technology Laboratory (NETL) of the U.S. Department of Energy. Leakage of injected CO_2 along preexisting structures, such as faults, is a widely acknowledged risk associated with CO_2 storage (Hawkes et al., 2005). During the injection of CO_2, a pressure-driven stress change increases the tendency of faults to dilate or slip, which promote leakage. An ideal CO_2 storage site selection should have little or no risk of leakage of injected CO_2 beyond the boundaries of the storage complex. It is essential to understand the structural framework of candidate storage sites, as well as the likelihood of dilation or slip along pre-existing faults. It is also important to understand the fault sealing characteristics to determine whether the fault is acting as a migration pathway or a fault seal for trapping the gas.

Unlike the western Gulf of Mexico, where the geologic framework has been defined by extensive oil and gas exploration, much less is known about the eastern Gulf of Mexico shelf due to a moratorium on drilling and production activities within 161 km (100 mi) of the shoreline. Published research in the eastern Gulf has focused mainly on the Triassic-Jurassic structures with the emphasis on crustal evolution and salt tectonics (Martin, 1987; Dobson and Buffler, 1991 ,1997; MacRae and Watkins, 1992, 1993, 1996; Nwafor, 2013; Pashin et al., 2016) and the depositional framework of the Norphlet Formation (Jurassic) which is a major ultra-deep natural gas reservoir (e.g., Mancini et al., 1985; Tew et al., 1991; Dobson and Bufler, 1997; Story, 1998; Hunt et al., 2017). Other studies have been focused on defining the correlation and distribution of Cretaceous formations (Petty 1995, 1997, 1999). Charbonneau (2018) described the

geology of the Sarasota Arch, South Florida Basin, and part of the Tampa Embayment and conducted a CO_2 storage assessment. To the author's knowledge, there have been few comprehensive structural framework studies in the eastern Gulf of Mexico area. Pashin et al. (2016) characterized the salt-related structures in the Jurassic-Neogene strata within the DeSoto Canyon Salt Basin and characterized the petroleum systems. The present study builds on the research of Pashin et al. (2016) to provide additional information on the fault networks and their implications for CO_2 storage. Another important objective of this research is to evaluate the likelihood of reactivation and sealing characteristics of the major extensional faults in the study area that offset the Cretaceous section.

3.3 Geological background

3.3.1 Study Area

The Gulf of Mexico Basin was formed by the rifting and drifting of the North American, South American, and African Plates beginning in the Late Triassic (Buffler and Sawyer, 1985; MacRae, 1993; Pindell, 1985). The Gulf of Mexico Basin formed as a result of extension and isostatic adjustment of the crust as the Yucatan block rotated counterclockwise relative to North America, (Pindell and Kennan, 2001; Sandwell et al., 2014). The basic structure of the continental shelf in the northeastern Gulf of Mexico includes alternating basement uplifts and basins, including the DeSoto Canyon Salt Basin, the Middle Ground Arch, the Tampa Embayment, the Sarasota Arch, and the

South Florida Basin (Figure 3.1). The DeSoto Canyon Salt Basin contains four structural provinces related to salt tectonics: (1) the Destin fault system, (2) the salt pillow province, (3) the salt diapir province, and (4) the salt roller province (Pashin et al., 2016) (Figure 3.2). The Destin fault system bounds grabens that were formed near the updip limit of salt. Broad salt pillows occur basinward of the Destin fault system, and the largest of these structures forms the core of Destin Dome. The diapir province is in the structurally deepest part of the salt basin, and the salt locally forms diapiric bodies that rise more than 6,700 m above the basement. The salt roller province contains a large array of normal faults and rollover structures that record gravitational shelf spreading during Jurassic time.

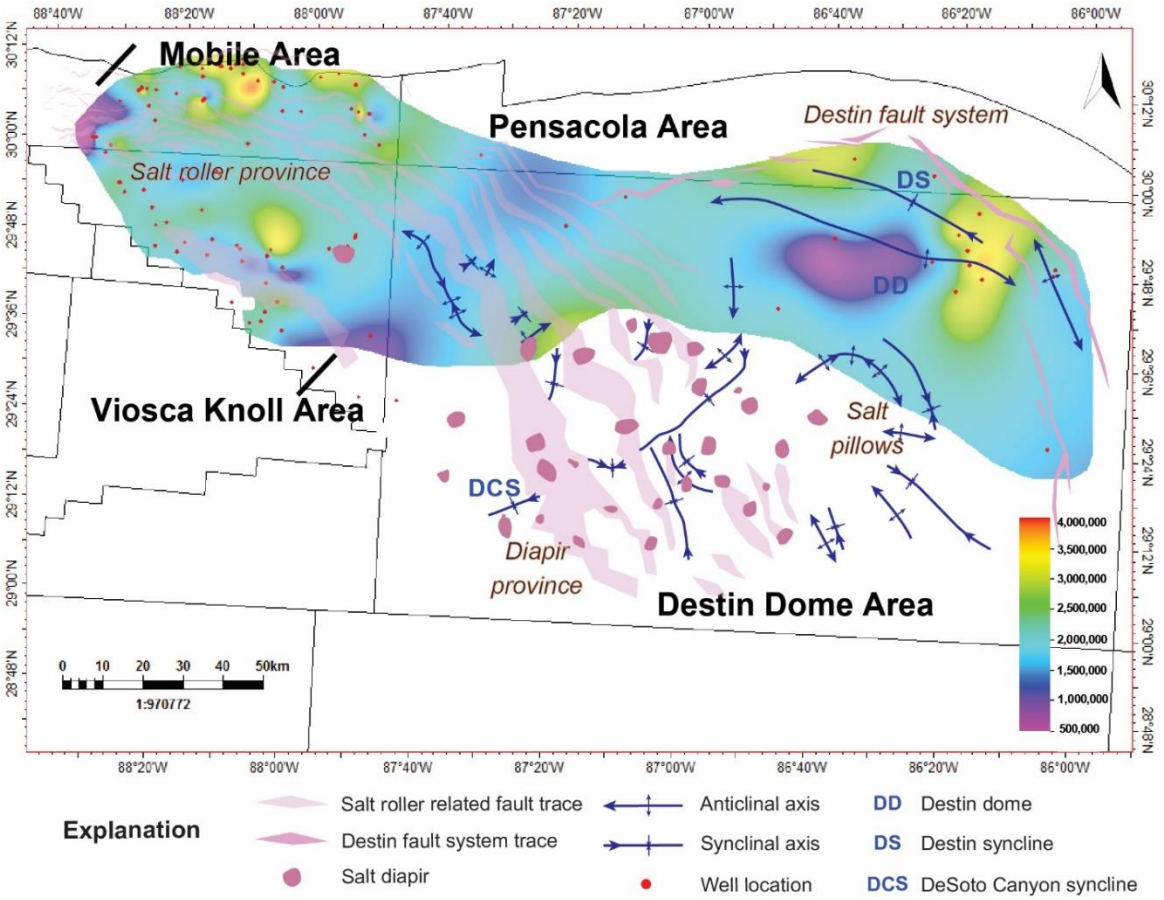

Figure 3.2. Cumulative storage resource map of the northern DeSoto Canyon Salt Basin (Paluxy Formation, Washita-Fredericksburg interval and lower Tuscaloosa Group). Contour interval = 500,000 tonnes/km^2 (Modified from Pashin et al., 2016; Chandra, 2018).

3.3.2 Stratigraphy

Strata in the study area include a thick succession of Mesozoic and Cenozoic siliciclastic rocks, carbonate rocks, and evaporites, which were deposited in a broad sedimentary wedge that was deposited upon extended Paleozoic basement (Galloway, 2008; Pashin et al., 2016; Figure 2. 2). Above basement is the Middle Jurassic Louann Salt. The Louann Salt is overlain by the sandstone of the Norphlet Formation and the

limestone and dolomite of the Smackover Formation. The Smackover Formation, in turn, is overlain by the Haynesville Formation, which is dominated by limestone. The Cotton Valley Group spans the Jurassic-Cretaceous boundary, containing mainly siliciclastic rocks, and capped by a prominent carbonate unit called the Knowles Limestone. Lower Cretaceous strata consist mostly of siliciclastic rocks in the northeastern part of the salt basin and carbonate rocks in the southern and western parts. Upper Cretaceous sedimentation culminated in formation of a chalk-rich carbonate ramp that spanned the width of the Lower Cretaceous platform. Paleocene through Oligocene strata are dominated by shale and limestone. Middle and Upper Miocene strata of the Pensacola Clay constitute the bulk of the Neogene section and contain siliciclastic strata deposited in shelf and shoreline environments (Smith, 1991).

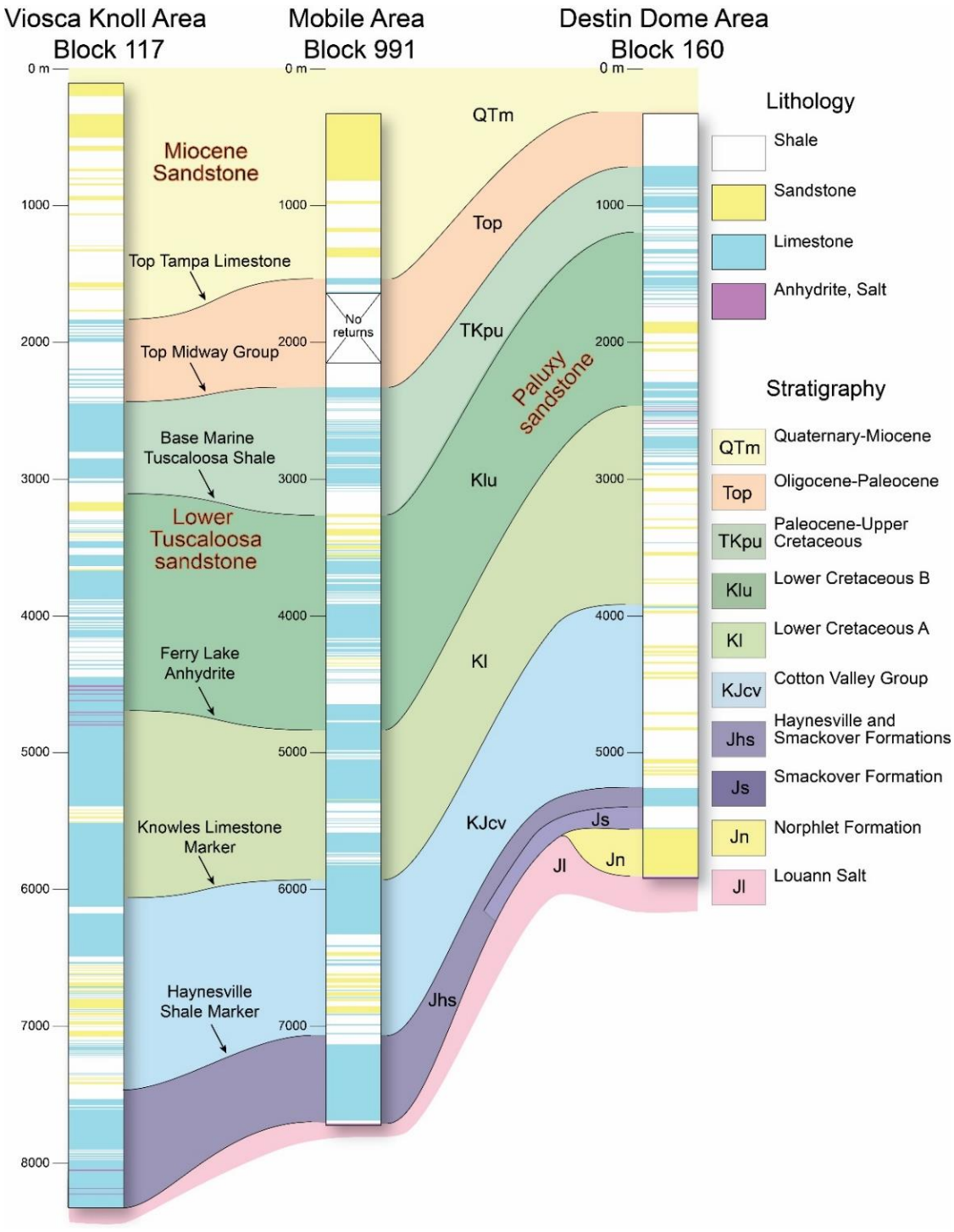

Figure 3.3. Stratigraphic columns showing rock types and major stratigraphic intervals of DeSoto Canyon Salt Basin (after Pashin et al., 2016).

3.3.3 Potential Reservoir Units

Preliminary investigation has reported about 28 Gt storage resource in Cretaceous sandstone of the DeSoto Canyon Salt Basin (Chandra, 2018), 879 Gt in Cretaceous carbonate of the Sarasota Arch (Charbonneau, 2018), and 120 Gt in Cenozoic sand of the DeSoto Canyon Area (Pashin et al., 2018). Previous lithological analysis identified several potential reservoir units in Cretaceous strata, including the Paluxy Formation, the Washita-Fredericksburg interval, Lower Tuscaloosa Group. These potential reservoirs are widespread, thick (3-40 m), possess high effective porosity that commonly exceeds 20%, and are confined by thick stacks (180-700 m) of shale and carbonate seals. The storage resource of the Paluxy Formation is concentrated largely in the withdrawal synclines around Destin Dome, whereas the storage resource in the Washita-Fredericksburg interval and Lower Tuscaloosa Group is concentrated mainly in the nearshore reaches of the Mobile and Viosca Koll Areas (Chandra, 2018) (Figure 3.2).

3.3.4 Stress field

The stress field in the DeSoto Canyon Salt Basin has been analyzed by Meng et al. (2018). The vector mean azimuth of maximum horizontal stress (SH_{max}) is dominantly northwest-southeast with an average of 114°. Both lithostatic stress (S_v) and hydrostatic pressure (P_p) have power-law relationships with depth (equations 3.1 and 3.2, where D is depth of the reservoir). The geometric mean of the minimum horizontal stress (Sh_{min})-depth data corresponds to a constant ratio of effective minimum horizontal stress and effective lithostatic stress of ~0.5 (equation 3.3).

$$S_v \text{ (MPa)} = 0.005812\text{D(m)}^{1.1583} \quad (3.1)$$

$$P_p \text{ (MPa)} = 0.005762\text{D(m)}^{1.0844} \quad (3.2)$$

$$Sh_{min} = 0.5(S_v - P_p) + P_p \quad (3.3)$$

3.4 Methodology

The analytical approach for this research consists of three main components: 1) structural framework analysis, 2) fault slip and dilation tendency analysis, and 3) fault seal analysis. Combining with the previous geologic and volumetric assessments (Pashin et al., 2016; Chandra, 2018), favorable storage sites were identified that have minimal risk of leakage of injected CO_2.

3.4.1 Structural framework analysis

Public domain 2D seismic reflection data and geophysical well logs were obtained from the Bureau of Safety and Environmental Enforcement (BSEE; Figure 3.1). Seismic profiles were interpreted using standard seismic-stratigraphic and sequence-stratigraphic procedures (Vail, 1987). Seismic markers from the base of the Louann Salt to the modern seafloor were identified, correlated, and traced throughout the study area using IHS Kingdom 2D/3D Pak. As markers were traced, discontinuous and offset reflections were used to define bed cutoffs and major fault planes. Faults intersecting two or more seismic markers were considered as major faults. Three dip-parallel seismic profiles were depth-converted in IHS Kingdom 2D/3D Pak using wellbore velocity

surveys. Major structural features, including dipping panels, folds, and faults were identified and characterized following depth conversion. Depth structural contour maps of selected markers were constructed to characterize the regional structural framework using Schlumberger Petrel software. Small-scale faults identified in the seismic profiles were not mappable due to the seismic line spacing (1-7 km). Fault planes were modeled in three dimensions using Petrel Software and prepared for slip and dilation tendency analysis and fault seal analysis.

3.4.2 fault slip and dilation tendency analyses

Slip and dilation tendency analyses were performed to determine the likelihood of fault movement during CO_2 injection. This part of the study aims to analyze the slip and dilation tendency for the faults observed in the seismic profiles associated with the four structural provinces in DeSoto Canyon Salt Basin and displace the potential reservoir sandstone and associated seals.

A fault surface is likely to slip when the resolved shear stress equals or exceeds the frictional resistance to sliding (Morris et al., 1996). Slip tendency (T_s) is the ratio of the shear stress (τ) to normal stress (σ_n) at the fault surface (Morris et al., 1996) and is expressed by

$$T_s = \frac{\tau}{\sigma_n} \qquad (3.4).$$

Dilation tendency is the ability of a fracture to dilate, and controlled largely by the normal stress on the fault surface, which can be normalized by the three principal stresses relative to the fault plane (Ferrill et al., 1999). The dilation tendency (T_d) can be computed using equation 3.5

$$T_d = \frac{\sigma_1 - \sigma_n}{\sigma_1 - \sigma_3} \quad (3.5),$$

where σ_1 is the maximum principal compressive stress, and σ_3 is the minimum principal compressive stress. Slip and dilation tendency values range from 0 to 1, with higher values indicating greater possibility of fault reactivation.

Slip and dilation tendency analysis was performed on the modeled faults using 3DStress software. Eleven fault surfaces mapped using Petrel Software were imported into 3DStress, and slip and dilation tendency at the potential reservoir depth were calculated. For a normal stress state in the Gulf of Mexico, S_v in equation (3.1) was entered into the 3DStress® software as the maximum compressional principal stress (σ_1), Sh_{min} equation (3.3) was entered as the minimum compressional principal stress (σ_3). The magnitude of SH_{max} cannot be determined without fracture test information, which is not available in the study area. Due to the uncertainty in SH_{max} (σ_2), an intermediate value between σ_1 and σ_3 was used as input in this study using possible stress magnitudes on the stress polygon following the approach of Zoback (2010). The

resulting slip and dilation tendency data were displayed by color mapping on the 3-D models of the faults to identify portions of the fault that may be prone to reactivation.

3.4.3 Fault seal analysis

Fault seal analysis evaluates whether a fault acts as a barrier or a conduit for flow during CO_2 storage. Two types of fault seal analyses have been performed to study the fault seal integrity, including juxtaposition seal analysis and fault rock seal analysis (Allan, 1989; Bouvier et al., 1989; Lindsay et al, 1993; Knipe, 1997; Knipe et al., 1998; Yielding et al., 1997). Juxtaposition seals occur when rock types with different permeability are juxtaposed by movement along a fault (Allan, 1989; Figure 3.4a). Fault rock seals occur where shale is smeared along the fault plane to form a membrane (Figure 3.4b). A fault is potentially sealed when a reservoir unit is juxtaposed with shale, tight limestone, evaporite, or clay smear. If a sandstone layer is juxtaposed with sandstone, or shale layers are not sufficiently thick and ductile to provide a shale smear in the fault zone, fluid is likely to be transmitted along or through the fault (Figure 3.4c). Therefore, fault rock seal is largely dependent on clay content and the continuity of shale smears (Bouvier et al., 1989; Lindsay et al, 1993; Yielding et al., 1997).

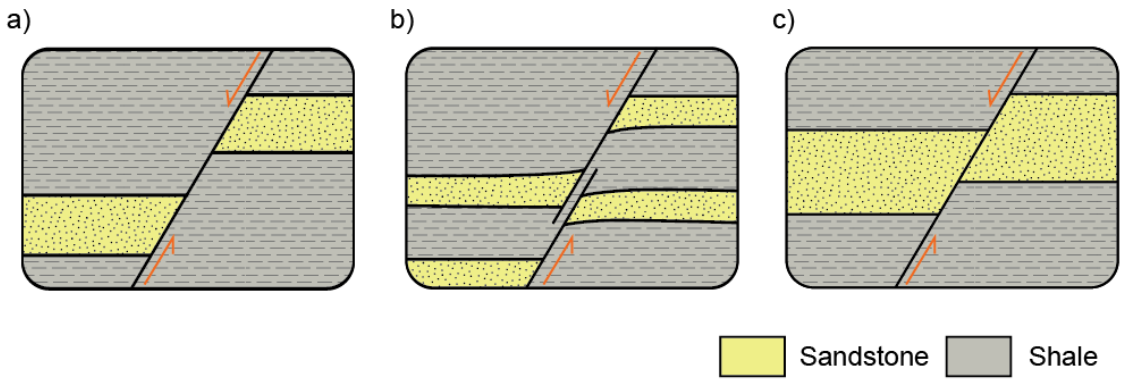

Figure 3.4. Aspects of fault juxtaposition. a) Juxtaposition seal; b) Clay smear; and c) Sand-sand juxtaposition (modified from Færseth et al., 2007).

In this study, juxtaposition analysis and clay smear analysis were performed to determine the seal properties of the largest fault in the DeSoto Canyon Salt basin. 1-D juxtaposition analysis was performed using geophysical well log data using the methods of Knipe (1997) and Knipe et al. (1998). Gamma ray (GR) and porosity log data were used for lithologic analysis. Shale volume (Vsh) from GR logs was used to estimate the clay content. A juxtaposition diagram was constructed in Petrel Software to plot bed cutoffs and the juxtaposed rock types on the fault plane following the approach of Allan (1989). The shale gouge ratio (SGR) algorithm of Yielding et al. (1997) was applied to estimate clay content in the fault zone, which is expressed as

$$\mathrm{SGR} = \frac{\sum(Shale\ layer\ thickness * Clay\ percentage)}{Fault\ throw} \qquad (3.6).$$

SGR estimates likelihood of clay mixing due to the presence of shale, which is a function of shale thickness and the magnitude of fault throw (Equation 3.6; Yielding et al., 1997). A high SGR value represents high clay content and low permeability (Foxford et al. 1998; Yielding, 2002; van der Zee and Urai, 2005; Bretan et al, 2011). Previous research has shown that SGR values lower than 15-20% pose a significant risk of leakage (Yielding, 2002). SGR values were gridded using Petrel Software to estimate clay content along the fault plane. Based on the results of juxtaposition and rock seal analyses, a 3D model was built showing conceptual sealing properties on the Fault.

3.5 Results

3.5.1 Structural Framework

Line d8519 (Figure 3.5) is an interpretation of a representative depth-converted seismic profile in the DeSoto Canyon Salt Basin. Basement generally contains chaotic and nonparallel reflections; weakly divergent reflections below Destin Dome define a Triassic graben (MacRae and Watkins, 1996). A distinct reflection marks the top of basement. Louann salt bodies (Jl) are readily identified because they are seismically transparent; that is, they contain few internal reflections. High-amplitude reflections formed by a marked impedance contrast at the top of salt was observed where salt is draped by higher velocity sediment in the Norphlet-Haynesville section. Strata in the Norphlet-Smackover section (Jsn) contain high amplitude reflections that define tilt blocks and rollover folds associated with salt rollers and the Destin Fault System.

The Knowles Limestone forms the top of the Cotton Valley Group and contains a moderate- to high-amplitude reflection that can be traced through much of the study area (top KJcvh). The Ferry Lake Anhydrite is a regional marker (Petty, 1995) and forms a high-amplitude reflection (top Kl) that helps subdivide the Lower Cretaceous section (Kl, Klu). A prominent downlap surface (base TKpu) corresponds with the contact between the sandstone of the Lower Tuscaloosa Group and the Marine shale of the Tuscaloosa Group. A weak reflector corresponding to the base of the Paleocene-Eocene Wilcox Group defines the top of interval TKpu. The top of the Tampa Limestone (top of interval Top) is identifiable as a regional strong reflector approximating the Oligocene-Miocene boundary. In the Miocene-Quaternary section (QTm), the Pensacola Clay contains weak to moderate reflections of variable geometry, and a distinct seismic marker at the top of interval QTm corresponds to the seafloor.

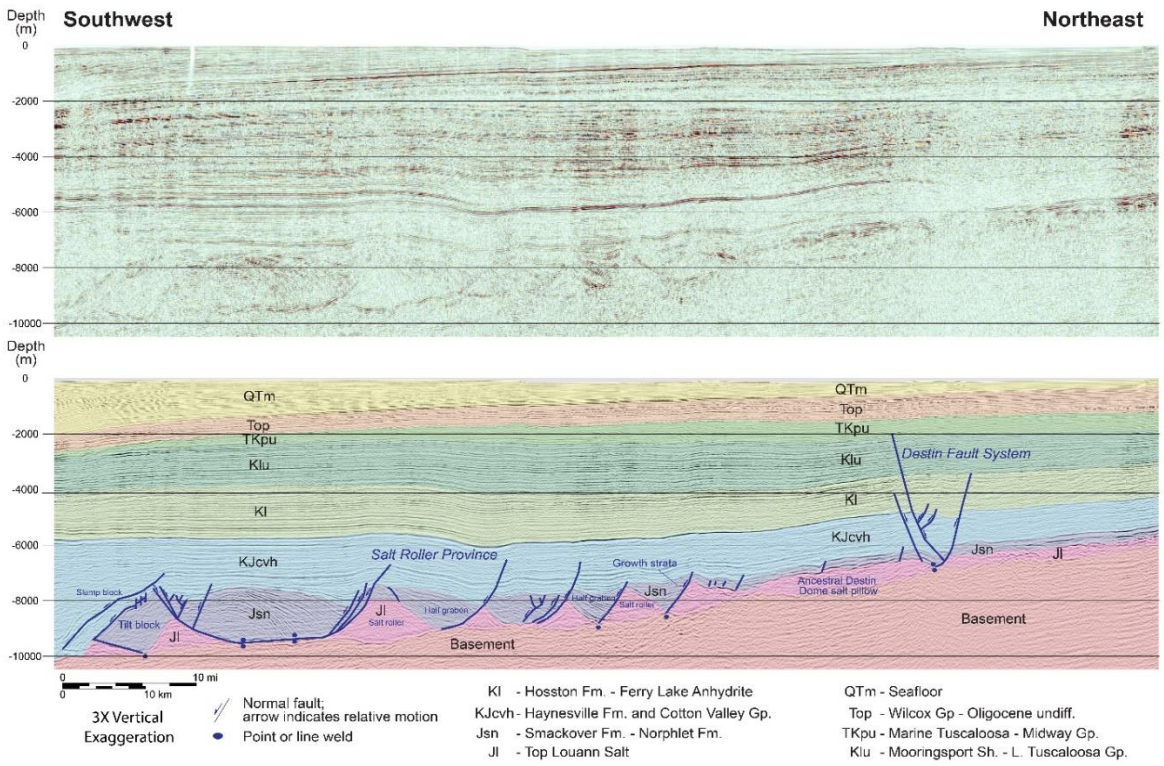

Figure 3.5. Uninterpreted and interpreted seismic profile (Line d8519) showing stratal geometry and structure in the western DeSoto Canyon Salt Basin (see Figure 3.1 for location).

3.5.1.1 Western DeSoto Canyon Salt Basin: Stable shelf

Line d8519 shows the structural style that is characteristic of the western to central DeSoto Canyon Salt Basin (Figure 3.5). In the western part of the DeSoto Canyon Salt Basin, numerous salt rollers are developed atop basement and are associated with regional and counterregional faults, rollover folds, and tilt blocks in the overlying Jurassic section (MacRae and Watkins, 1993; Pashin et al., 2016). The salt rollers are typically bounded by regional-dipping normal faults that have a planar to listric

geometry. Seismic profiles and structural contour maps show that the vast majority of the faults offset strata no younger than the Knowles Limestone of the Cotton Valley Group. The few faults that offset the Knowles Limestone are in the updip portions of the salt roller province in the Mobile and Viosca Knoll Areas (Pashin et al., 2016; Figure 5). The normal faults have maximum displacement at the top of the Louann Salt, and displacement decreases toward the upper fault tips, indicating synsedimentary growth. Strata between the top of the Knowles Limestone and the seabed lack imaged faults in the western DeSoto Canyon Salt Basin. Subsurface horizons in the Mobile and Viosca Knoll Areas dip approximately 0.3-0.6° SW, and regional structural relief is about 800 m. Seismic profiles and structure maps both indicate a four-way structural closure in the southwestern part of the basin (Figures 3.5, 8). This structural element is the strata above the salt roller with maximum relief at the top of the salt (Jl) and with relief decreasing upward to the top of the Lower Tuscaloosa Group (Klu).

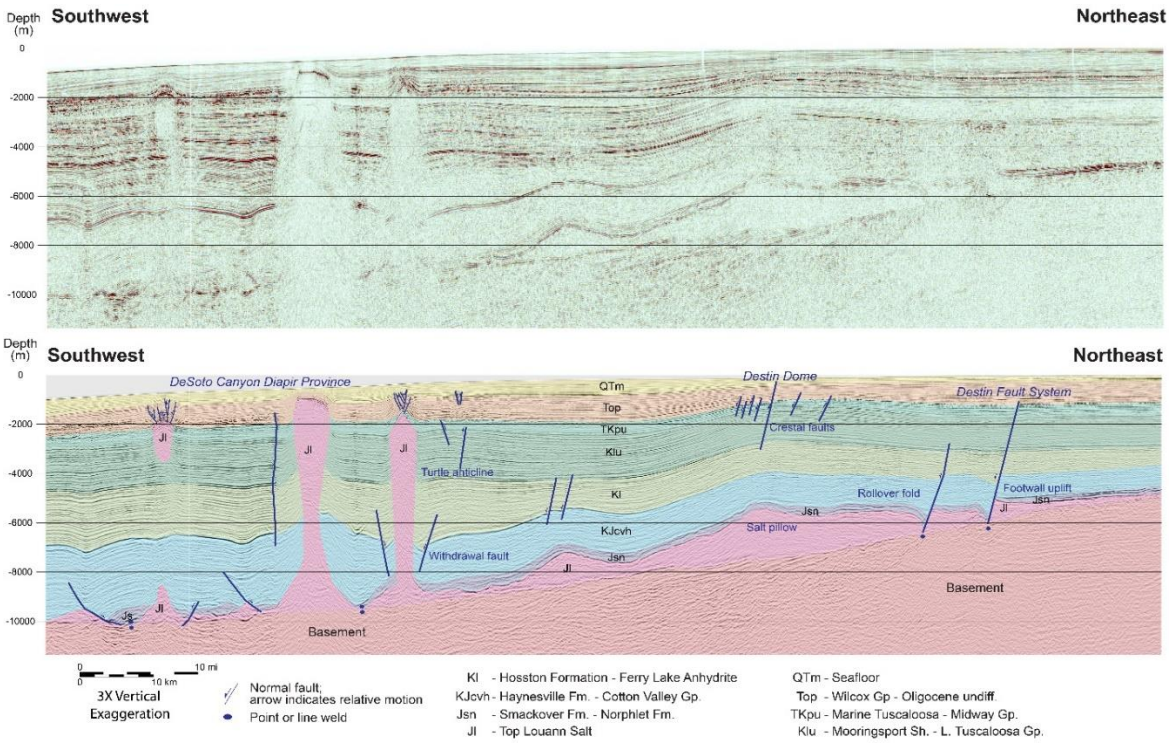

Figure 3.6. Uninterpreted and interpreted seismic profile (Line d8537) showing stratal geometry and structure from the Destin Fault System to the salt diapir province (see Figure 3.1 for location).

3.5.1.2 Central DeSoto Canyon Salt Basin: Peripheral faults, salt pillows, and diapirs

The central DeSoto Canyon Salt Basin exhibits a range of structural styles related to salt tectonics, and strata as young as Paleocene-Miocene are deformed (Figure 3.6). Regional and counterregional faults were observed in this area. Seismic profiles indicate that, in contrast to the salt roller province, the faults composing the Destin Fault System offset Cretaceous and younger strata (Figures 3.5, 3.6). The Destin Fault System contains

a group of normal faults striking northwest-southeast in the northeastern part of the DeSoto Canyon Salt Basin. A group of east-west trending faults is in the north-central part of the salt basin and constitutes the western part of the Destin Fault System. Strata in the central DeSoto Canyon Salt Basin have regional dip of 0.5-0.8° toward the southwest, and structural relief is about 1700-2600 m (Figures 3.7, 3.8).

Basinward of the Destin Fault System, broad salt pillows form the cores of large anticlines (MacRae and Watkins, 1992, 1993; Pashin et al., 2016). Numerous small-displacement normal faults are imaged in the crestal regions of the anticlines, offsetting Cretaceous and younger strata (Figure 3.6). Displacement appears to be greatest (~150 m) in the central parts of the crestal faults in the Lower Cretaceous section, and diminishes toward the tips. A majority of the crestal faults have trace lengths smaller than the spacing between seismic profiles (5 km), and regional and counterregional faults were observed in the seismic surveys (Pashin et al, 2016). Jurassic strata maintain uniform thickness over the crest of the dome, whereas significant thinning of strata over the crest of the dome was observed in younger strata. Destin Dome, which is the largest pillow-cored anticline, is a salient feature in the structural contour map. Structural relief of the Destin Dome decreases upward from about 1,000 m at the top of the Cotton Valley Group (KJcv), to about 600 m in the Midway Group (top TKpu), and is negligible at the modern seafloor.

Salt diapirs are numerous in the central DeSoto Canyon Salt Basin. The diapirs appear to be rooted at the top of basement and terminate in the Cretaceous-

Quaternary section. Height of the diapirs is as great as 8,400 m (Figure 3.6). Reactive and passive diapirs (Hudec and Jackson, 2007) are developed in the lower parts of the structures where salt movement is controlled by extension (Pashin et al., 2016). Normal faults and rim synclines are common near the bases of the diapirs, and maximum fault displacement is about 500 m. The tops of most diapirs represent active piercements (Figure 3.6), where the diapirs have deformed the overburden by extension. Displacement of the faults around diapirs in the Lower Cretaceous section (Klu) is generally less than 180 m, and interpreting the seismic profiles adjacent to the salt bodies is a challenge.

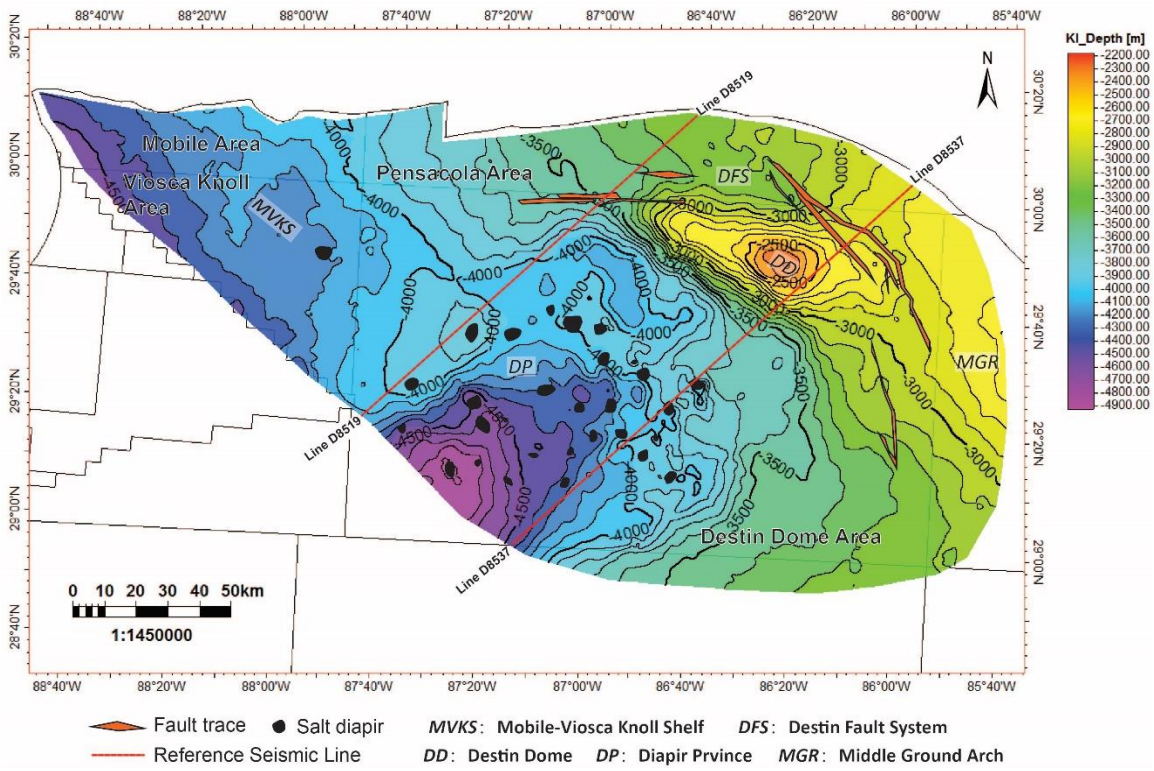

Figure 3.7. Subsea structural contour map of the top of Ferry Lake Anhydrite (top Kl) (contour interval = 100 m).

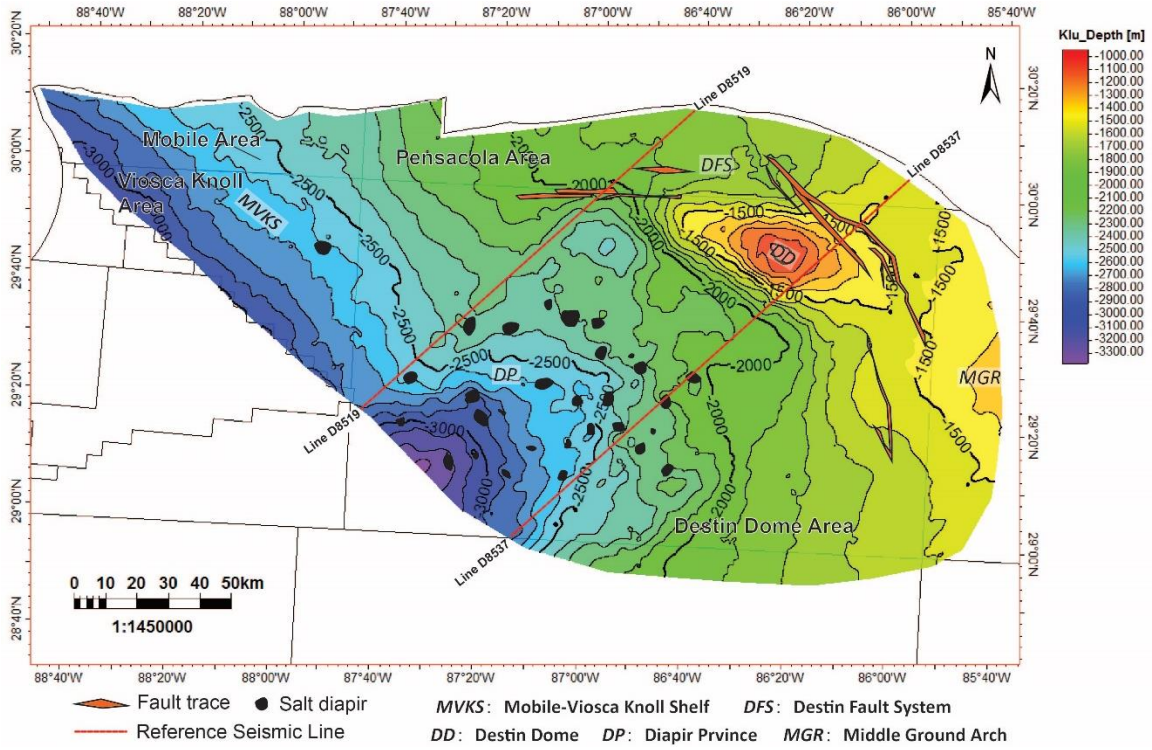

Figure 3.8. Subsea structural contour map of the Base of Marine Tuscaloosa Shale (top Klu) (contour interval = 100 m).

3.5.2 Slip and dilation tendency

Three distinct groups of faults were identified in the Destin Fault System (Figure 3.9). The NW-SE trending faults (faults 1-5, faults 6-7) strike between N. 42° W. and N. 4° E., and most of the faults dip southwest. The E-W trending faults (8-11) strike between N. 88°W. and N. 88° E., and mostly dip south. The majority of the faults dip less than 60°, although some steep fault segments have dip approaching 80° in some areas. Length of the fault traces ranges from 10.7 to 79.4 km, and height ranges from 3.7 to 5.6 km (Table 3.1). Displacement along the faults is greatest at the top of the Louann Salt (900 m), decreases upward in in section, with most faults terminating in or near the

Upper Cretaceous section. Displacement of the faults is ~110 m at the top of the Ferry Lake Anhydrite (top Kl) and decreases to ~50 m at top of the Lower Tuscaloosa Group (top Klu).

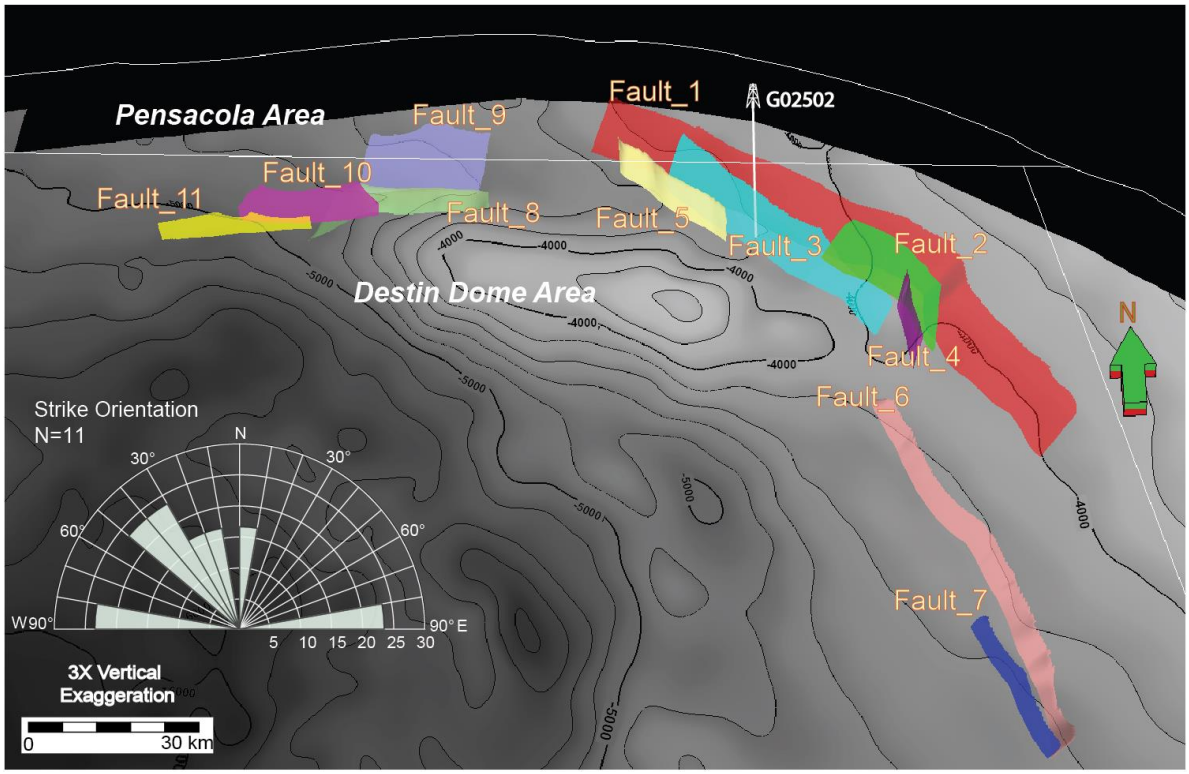

Figure 3.9. 3D visualization of the major faults in the Destin Fault System. Rose diagram showing the fault orientation. Contoured surface is the top of the Knowles Limestone (top KJcvh).

Results of slip and dilation tendency analysis of the faults in the middle part of the Lower Cretaceous section (Paluxy Formation) are shown in Figures 3.10 and 3.11. Analysis of borehole breakouts in the DeSoto Canyon Salt Basin indicates that SH_{max} is

oriented 114° (Meng et al., 2018). The magnitude of the three principal stresses for the Paluxy Formation was estimated at σ_1' = 20 MPa, σ_2' = 16 MPa, and σ_3' = 12 MPa based on the stress gradients calculated by Meng et al. (2018). Slip tendency of the Paluxy Formation is very low, with all of the faults having slip tendency values less than 0.30 out of a possible 1.00. Fault 1 is the largest fault in the study area and has a strike of about N. 55°W. in the northwestern segment and about N. 20°W. in the southeastern segment; multiple strike bends were identified along the fault (Figure 3.9). The northwestern segment of Fault 1 has a slip tendency of 0.26. The southeastern fault segment has a very low slip tendency with typical values on the order of 0.15 and maximum values of about 0.60 (Figure 3.10). Interestingly, major changes in average slip tendency correspond with major strike bends along the fault.

The dilation tendency value of most fault planes is typically higher than 0.30 and is about 0.90 in places with high dip angle (Figure 3.11). Large parts of most faults have dilation tendency greater than 0.50, and the highest dilation tendency values were modeled on faults 3, 5, 10, and 11.

Table 3.1. Fault attributes in the Destin fault system.

Fault Group	Fault Name	Strike Azimuth (°)	Dip (°)	Dip Direction	Length (m)	Height (m)
Group_1	Fault_1	N. 47°W.	40	SW	79,353	4,485
	Fault_2	N. 38°W.	52	SW	13,403	4,380
	Fault_3	N. 40°W.	54	SW	40,265	5,195
	Fault_4	N. 4°E.	62	E	10,763	4,605
Group_2	Fault_5	N. 42°W.	59	NE	21,812	4,633
	Fault_6	N. 13°W.	54	SW	35,808	4,228
	Fault_7	N. 30°W.	40	SW	14,766	3,697
Group_3	Fault_8	N. 82°E.	46	S	25,187	5,556
	Fault_9	N. 87°W.	52	N	17,834	6,167
	Fault_10	N. 88°W.	55	S	20,100	4,935
	Fault_11	N. 88°E.	58	S	22,146	2,892

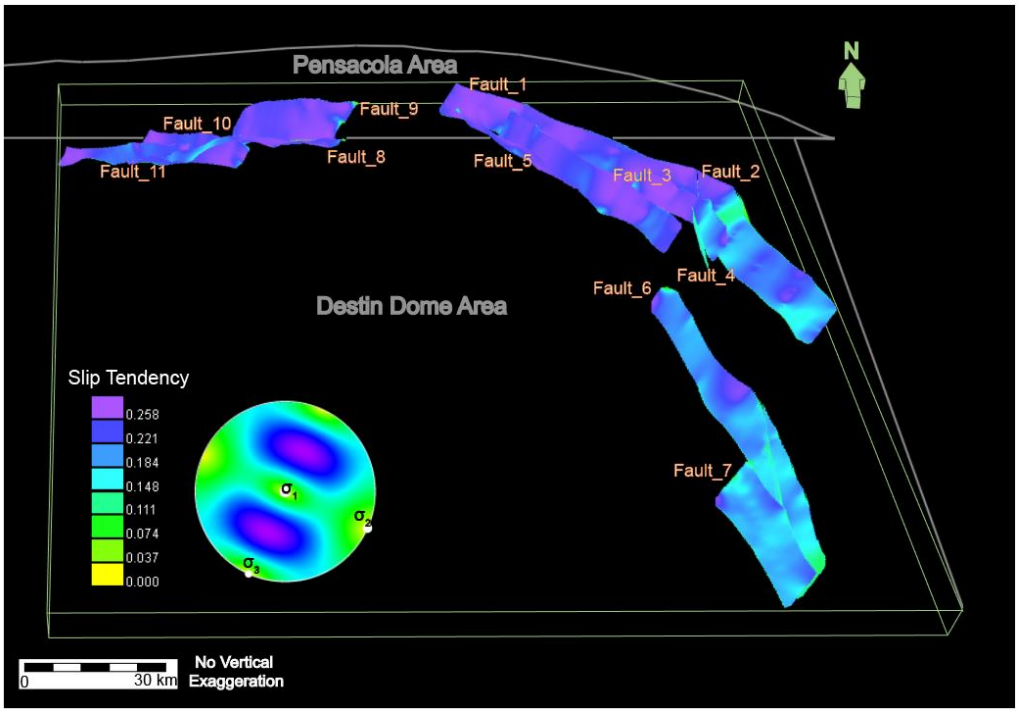

Figure 3.10. 3D visualization of slip tendency of faults in Lower Cretaceous strata in the Destin Fault System. Results indicate that the faults in the DeSoto Canyon Salt Basin are effectively stable with slip tendency less than 0.30.

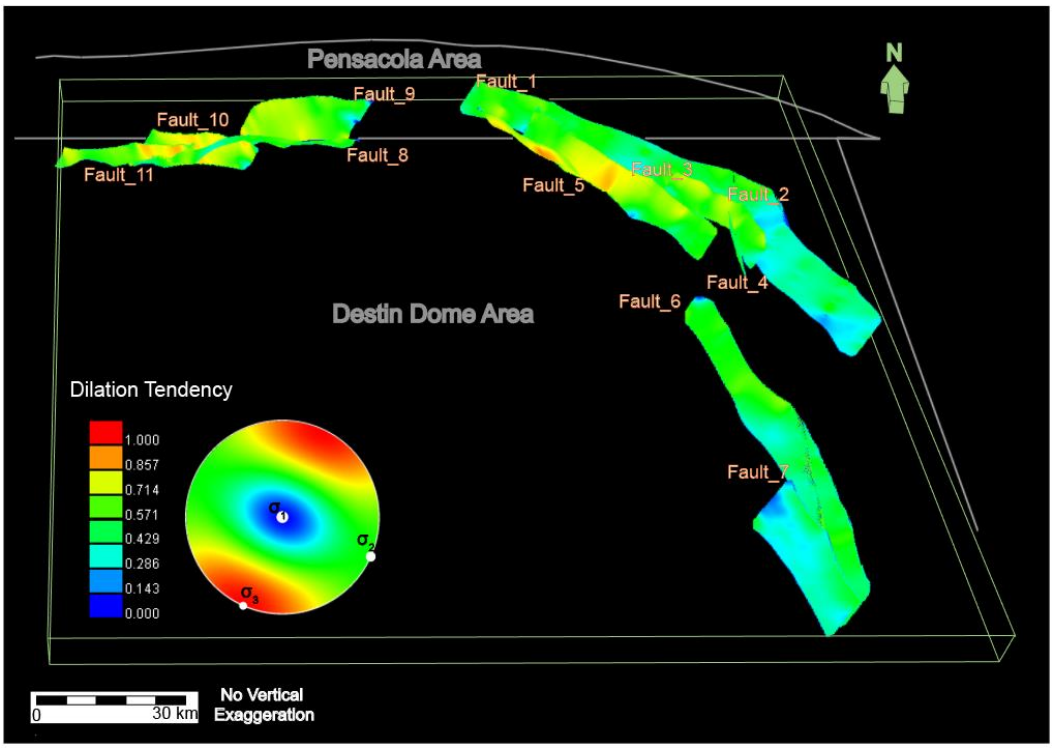

Figure 3.11. 3D visualization of dilation tendency analysis of faults in Lower Cretaceous strata in the Destin Fault System. Results indicate that large parts of most faults in the Destin Fault system have dilation tendency higher than 0.50 and that values locally approach 0.90 in steeply dipping fault segments.

3.5.3 Fault seal analysis

Figure 3.12 shows the fault juxtaposition analysis of an example well (Well G02502) that penetrates the hanging wall block of Fault_1 (Figure 3.9). This diagram provides an estimation of rock types that are juxtaposed as a function of fault throw. The depth of the Paluxy Formation is between 2,559 to 2,607 m. Associated top seals include tight shale and limestone in the Washita-Fredericksburg Interval, and the

bottom seal includes tight limestone in the Mooringsport Formation. The hanging wall-footwall juxtapositions on the diagram include sandstone over sandstone, shale over shale, limestone over limestone, sandstone over shale, and sandstone over limestone. The sandstone over sandstone juxtaposition of the reservoir unit generally occurs where throw is less than 40m. The SGR value was gridded for the sandstone and shale layers along the fault plane (Figure 3.13). Red and orange indicate low SGR, whereas yellow and green indicate high SGR. Results of the SGR analysis show that sandstone-sandstone juxtaposition zones contain SGR values of 18%-45% along the fault plane. The rest of the zones where shale-sandstone juxtaposition and shale-shale juxtaposition are developed along the fault have the SGR values ranging from 48% to 94%.

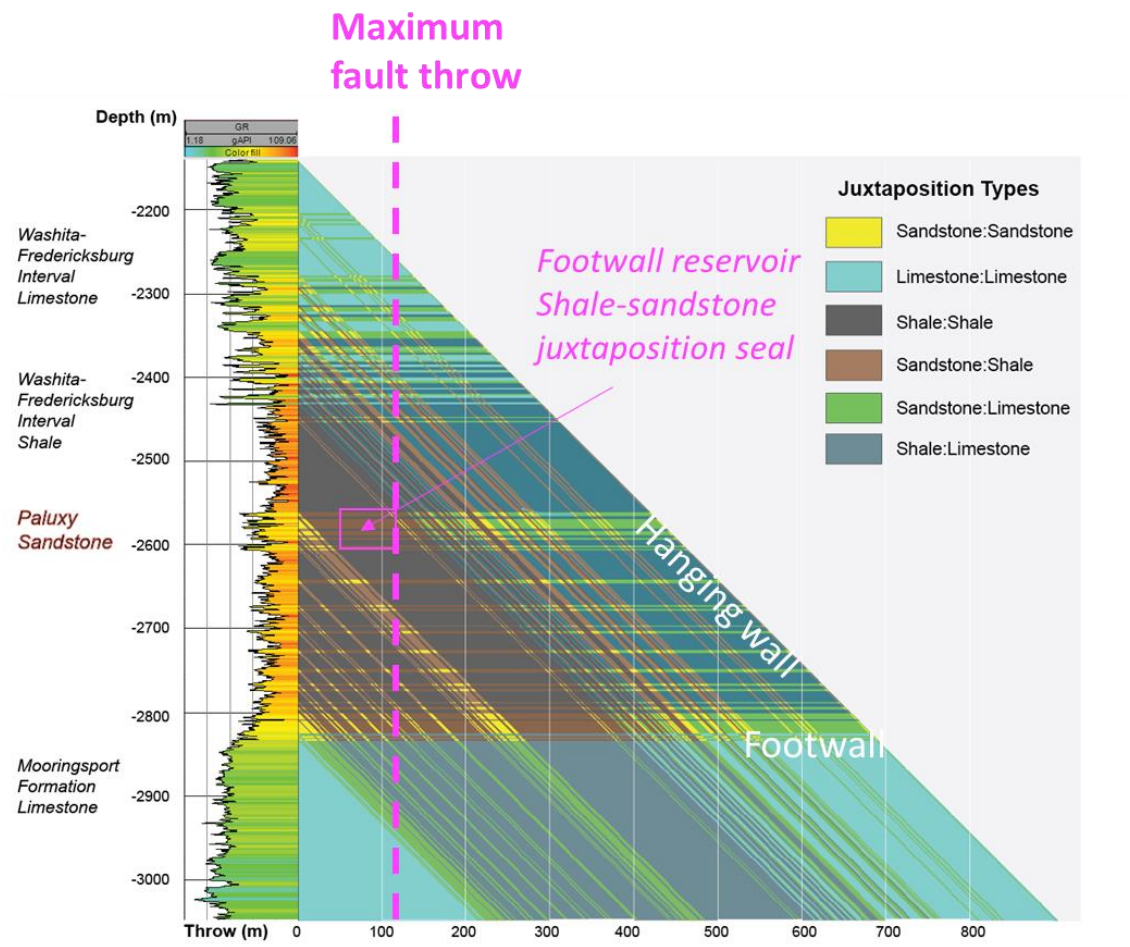

Figure 3.12. Fault juxtaposition triangle diagram showing the juxtaposition relationship of Paluxy reservoir and associated seals.

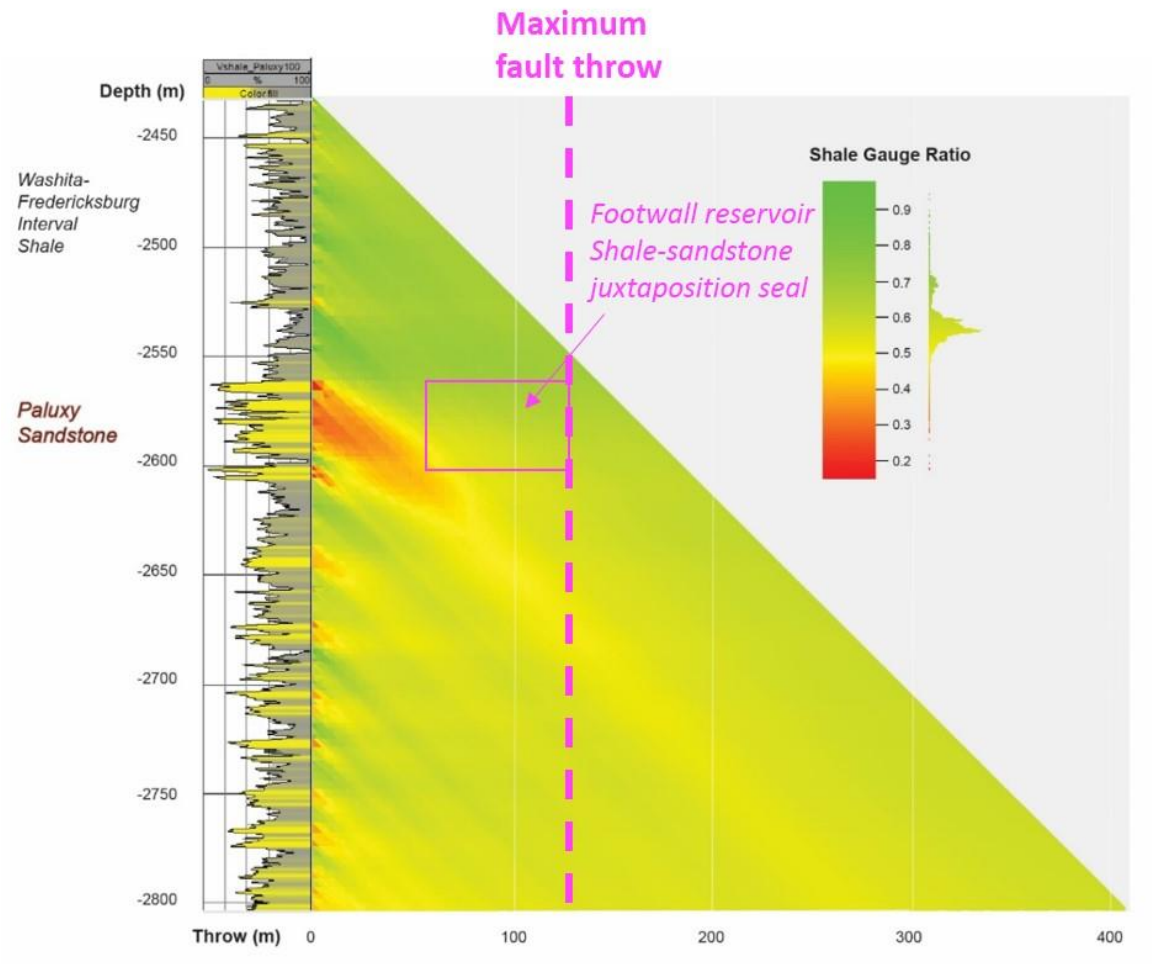

Figure 3.13. SGR value of the Paluxy sandstone and associated shale seals along the fault plane. Sandstone and shale are labelled grey and yellow, respectively.

3.6 Discussion: Leakage risk and recommendations for CO_2 storage

Analysis of the structural framework indicates that the structural style of Cretaceous strata is variable and is most complex in the Destin Fault System and the Salt Diapir province of the eastern DeSoto Canyon Salt Basin. In the Mobile and Viosca Knoll Areas in the western part of the salt basin, salt rollers are developed mainly in the

Jurassic section, and imageable deformation of Cretaceous and younger strata is limited to subtle folds and local diapirism. The four-way structural closure in the western Destin Dome Area may help trap CO_2 at multiple structural levels from the Paluxy Formation and Washita-Fredericksburg interval (Klu) through the top of the lower Tuscaloosa group (Klu). In the northeastern DeSoto Canyon Salt Basin, the Destin Fault System offsets Jurassic through Upper Cretaceous strata. Basinward of the Destin Fault System, anticlines are developed above broad salt pillows, and faults are imaged in Jurassic and Cretaceous strata in the crestal regions of the structures and thus pose potential risks for cross-formational migration of CO_2 along the fault planes. The diapir province in the heart of the salt basin contains numerous salt diapirs and associated folds and faults, including withdrawal synclines, reactive faults, and crestal graben systems that deform Jurassic through Neogene strata and also pose potential cross-formational migration risk.

Previous research indicates that porous sandstone of Cretaceous-Neogene age provides the major storage opportunities in the DeSoto Canyon Salt Basin (Chandra, 2018). Potential storage reservoirs in the Cretaceous section are intercalated with and overlain by thick (200-425 m) successions of shale and nonporous carbonate, which form baffles, barriers, and regional seals for potential carbon storage (Chandra, 2018; Figure 3.3). Considering the lack of faults in these strata in the western part of the salt basin, the stable shelf areas of the Mobile and Viosca Knoll Areas provide favorable storage opportunities.

Cross-formational migration of injected CO_2 could conceivably occur through natural (e.g., subseismic faults), or manmade pathways (e.g., wells). Most wells penetrating the Cretaceous section were drilled in search of petroleum objectives in the Jurassic section, and multiple casing strings are typical of wells penetrating the Jurassic Cretaceous section, even in dry holes (Chandra, 2018). Shallow petroleum objectives are mainly in Miocene strata (Smith and Mink, 1997, 1998). Vertical fractures, such as orthogonal joints, have not been observed in cores from sandstone and shale units in the Cretaceous section in onshore areas (e.g., Koperna et al., 2009, 2012; Pashin et al., 2014; Folaranmi, 2015). Accordingly, the greatest risk of leakage of injected CO_2 from storage reservoirs in the DeSoto Canyon Salt Basin is along faults and fault-related fractures.

During injection, an increase of pore pressure will increase the tendency of a pre-existing fault and associated fractures in the caprock to slip or open, thereby forming a potential fluid migration pathway (Hawkes et al., 2005). Therefore, it is essential to devise injection strategies that maintain pressure below the minimum horizontal stress at all times (Meng et al., 2018). Slip tendency values tend to be lower than 0.30 (Figure 3.10), indicating that the risk of fault movement during injection is low. Major changes of slip tendency correspond with bends of fault strike. In general, faults striking close to SH_{max} (114°) have higher slip tendency than those that are oblique to SH_{max}.

Dilation tendency values commonly exceed 0.50, and so the risk of fault dilation is substantially higher than that of slippage (Figure 3.11). Zones with dilation tendency approaching 0.90 occur along some steeply dipping fault segments. Where fault dip is relatively low, overburden stress (Sv) impedes slippage and dilation, but where a fault approaches vertical, only the lesser horizontal stresses (SH_{max}, Sh_{min}) impede slippage and dilation (Ferrill et al., 1999). Indeed, in regions under active tension, Sh_{min} may actually promote dilation. Accordingly, injection programs should avoid pressurizing faults to help ensure safe storage by minimizing the probability of slip and dilation. In the Cretaceous-Neogene section, this means that caution should be applied near the peripheral faults of the Destin Fault System and the crestal faults in anticlines above the major salt pillows.

The diapir province in the heart of the salt basin has yet to be tested for hydrocarbon potential, and potential may exist for storage in Cretaceous strata flanking the diapirs. The faulted strata atop the diapirs may contain targets for petroleum exploration, but close fault spacing combined with the potential for fault dilation appear to make shallow targets above the diapirs questionable objectives for subseafloor CO_2 storage. Although it is not feasible to map and analyze reactivation tendency in such localized fault systems with the available data, faults that strike along SH_{max} and dip steeply are predicted to pose elevated risk of slip or dilation.

Based on the results of the fault seal analyses, a conceptual 3D model was built to display the potential sealing properties of faults in the DeSoto Canyon Salt Basin

(Figure 3.14). Fault juxtaposition analysis indicates that there are multiple juxtaposition types occurring at the fault planes. According to the 1D juxtaposition result, a sandstone-sandstone juxtaposition occurs where fault throw is less than 40m. Fault throw in Cretaceous formations is less than the fault throw at Ferry lake Anhydrite (110 m). A sandstone-sandstone juxtaposition may facilitate migration of injected CO_2 across or into the fault zone (Figure 3.14). Rock seal analysis shows the SGR value of the Paluxy sandstone ranges from 18% to 45%. The high SGR zones of the fault plane have potential for sealing by clay smear, whereas the low SGR zones have high risk of migration into the fault zone and across the fault. Therefore, significant caution is required when considering injecting CO_2 near faults, especially where sandstone-sandstone juxtapositions are developed.

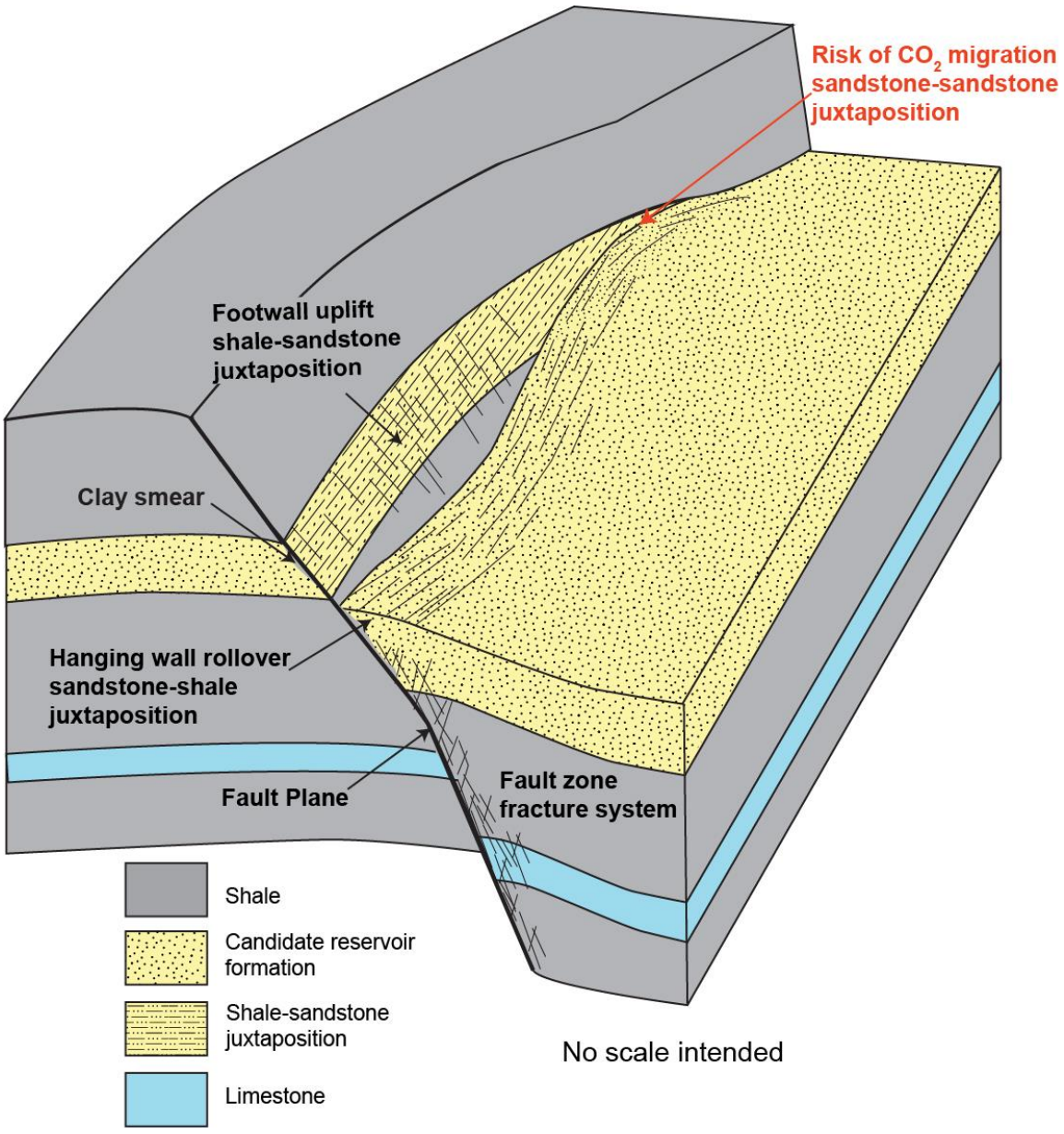

Figure 3.14. Conceptual 3D model showing the seal properties of Fault (modified from Pashin et al., 2000).

When a sand layer in a footwall is juxtaposed with a shale bed or clay smear, the fault will tend to act as a barrier to flow. In the area of the Destin Fault System, hanging-

wall rollover provide a closure at the crest of the rollover fold, where it is suitable for carbon storage. The footwall uplifts also provide prospective reservoirs. Indeed, many traps in the east Gulf of Mexico region are in footwall uplifts (Qi et al., 1998; Pashin et al., 2000). Favorable injection sites are located at these structures where shale-sandstone juxtapositions exist. However, for faults with high dilation tendency, reactivation of the fault by CO_2 injection could affect the clay content along the fault plane. Fault shear and opening process may produce a segment of the clay smear (Vrolijk et al., 2016), particularly where reservoir strata in the footwalls are juxtaposed with clay smear in the hanging walls, thus increasing the risk of migration out of zone. Therefore, further research needs to focus on characterizing and simulating the physical and hydraulic properties of the fault damage zone during CO_2 injection process, and its influence on fluid migration pathways. Additional high resolution seismic survey and geophysical well survey are therefore suggested for establishing geological storage potential adjacent the Destin Fault system. Strata in the hanging wall section is thicker than that in the footwall due to the synsedimentary growth, thus affectting the juxtaposition relationship along the fault. Hence, it is also essential to model the 3D fault zone facies distribution and seal properties and incorporating synsedimentary fault growth into the analysis.

3.7 Conclusions

Variable structural styles exist in the DeSoto Canyon Salt Basin in the east-central Gulf of Mexico Area. Understanding the structural styles and how they affect the CO_2 storage is essential for ensuring safe carbon storage and minimizing the risk of gas migration from the storage complex. The stable shelf of the Mobile and Viosca Koll Areas, and the four-way structural closure in the western Destin Dome Area can help trap CO_2 at multiple structural levels from the Cretaceous strata, which provide favorable storage opportunities. The Destin Fault System, salt pillows, salt diapirs, and the associated faults form a structurally complex zone in the Basin. Three groups of peripheral faults and multiple small-scale crestal faults occur at top of the pillow-cored anticlines pose potential risks for cross-formational migration of CO_2 along the fault planes.

Eleven major faults were mapped in the Destin Fault System for reactivation tendency analysis. The slip tendency of those faults in the Paluxy Reservoir is very low overall with slip tendency values less than 0.30. Dilation tendency of those faults is relatively high, with an average value around 0.50 and maximum values approaching 0.90 in steeply dipping fault segments. Faults that strike along SH_{max} and dip steeply (approaching vertical) are predicted to pose elevated risk of slip or dilation, particularly in steep fault segments where lithostatic stress may be insufficient to keep faults closed during nearby injection operations.

Significant caution is required when considering injecting CO_2 near the Destin Fault system, especially where sandstone-sandstone juxtapositions are developed. Favorable CO_2 injection sites with minimal gas migration risk in faulted areas are located in hanging-wall rollover folds and in footwall uplifts that are sealed by shale-sandstone juxtapositions. Further geomechanical, pressure, and flow simulation of the potential reservoirs and seals in structurally complex regions.

References

Allan, U.S., 1989. Model for hydrocarbon migration and entrapment within faulted structures. AAPG Bulletin 73, 803-811.

Bouvier, J.D., Kaarssijpesteijn, C. H., Kluesner, D. F., Onyejekwe, C. C., Vanderpal, R. C., 1989. Three-dimensional seismic interpretation and fault sealing investigations, Nun River Field, Nigeria. AAPG Bulletin 73, 1397-1414.

Buffler, R.T., Sawyer, D.S., 1983. Distribution of crust and early history, Gulf of Mexicobasin. Gulf Coast Association Geological Society Transcripts 35, 334–344.

Bretan, P., Yielding, G., Mathiassen, O. M., and Thorsnes, T., 2011. Fault-seal analysis for CO_2 storage: an example from the Troll area, Norwegian Continental Shelf. Petroleum Geoscience 17, 181-192.

Chandra, A., 2018. Geological Characterization and CO_2 Storage Potential of Cretaceous Sandstone in the DeSoto Canyon Salt Basin of the MAFLA Shelf. Master's thesis: Oklahoma State University.

Charbonneau, P., 2018. Geologic framework for the assessment of offshore CO_2 storage resources in the West Florida Platform: Master's thesis. Oklahoma State University.

Dobson, L.M., Buffler, R.T., 1991. Basement rocks and structure, northeastern Gulf of Mexico. GCAGS Transactions 41, 191-206.

Dobson, L.M., Buffler, R.T., 1997. Seismic stratigraphy and geologic history of Jurassic rocks, northeastern Gulf of Mexico. AAPG Bulletin 81. 100-120.

Ferrill, D. A., Winterle, J., Wittmeyer, G., Sims, D., Colton, S., Armstrong, A., Morris, A. P., 1999. Stressed rock strains groundwater at Yucca Mountain, Nevada. GSA Today 9, 1-8.

Folaranmi, A. T., 2015. Geologic characterization of a saline reservoir for carbon sequestration: The Paluxy Formation, Citronelle Dome, Gulf of Mexico Basin, Alabama. Master's thesis, Oklahoma State University.

Farseth, R.B., Johnsen, E. Sperrevik, S., 2007. Methodology for risking fault seal capacity: Implications of fault zone architecture. AAPG Bulletin 91, 1231-1246.

Foxford, K.A., Walsh, J.J., Watterson, J., Garden, I.R., Guscott, S.C., Burley, S.D. ,1998. Structure and content of the Moab Fault Zone,Utah, USA, and its implications for fault seal prediction. In:Jones, G.,Fisher, Q.J. & Knipe, R.J. (eds)Faulting, Fault Sealing and FluidFlow in Hydrocarbon Reservoirs. Geological Society, London, Special Publications 147, 283–297.

Galloway, W. E., 2008, Depositional evolution of the Gulf of Mexico sedimentary basin. Elsevier, Sedimentary Basins of the World 5, 505-549.

Goodman, A., Hakala, A., Bromhal, G., Deel, D., Rodosta, T., Frailey, S., Small, M., Allen, D., Romanov, V., Fazio, J., 2011. US DOE methodology for the development of geologic storage potential for carbon dioxide at the national and regional scale. International Journal of Greenhouse Gas Control 5, 952-965.

Hawkes, C. D., Bachu, S., Haug, K., Thompson, A., 2005. Analysis of in-situ stress regime in the Alberta Basin, Canada, for performance assessment of CO_2 geological

sequestration sites, *in* Proceedings Fourth Annual Conference on Carbon Capture and Sequestration, 2-5.

Hudec, M. R., Jackson, M. P., 2007. Terra infirma: Understanding salt tectonics: Earth-Science Reviews 82, 1-2, 1-28.

Hunt, B., Robinson, D. M., Weislogel, A. L., Ewing, R. C., 2017. Sediment source regions and paleotransport of the Upper Jurassic Norphlet Formation, eastern Gulf of Mexico. AAPG Bulletin 101, 1519-1542.

Knipe, R.J., 1997. Juxtaposition and seal diagrams to help analyze fault seals in hydrocarbon reservoirs. AAPG bulletin 81, 187-195.

Knipe, R.J., Jones, G. Fisher, Q.J., 1998. Faulting, fault sealing and fluid flow in hydrocarbon reservoirs: an introduction. Geological Society, London, Special Publications 147, vii-xxi.

Koperna, G., Riestenberg, D., Kuuskraa, V., Rhudy, R., Trautz, R., Hill, G.R., Esposito, R., 2012. The SECARB anthropogenic test: a US integrated CO_2 capture, transportation and storage test. International Journal of Clean Coal and Energy 1, 13-26.

Koperna, G., Riestenberg, D., Petrusak, R., Esposito, R., Rhudy, R., 2009. Lessons learned while conducting drilling and CO_2 injection operations at the Victor J. Daniel power plant in Mississipp. SPE 124003. 2009 SPE Annual Technical Conference and Exhibition Proceedings, New Orleans, 4-7.

Lindsay, N.G., Murphy, F.C., Walsh, J.J., Watterson, J., Flint, S. Bryant, I.D., 1993. Outcrop studies of shale smears on fault surfaces. The geological modelling of hydrocarbon reservoirs and outcrop analogues 15, 113-123.

MacRae, G., Watkins, J. S., 1992. Evolution of the Destin Dome, offshore Florida, north-eastern Gulf of Mexico. Marine and petroleum geology 9, 501IN1505-1504IN2509.

MacRae, G., Watkins, J. S., 1993. Basin architecture, salt tectonics, and Upper Jurassic structural styles, DeSoto Canyon salt basin, northeastern Gulf of Mexico. AAPG Bulletin 77, 1809-1824.

MacRae, G., Watkins, J.S., 1996, DeSoto Canyon salt basin: Tectonic evolution and salts [sic] structural styles, in Jones, J.O., and Freed, R.L., eds., Structural framework of the northern Gulf of Mexico. GCAGS Special Publication, 53-61.

Meng, J., Pashin, J.C., Nygaard, R., Chandra, A., 2018. Analysis of the stress field in the DeSoto Canyon Salt Basin for ensuring safe offshore carbon storage. International Journal of Greenhouse Gas Control 79, 279-288.

Mancini, E.A., Mink, R.M., Bearden, B.L., and Wilkerson, R.P., 1985. Norphlet Formation (Upper Jurassic) of southwestern and offshore Alabama: Environments of deposition and petroleum geology. AAPG Bulletin 69, 881-898.

Martin, R.G., 1978. Northern and eastern Gulf of Mexico continental margin stratigraphic and structural framework: AAPG Studies in Geology 7, 21-42.

Morris, A., Ferrill, D. A., and Henderson, D. B., 1996. Slip-tendency analysis and fault reactivation: Geology 24, 275-278.

Nwafor, E., 2013. Crustal structure of the eastern Gulf of Mexico, Master thesis: The University of Alabama.

Pashin, J.C., Raymond, D.E., Alabi, G.G., Groshong, R.H., Jr., and Guohai Jin, 2000. Revitalizing Gilbertown oil field: Characterization of fractured chalk and glauconitic sandstone reservoirs in an extensional fault system. Alabama Geological Survey Bulletin 168, 81 p.

Pashin, J.C., M.R. McIntyre-Redden, G. Jin, S.D. Mann, 2014. Site Characterization for CO_2 Storage from Coal-fired Power Facilities in the Black Warrior Basin, Alabama. Geological Survey of Alabama Open File Report 1401, 154 p.

Pashin, J. C., Jin, G., Hills, D. J., 2016. Mesozoic Structure and Petroleum Systems in the DeSoto Canyon Salt Basin in the Mobile, Pensacola, Destin Dome, and Viosca Knoll Areas of the MAFLA Shelf. *in* Proceedings 35th Annual Gulf Coast Section SEPM (GCSSEPM) Foundation Bob F. Perkins Research Conference, Houston, Texas, 315-340.

Petty, A.J., 1995. Ferry Lake, Rodessa, and Punta Gorda Anhydrite Bed Correlation, LowerCretaceous, Offshore Eastern Gulf of Mexico. Gulf Coast Association of Geological Societies Transactions 45, 487–495.

Petty, A. J., 1997. Lower Tuscaloosa clastic facies distribu-tion (Upper Cretaceous), federal and state waters, east-ern Gulf of Mexico. GCAGS Transactions 47, 453–462.

Pindell, J., Kennan, L., 2001. Kinematic evolution of the Gulf of Mexico and Caribbean, *in* Proceedings Petroleum Systems of Deepwater Basins. GCSSEPM 21st Annual Bob F. Perkins Research Conference Proceedings, 193-220.

Pindell, J. L., 1985. Alleghenian reconstruction and subsequent evolution of the Gulf of Mexico, Bahamas, and Proto-Caribbean. Tectonics 4, 1-39.

Qi, J., Pashin, J.C., and Groshong, R.H., Jr., 1998. Structure and evolution of North Choctaw Ridge Field, Alabama, a salt-related footwall uplift along the peripheral fault system, Gulf Coast basin. GCAGS Transactions 48, p. 349-359.

Roberts-Ashby, T. L., Brennan, S. T., Merrill, M. D., Blondes, M. S., Freeman, P., Cahan, S. M., DeVera, C. A., Lohr, C. D., 2015. Geologic framework for the national assessment of carbon dioxide storage resources– South Florida Basin: Chapter L in Geologic framework for the national assessment of carbon dioxide storage resources. US Geological Survey, 2331-1258.

Roberts, G., Erickson, J., 2009. The Norphlet sandstone and other petroleum plays along and outboard of the Florida Escarpment, eastern Gulf of Mexico. Spectrum Geo Technical Paper, 6 p.

Sandwell, D. T., Müller, R. D., Smith, W. H., Garcia, E., Francis, R., 2014. New global marine gravity model from CryoSat-2 and Jason-1 reveals buried tectonic structure. Science 346, 65-67.

Smith, C. C., 1991. Foraminiferal biostratigraphic framework, paleoenvironments, rates of sedimentation, and geologic history of the subsurface Miocene of southern

Alabama and adjacent state and federal waters. Geological Survey of Alabama, 223 p.

Smith, C. C., Mink, R. M., 1997. Upper Miocene Dauphin natural gas sands in offshore Alabama. Gulf Coast Association of Geological Societies Transactions 47, 541-548.

Smith, C. C., Mink, R. M., 1998. Middle and upper Miocene natural gas sands of onshore and coastal Alabama. Gulf Coast Association of Geological Societies Transactions 48, 417-422.

Southern States Energy Board, 2013. Preliminary Evaluation of Offshore Transport and Geologic Storage of Carbon Dioxide, 110 p.

Story, C., 1998. Norphlet geology and 3-D geophysics of Fairway field, Mobile Bay, Alabama, in Allen, J.L., and others, eds., 3-D seismic case histories from the Gulf Coast basin. Austin, Texas, GCAGS, 123-129.

Tew B. H., Mink R. M., Mann S. D., Bearden B. L., Mancini E. A., 1991. Geologic framework of Norphlet and pre-Norphlet strata ofthe onshore and offshore eastern Gulf of Mexico area, Trans. Gulf Coast Assn. Geol. Soc. 41, 590–600.

Van der Zee, W., Urai, J.L., 2005. Processes of fault evolution in asiliciclastic sequence: a case study from Miri, Sarawak, Malaysia. Journal of Structural Geology 27, 2281–2300.

Vail, P.R., 1987. Seismic stratigraphy interpretation procedure. In:Bally, A.W. (Ed.), Atlas of Seismic Stratigraphy 27. AAPG Studies in Geology, 1–10.

Vrolijk, P. J., Urai, J. L., Kettermann, M., 2016, Clay smear: Review of mechanisms and applications. Journal of Structural Geology 86, 95-152.

Yielding, G., Freeman, B. Needham, T., 1997. Quantitative fault sealprediction. AAPG Bulletin 81, 897–91

Yielding, G., 2002. Shale Gouge Ratio – calibration by geohistory.In:Koestler, A.G. & Hunsdale, R. (eds)Hydrocarbon Seal Quantification.Norwegian Petroleum Society (NPF) Special Publication, Elsevier, Amsterdam 11, 1–15.

Zoback, M. D., 2010. Reservoir geomechanics, first ed. Cambridge University Press, Cambridge.

CHAPTER IV

PAPER III: GEOMECHANICAL CHARACTERISTICS OF POTENTIAL CO_2 STORAGE RESERVOIRS, DESOTO CANYON SALT BASIN, EASTERN GULF OF MEXICO

4.1 Abstract

Recent studies indicate vast storage capacity exists in Cretaceous and Paleocene-Miocene sandstones in the eastern Gulf of Mexico. Understanding the geomechanical integrity of reservoirs and associated seals is very useful for reducing the risk of migration of injected CO_2 out of the storage complex. Rock mechanical properties and reservoir-seal integrity of three potential reservoir units were analyzed using geophysical well logs. Geomechanical analysis shows the Cretaceous reservoir units contain competent carbonate caprocks that arrest the fracture propagation from injection. Results of the reservoir and seal integrity analyses indicate all three potential reservoirs and associated seals are geomechanically stable. Injection pressure of CO_2 should keep below the minimum horizontal stress to prevent the occurrence of tensile hydraulic fractures. Combined with structural framework and reservoir property studies,

the Lower Tuscaloosa sandstone reservoir is a target for long-term commercial carbon storage.

Future work should focus on geomechanical simulation of the reservoir units and other leakage risk assessment to further ensure safe carbon storage during and after CO_2 injection. Laboratory tri-axial tests are recommended in the future to confirm the accuracy of the UCS correlations for the DeSoto Canyon Salt Basin.

4.2 Introduction

The study area for this research encompass the offshore Mississippi-Alabama-Florida shelf and is part of Central and Eastern Gulf of Mexico (GOM) planning areas of the Bureau of Ocean Energy Management (BOEM) (Figure 4.11). Recent studies indicate that vast storage capacity exists in Cretaceous and Paleocene-Miocene sandstone (Chandra, 2018; Charbonneau, 2018; Pashin et al., 2018). The sandstone reservoirs are overlain by thick sections of shale, limestone and chalk, which form regionally extensive seals. Volumetric assessment of the Creataceous reservoirs show gigatonne (Gt) class storage capacity. Each offshore block of the study area can store an average of 69 megatonnes (Mt) of CO_2 in Cretaceous strata, which is equivalent to annual CO_2 emissions from 13 major coal-fired power plants (Chandra, 2018).

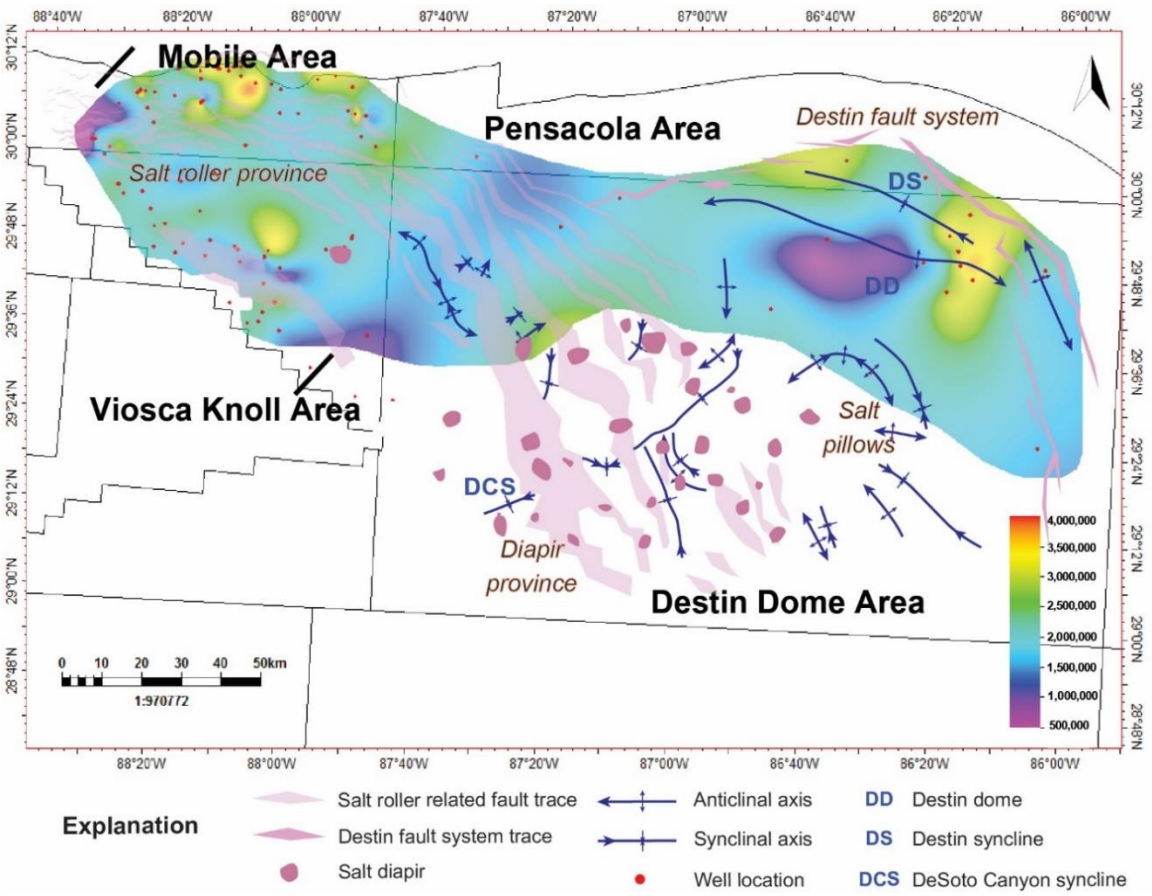

Figure 4.1 Map showing the key structural elements and cumulative storage resource map of the DeSoto Canyon Salt Basin (Paluxy Formation, Washita-Fredericksburg interval and lower Tuscaloosa Group). Contour interval = 500,000 tonnes/km^2 (modified from Pashin et al., 2016; Chandra, 2018).

Ensuring safe, permanent storage of CO_2 is vital for the success of subsurface geologic CO_2 storage projects. Determination of the in-situ stress field and geomechanical properties of the potential storage units can be very useful for testing whether the injection operations can be conducted in a safe, environmentally responsible manner, and therefore facilitates effective long-term storage of CO_2 (Haug

et al., 2007, Meng et al., 2018). Three main potential leakage mechanisms are identified to be associated with the carbon storage process (Hawkes et al., 2004, 2005). They are: 1) poor cement emplacement in enlarged boreholes; 2) reactivation of the existing faults; and 3) induced shear and tensile fracture of the caprock (Figure 4.2). Previous research has estimated the in-situ stress field in the DeSoto Canyon Salt Basin (Meng et al., 2018). To the author's knowledge, no comprehensive research has been performed in the DeSoto Canyon Salt Basin regarding the geomechanical aspects of potential CO_2 storage. Additionally, no core samples are available for laboratory testing. To help fill this gap, the purpose of this study is to evaluate the geomechanical integrity of reservoirs and seals using the available empirical methods. This analysis provides insight on determining the seal integrity for each potential reservoir unit.

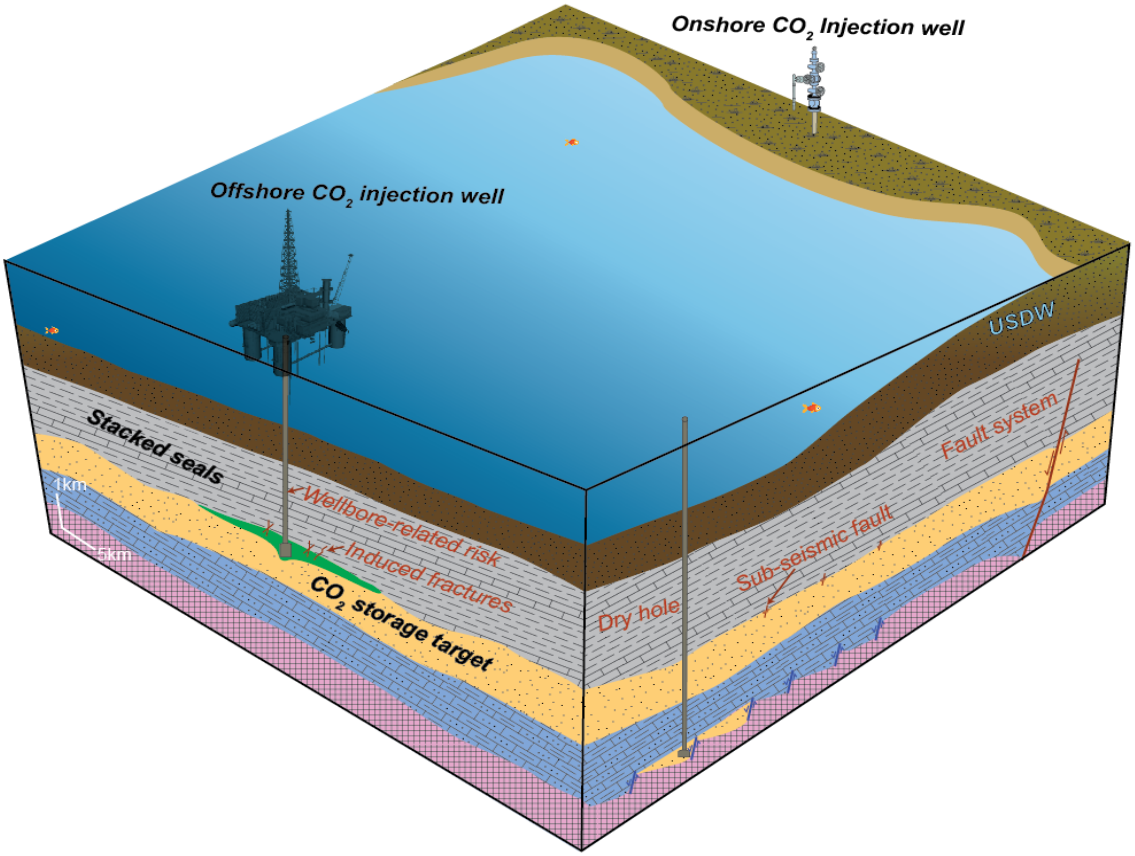

Figure 4.2. Conceptual model showing possible leakage risks controlled by geomechanical factors in the western DeSoto Canyon Salt Basin (modified from Hawkes et al., 2005; Meng et al., 2017).

4.3 Geological Background

4.3.1 Study Area

The DeSoto Canyon Salt Basin is located offshore of Mississippi, Alabama, and the western Florida Panhandle, and is part of the Gulf of Mexico continental shelf. During Mesozoic to Cenozoic, the Gulf of Mexico basin formed by rifting and drifting as a result of extension and isostatic adjustment of the crust as the Yucatan block rotated

counterclockwise relative to North America (Buffler and Sawyer, 1985; Pindell, 1985; MacRae and Watkins, 1993; Pindell and Kennan, 2001; Sandwell et al., 2014). Strata in the study area include a thick succession of Mesozoic and Cenozoic siliciclastic rocks, carbonate rocks, and evaporites, which were deposited in a broad sedimentary wedge that was deposited upon extended Paleozoic basement (Figure 4.3, Galloway, 2008; Pashin et al., 2016). The Desoto Canyon Salt Basin contains four distinctive structural provinces, including the Destin fault system, the salt pillow province, the salt diapir province, salt roller province (Figure 4.1, Pashin et al., 2016).

4.3.2 Onshore and offshore storage potential

Numerous studies have assessed the potential for onshore CO_2 storage in the Southeastern U.S. (Pashin et al., 2008; Koperna et al., 2009; Esposito et al., 2010; Koperna et al., 2012).The onshore Southeastern Regional Carbon Sequestration Partnership (SECARB) test at Plant Daniel in southeast Mississippi evaluated the lower Tuscaloosa Group as a highly porous and permeable storage target sealed by the Marine shale of the Tuscaloosa Group (Koperna et al., 2009; Petrusak et al., 2009). The SECARB III Anthropogenic test of the Citronelle Field in southwest Alabama also proved the potential of the Paluxy Formation to store commercial quantities of anthropogenic CO_2 (Pashin et al., 2008; Folaranmi, 2015). The primary confining unit above the Paluxy Formation is the basal shale of the Washita-Fredericksburg interval, and secondary seals higher in the section provide additional storage security and include the marine shale of

the Tuscaloosa Group, the chalk of the Selma Group, and the basal mudstone of the Midway Group.

Previous studies identified several potential reservoir units in Cretaceous strata, including the Paluxy Formation, the Washita-Fredericksburg interval, Lower Tuscaloosa Group, and Paleocene-Miocene sandstones. Paluxy sandstone bodies are 15-115 m (50-370 ft) thick with porosity commonly exceeding 20%, and are sealed by thick succession of shale and tight limestone in the Washita-Fredericksburg interval (Figure 4.3a). The Washita-Fredericksburg Interval contains minor amounts of reservoir quality sandstone, and stacked sandstone layers have net thickness of 0-40 m (0-120 ft). Lower Tuscaloosa sandstone thickness ranges from 30-100 m (100-300 ft) with porosity commonly exceeding 15%. The Marine shale of the Tuscaloosa Group contains a thick section of shale that overlies lower Tuscaloosa sandstone and forms a regionally extensive reservoir seal (Figure 4.3b). Additionally, the Cretaceous reservoirs are also confined regionally by the chalk of the Selma Group and the basal mudstone of the Midway Group. Multiple sandstone intervals have been recognized in the Paleocene-Miocene section, and the individual sandstone intervals range from 10-80 ft (3-25m) in thickness and are overlain by shale and chalky limestone of Paleocene-Miocene age. The porosity of the Paleocene-Miocene sandstone commonly exceeds 30% (Figure 4.3c). The Paleocene-Miocene sandstone units contain natural gas reservoirs in the region that are sealed by thick shale units (Smith, 1991). The storage resource of the Paluxy Formation is concentrated largely in salt withdrawal synclines in the Destin Dome structural province. By comparison, the storage resource of the Washita-Fredericksburg interval

and the Lower Tuscaloosa Group is concentrated mainly in the Mobile and Viosca Koll Areas (Figure 4.11). Volumetric assessment indicates that 28 Gt of P_{50} storage capacity exists in the Cretaceous storage units (Chandra, 2018).

4.3.3 Stress and pressure in the reservoir

Stress in the earth is defined by three mutually perpendicular principal stresses ($\sigma_1 > \sigma_2 > \sigma_3$). When discussing a subsurface reservoir, these stresses are typically called vertical stress (Sv), maximum horizontal stress (SH_{max}), and minimum horizontal stress (Sh_{min}). Another important stress parameter is pore pressure (Pp), which is the pressure exerted by fluids within the pore space of the rock.

The stress field in the DeSoto Canyon Salt Basin has been analyzed by Meng et al. (2018). The vector mean azimuth of the maximum horizontal stress (SH_{max}) is dominantly oriented northwest-southeast with an average azimuth of 114°. Both lithostatic stress (S_v) and hydrostatic pressure (P_p) have a power-law relationship with depth (equations 4.1 and 4.2, where D is depth of the reservoir). The geometric mean of the minimum horizontal stress (Sh_{min})-depth data corresponds to a constant ratio of effective minimum horizontal stress and effective lithostatic stress of ~0.5 (equation 4.3).

$$S_v = 0.005812D^{1.1583} \quad (4.1)$$

$$P_p = 0.005762D^{1.0844} \quad (4.2)$$

$$Sh_{min} = 0.5(S_v - P_p) + P_p \quad (4.3)$$

Stress unit and pressure: MPa; Depth unit: meter.

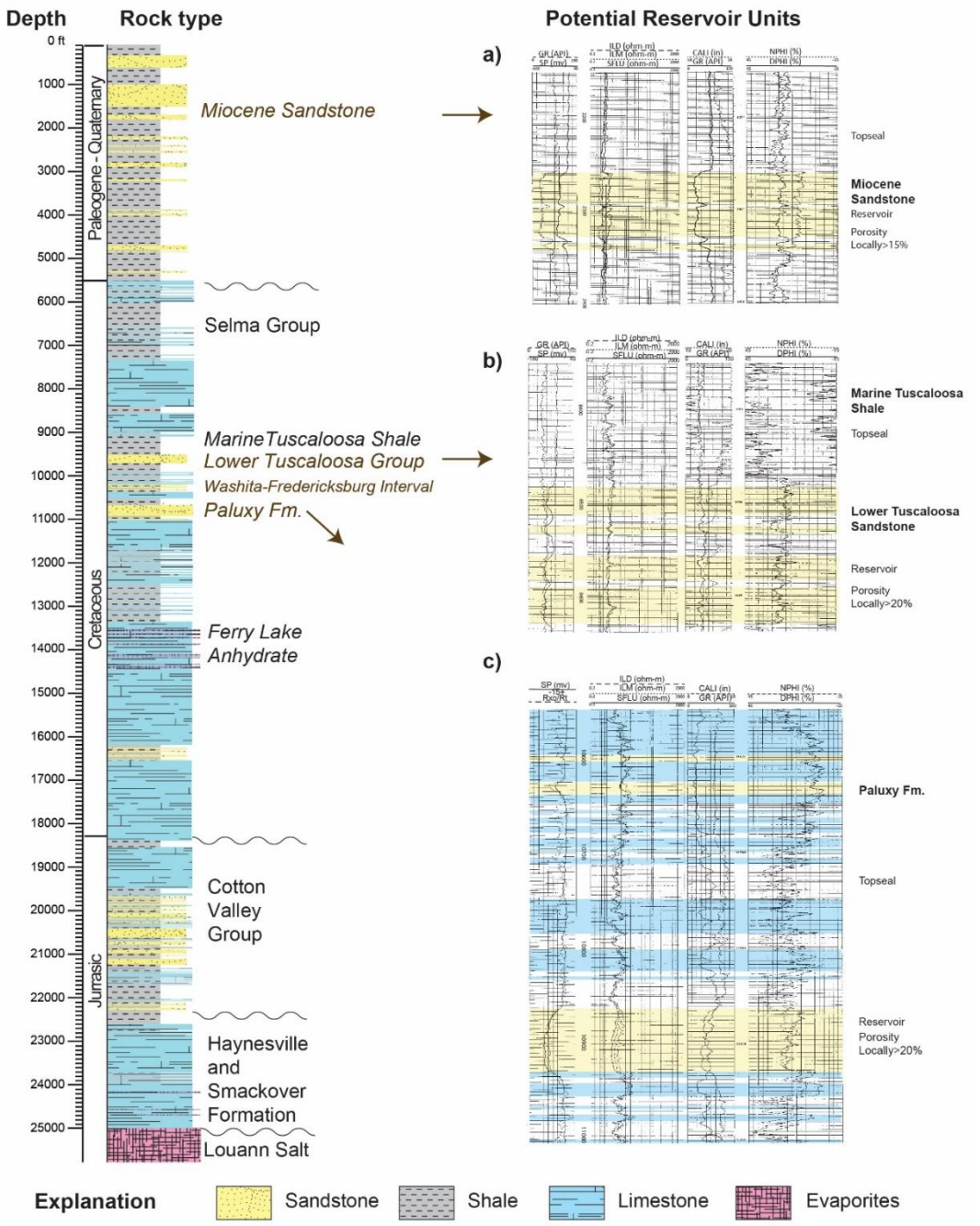

Figure 4.3. Stratigraphic column of the DeSoto Canyon Salt Basin and sample well logs showing potential reservoir formations and associated topseals, including a) Paleocene-Miocene sandstone, b) lower Tuscaloosa sandstone, and c) Paluxy sandstone.

4.4 Methodology

This study analyzes stress and pressure information in target reservoirs, as well as rock strength in candidate injection zones and in reservoir seals. Rock strength of the Paluxy, Lower Tuscaloosa, and the Paleocene-Miocene storage targets were estimated and used to evaluate the reservoir and seal integrity.

4.41 Rock strength in selected reservoirs

Rock strength is a geomechanical parameter that describes the resistance of a rock to different types of stress. The most accurate method to test rock strength is to conduct tri-axial strain tests under confining stress. Different values of σ_1, σ_2 and σ_3 can be applied on a rock sample until failure, and the result can be plotted on the Mohr Circle to define the Mohr-Coulomb failure envelope (Figure 4.4). A simplified experiment applies a uniaxial stress on the rock (σ_3=0). In this case the measured strength is the unconfined compressive strength (UCS). The failure envelope can be determined by three parameters, including 1) UCS, 2) friction angle (φ; the angle between the failure envelope and X axis), and 3) cohesion (c; the intercept of failure envelope and Y axis).

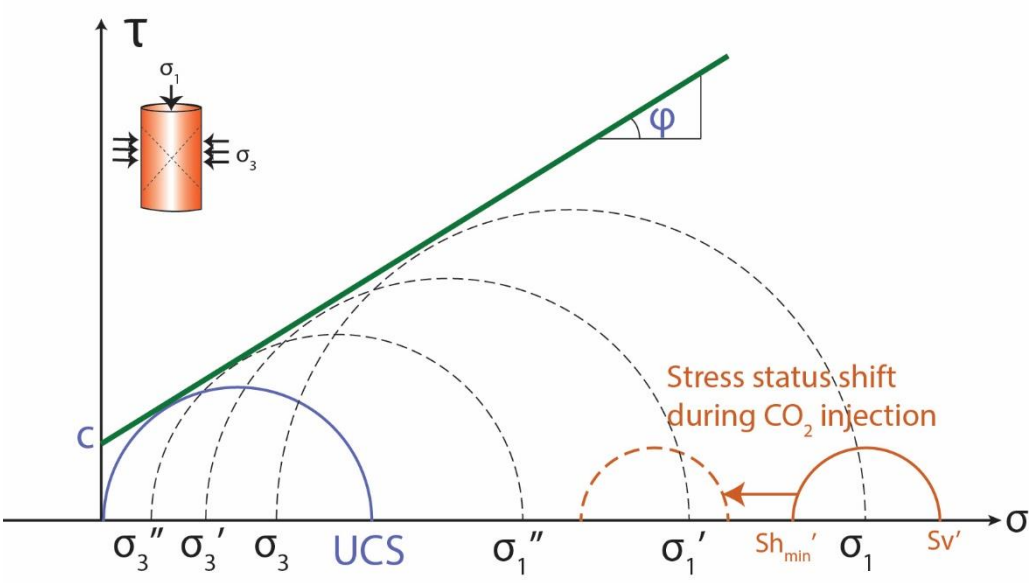

Figure 4.4. Mohr-Coulomb failure envelope describing the rock strength measurement in lab setting, and the effective stress status evolution during CO_2 injection.

No cores are available for geomechanical laboratory tests in the DeSoto Canyon Salt Basin. As a result, the rock strength of the reservoir and seal rock were calculated from geophysical well logs. The use of well log data to determine the geomechanical parameters and to define failure envelope is well established (Chang et al., 2006; Hareland and Nygaard, 2007; Onyia, 1988). Chang et al. (2006) summarized several correlations to predict UCS and frictional angle using well log information, including several correlations derived from sandstone and shale in the Gulf of Mexico area. Hadi and Nygaard (2018) presented a set of correlations to predict UCS and frictional angle for three carbonate rock types (limestone, dolomite and chalk). These correlations are based on a large number of petrophysical-geomechanical tests in a range of geological locations and settings.

In this study, rock types were interpreted using basic well log interpretation procedures (Asquith et al., 2004). UCS correlations from Chang et al. (2006) were used for reservoir sandstone and shale caprock units in the Gulf of Mexico (equations 4.4, 4.5). For the limestone of the Washita-Fredericksburg interval and chalk of the Selma Group, UCS correlations from Hadi and Nygaard (2018) were used to estimate the strength of the caprock (equation 4.6-4.7).

$$UCS_{sandstone}=3.87\exp(1.14\times10^{-10}\rho Vp^2) \quad (4.4)$$

$$UCS_{shale}= 0.5\ (304.8\ /\Delta tc)^3 \quad (4.5)$$

$$UCS_{limestone}= 55\text{-}94\phi+102.4\exp(-4.46\phi) \quad (4.6)$$

$$UCS_{chalk}= 46\text{-}134.6\phi+117.3\exp(-5.62\phi) \quad (4.7),$$

where Vp (m/s) is the compressional velocity (Δt) from a sonic log; ρ (kg/m^3) is the bulk density acquired from density logs, and ϕ (%) is the porosity of the rock.

Cohesion(c) of the Mohr-Coulomb failure envelope will be calculated using equation 4.8. Friction angle will be estimated based on sonic and density log data (Chang et al., 2006; Edimann et al., 1998; Lal, 1999; Weingarten and Perkins, 1995). Empirical relationships between friction angle and other logged measurements are given in equation 4.9 (sandstone), 4.10 (shale) and 4.11 (carbonate):

$$UCS=2c*\tan(45°+\varphi/2) \quad (4.8)$$

$$\varphi_{sandstone}=57.8-105\phi \quad (4.9)$$

$$\varphi_{shale}= \sin^{-1}[(Vp-1000)/(Vp+1000)] \quad (4.10)$$

$$\varphi_{carbonate}= -0.78\phi+41.929 \quad (4.11)$$

4.42 Reservoir and seal integrity evaluation

Using the methods given above, the three parameters, UCS, friction angle (φ), and cohesion (c) were obtained for candidate reservoir units. The Mohr-Coulomb failure envelopes of the reservoir and seal rocks were determined and plotted in the X-Y plane. The current effective in-situ stress at reservoir depth also was plotted on the Mohr circle (Figure 4.4). When injecting CO_2, pore pressure (Pp) will increase in the reservoir formation, thus leading to a decrease of effective maximum stress (Sv) and minimum stress (Sh_{min}). The stress Mohr circle will therefore shift leftward (e.g. Figure 4.4). During the alteration of the reservoir stress status, any stress status below the failure envelope can be considered stable. Shear failures will be generated when the stress circle cross-cut the failure envelopes. Tensile failure will occur when the stress circle pass the zero normal effective stress status (Y axis). Prospective reservoirs were then ranked according to stability to facilitate future development.

4.5 Results

4.51 Paluxy Formation

Effective stress from Meng et al (2018) and the average value of the rock mechanical properties for each reservoir and caprock are shown in Table 4.1, and used as input to plot the Mohr-failure envelope plane for reservoir and seal analyses. Figure 4.5 is a lithology-UCS correlation of the Paluxy sandstone and associated topseals (Washita-Fredericksburg shale and limestone). This graphic, associated with the

histogram analysis of the UCS for each rock type (Figure 4.6), shows that the limestone caprock of the Washita-Fredericksburg interval has the highest UCS, ranging from 115 to 150 MPa and averaging 131 MPa. The UCS of Paluxy sandstone ranges from 33 to 45 MPa with an average of 35 MPa. The shale caprock of the Washita-Fredericksburg interval has the lowest UCS, ranging from 10 to 45 MPa and averaging 22 MPa. Plotting the results on the Mohr circle indicates that the Paluxy reservoir does not intersect any of failure envelope (Figure 4.7). The limestone in the Washita-Fredericksburg interval has a much higher failure strength than sandstone and shale.

Table 4.1. Summary of stress field and geomechanical parameters for each candidate reservoir units in the DeSoto Canyon Salt Basin calculated from well log data.

Potential Reservoir	**Effective Stress (MPa)**		**Reservoir Unit**	**UCS (MPa)**		**Frictional Angle (°)**		**Cohesion (MPa)**
				Average	Standard Deviation	Average	Standard Deviation	Average
Paleogene-Neogene	σ_1'	9	Sandstone Reservoir	16.3	1.3	13.5	4.5	6.6
	σ_3'	4.5	Shale Caprock	6.7	1.2	22.6	2.1	2.2
Lower Tuscaloosa Group	σ_1'	20.9	Sandstone Reservoir	26.7	4.2	34.1	5.1	7.0
	σ_3'	10.4	Shale Caprock	10.8	2.6	28.0	2.4	3.2
			Chalk Caprock	52.1	23.2	41.8	0.1	11.6
Paluxy Formation	σ_1'	31.8	Sandstone Reservoir	35.4	1.8	43.7	2.4	7.5
	σ_3'	15.9	Shale Caprock	21.9	5.6	35.5	2.5	5.6
			Limestone Caprock	130.9	7.0	41.9	0.0	29.2

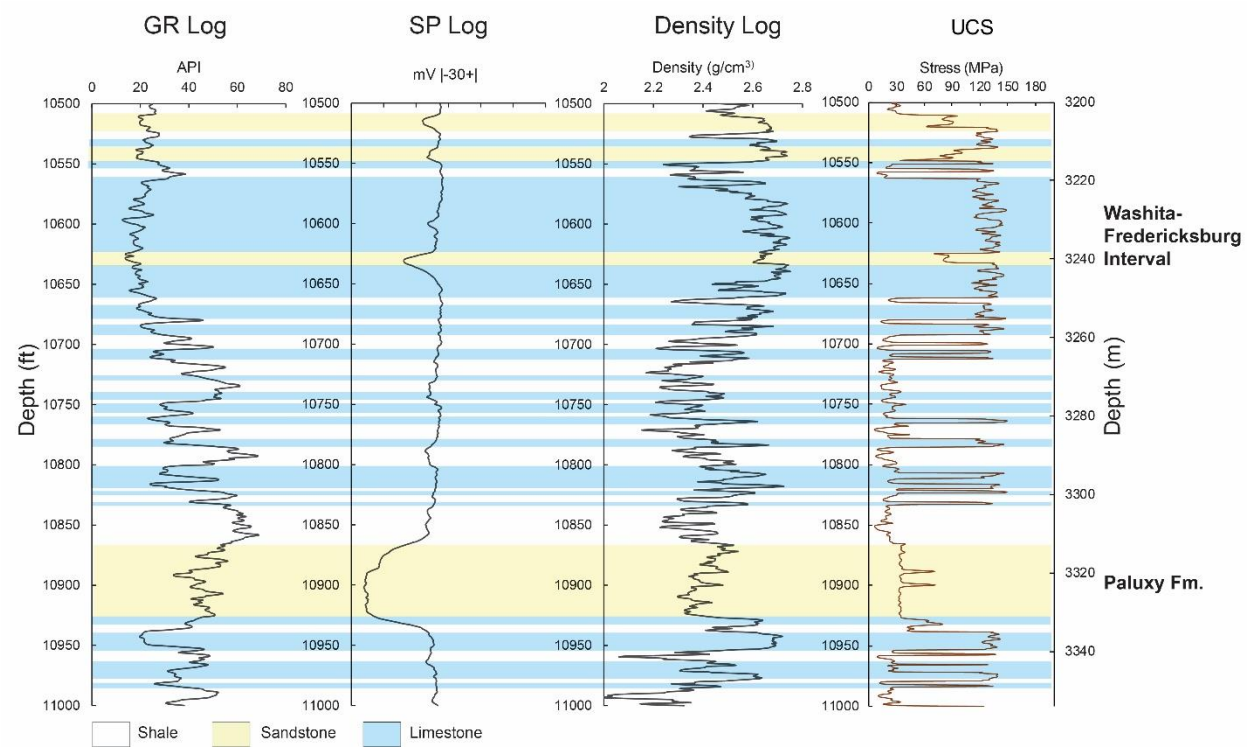

Figure 4.5. Well log-UCS correlation of Paluxy sandstone and associated topseals.

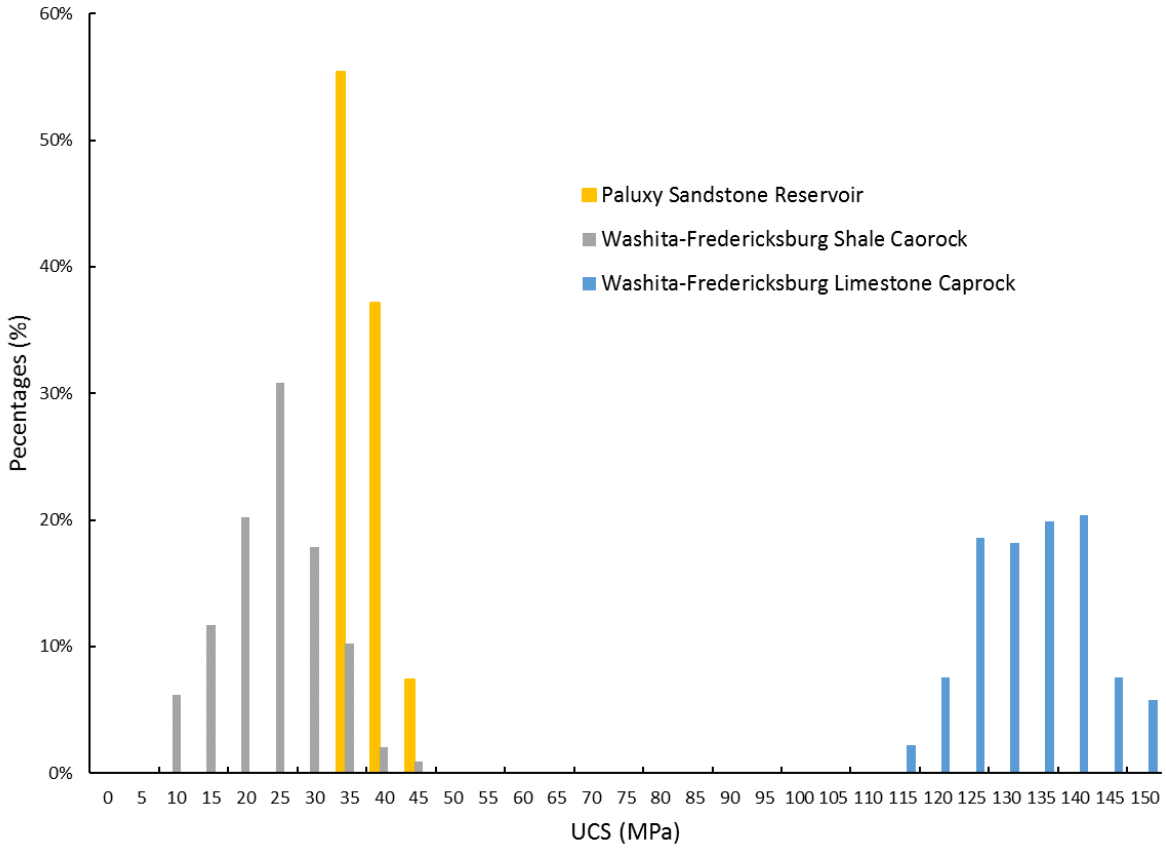

Figure 4.6. Histograms of UCS for Paluxy sandstone, Washita-Fredericksburg shale, and Washita-Fredericksburg limestone (n=685).

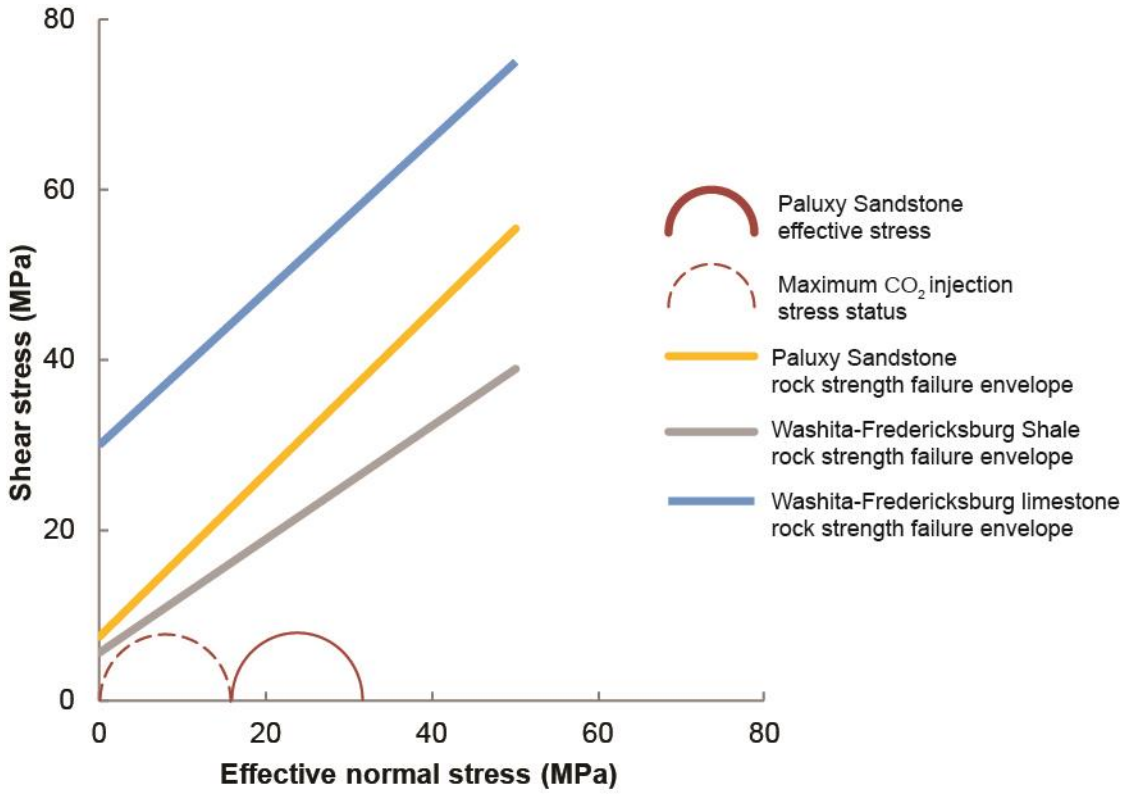

Figure 4.7. Mohr circle for effective stress at the depth of Paluxy Formation sandstone and the corresponding failure lines for the reservoir and caprock. Solid half circle representing the original status of reservoir stress, dashed half circle representing the final status when tensile fractures occur.

4.52 Lower Tuscaloosa Group reservoir unit

Figures 4.8 and 4.9 are the lithology-UCS correlation and a histogram of the UCS of the Lower Tuscaloosa sandstone potential reservoir and associated topseals (Marine Tuscaloosa shale and Selma Group chalk). The chalk caprock of the Selma Group has highly variable of UCS ranging from 10 to 100 MPa and averaging 52 MPa. The UCS of Lower Tuscaloosa sandstone ranges from 15 to 45 MPa and averages 27 MPa. The shale caprock of the Marine Tuscaloosa has the lowest UCS values, which range from 8 to 34

MPa and average 11 MPa. Like in the Paluxy, the Lower Tuscaloosa effective stress also plots below the failure lines of the sealing strata (Figure 4.10). Selma chalk has a higher failure strength than the reservoir sandstone and Marine shale caprock.

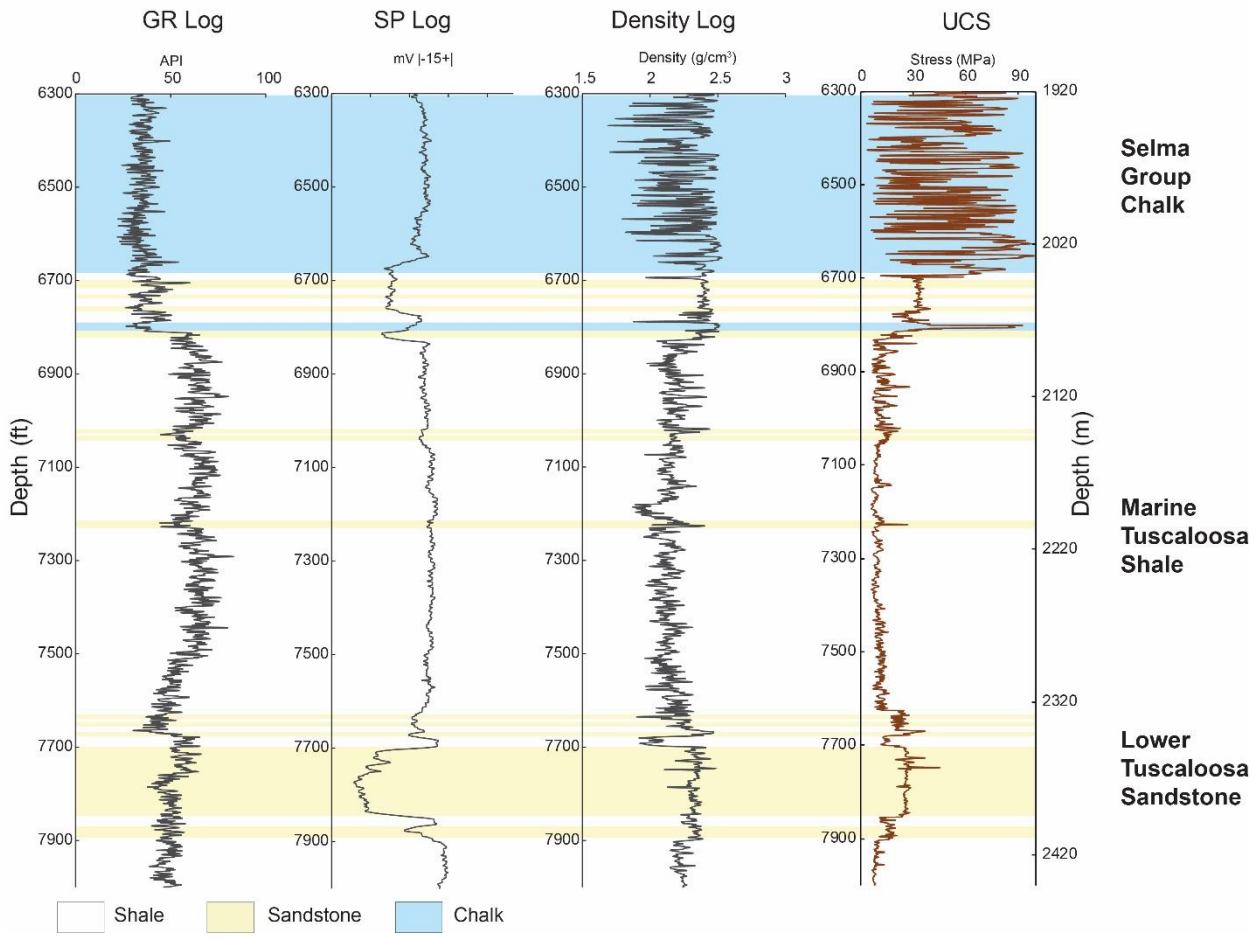

Figure 4.8. lithology-UCS correlation of lower Tuscaloosa sandstone and associated topseals.

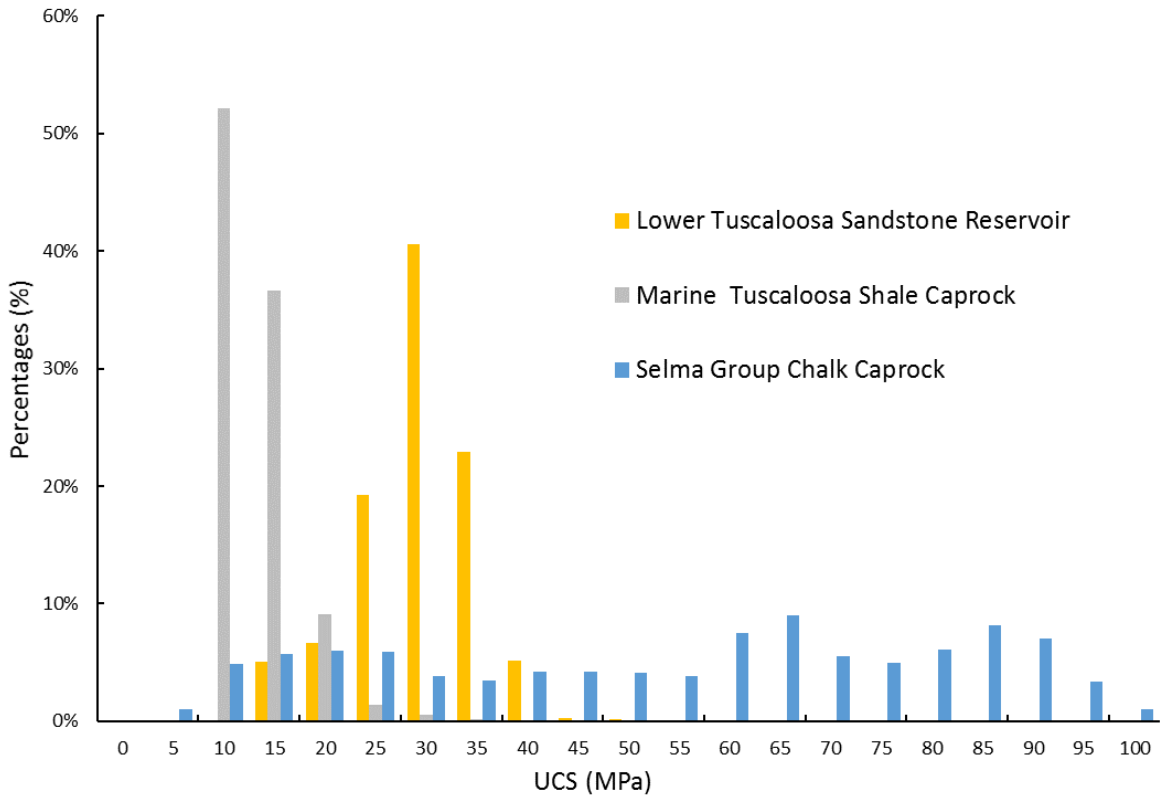

Figure 4.9. Histograms of UCS for Lower Tuscaloosa sandstone, Marine Tuscaloosa shale, and Selma Group chalk (N=3400).

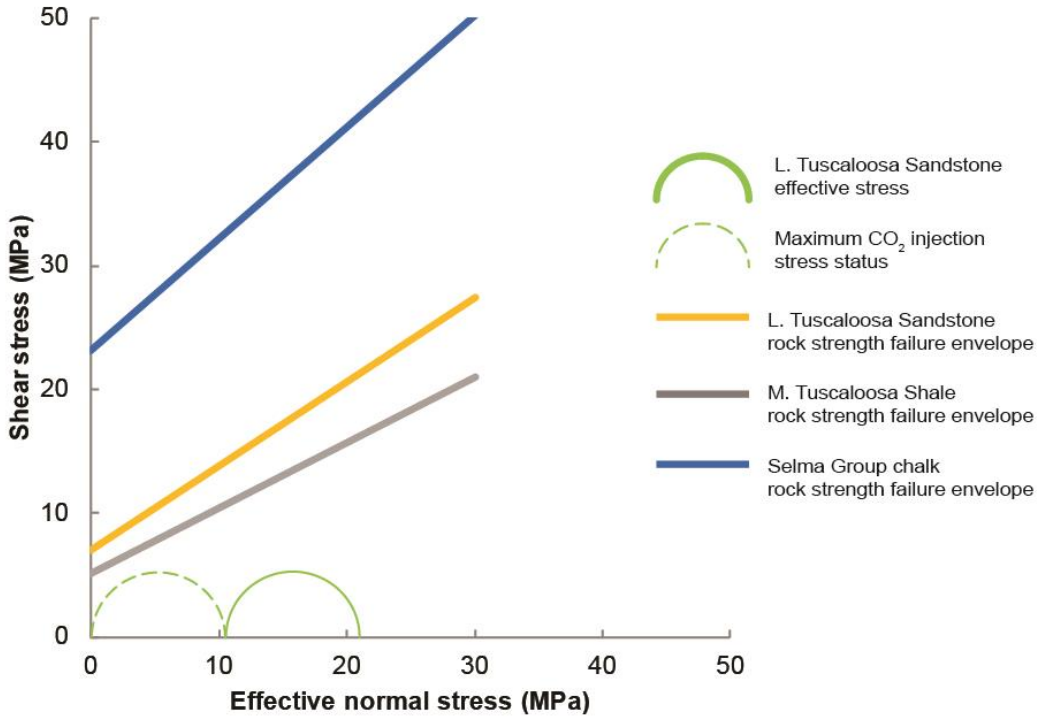

Figure 4.10. Mohr circle for effective stress at the depth of Lower Tuscaloosa sandstone and the corresponding failure envelope for the reservoir and caprock. Solid half circle representing the original status of reservoir stress, dashed half circle representing the final status when tensile fractures occur.

4.53 Paleocene-Miocene reservoir unit

Paleocene-Miocene sandstone and the associated caprock has lower UCS than the other units that were analyzed (Figure 4.11, 4.12). The UCS of Paleocene-Miocene sandstone ranges from 14 to 22 MPa and averages 16 MPa. The caprock of the Marine shale contains the lowest UCS values, ranging from 5 to 12 MPa and averaging 7 MPa.

However, the Paleocene-Miocene shale caprock has a lower failure strength than the reservoir sandstone.

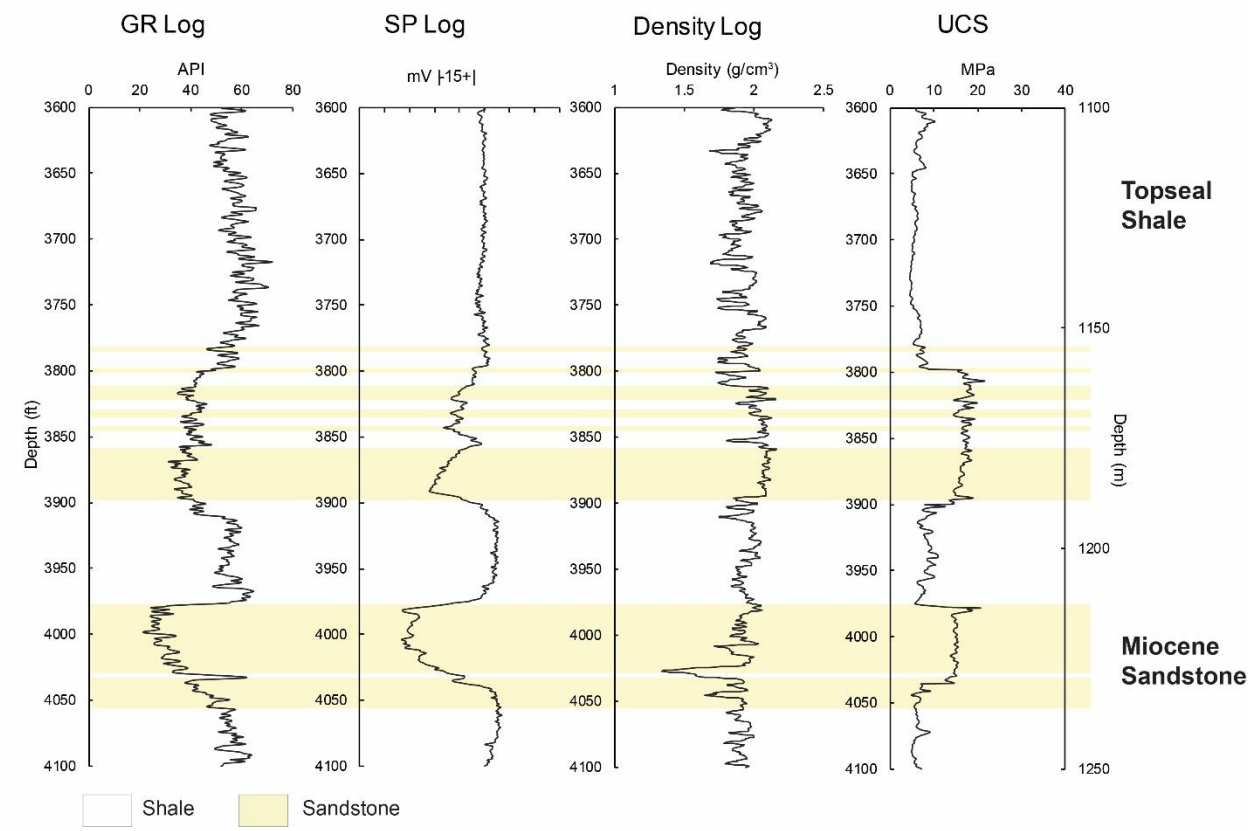

Figure 4.11. lithology-UCS correlation of Paleocene-Miocene sandstone and associated shale topseals.

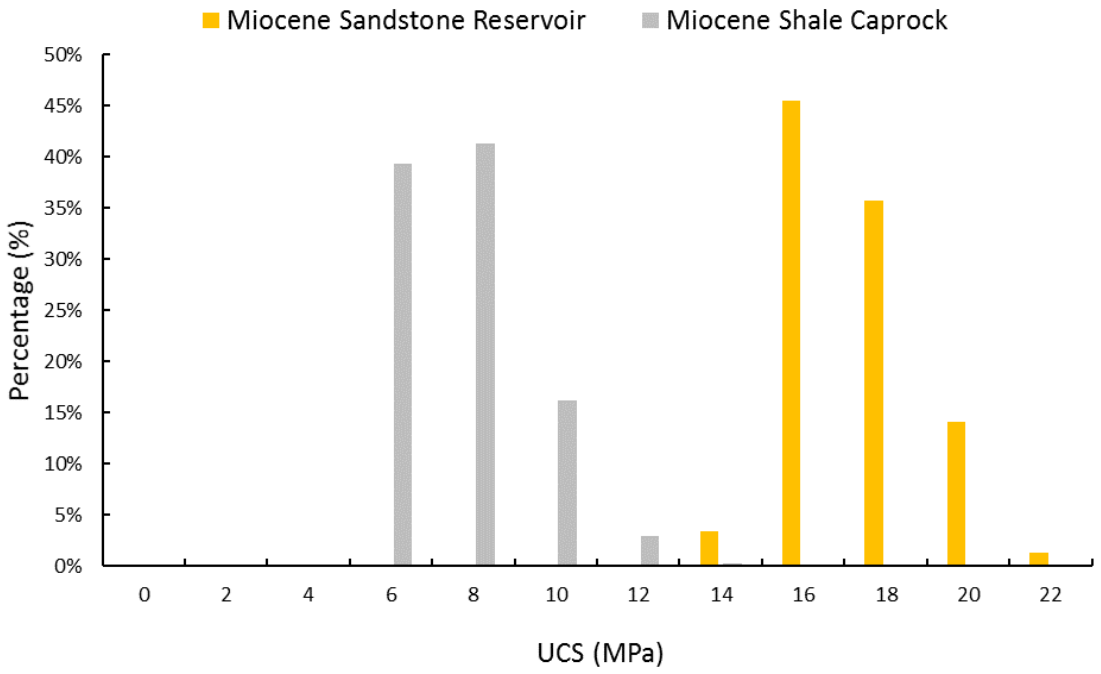

Figure 4.12. Histograms of UCS for Paleocene-Miocene sandstone and shale (n=1000).

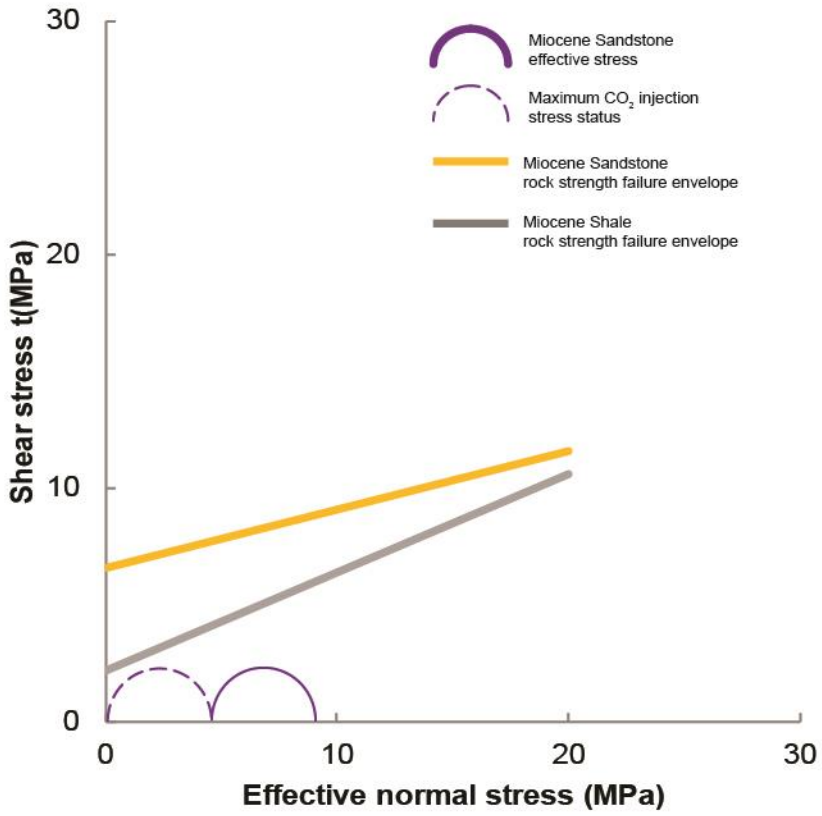

Figure 4.13. Mohr circle showing effective stress in Paleocene-Miocene sandstone and the corresponding failure lines for the reservoir and caprock. Solid half circle representing the original status of reservoir stress, dashed half circle representing the final status when tensile fractures occur.

4.6 Discussion

Results of the reservoir and seal integrity analyses show that the Mohr circles for all three target reservoir intervals Mohr circles sit below the reservoir and caprock failure envelopes (Figure 4.7, 4.10, 4.13). Hence, all the potential reservoirs are under stable stress conditions. During injection, the effective stresses will reduce and the Mohr circle for each candidate reservoir will move to the left. Since reservoir sandstone

maintains a higher failure strength than the in-situ stress, it is unlikely that shear fracturing will occur during injection since even at zero effective horizontal stress the Mohr circle will not intersect any of the shear failure lines. The most likely fracturing scenario is formation of tensile hydraulic fractures as the Mohr circle passes through the compressional XY plane. Even this situation is unlikely to occur, as long as the injection pressure is kept below the minimum effective horizontal stress (Meng et al., 2018) and made sure the stress circle stays on the first quartile of the compressional XY plane. The limestone caprock of the Washita-Fredericksburg Interval and chalk caprock from the Selma Group have much higher failure strength than the reservoir and shale caprocks, and so will help in arresting any tensile fractures or shear fractures that may form in weak parts in the reservoir.

When injecting CO_2 into deep saline aquifers, the maximum bottom hole injection pressure is commonly set at 90% of the fracture pressure (Hawkers et al., 2005). Therefore the headroom for each reservoir for injecting CO_2 should be set up as at 90% of the fracture pressure minimum effective horizontal stress at each reservoir depth. Chandra (2018) reported that the Paluxy sandstone has ~17 Gt storage resource mainly in the east-central part of the DeSoto Canyon Salt Basin, and the allowable injection headroom is the highest of the three candidate reservoirs (~14.3 MPa in the reference well). However the storage resource is concentrated in the withdrawal synclines around the Destin Dome structural province with high dilation tendency (Pashin et al, 2016, Chandra, 2018; Meng et al, in preparation). Therefore, injection site for Paluxy reservoirs should be avoid the fault system. Further pressure and flow

simulation is needed to determine safe injection pressure and distance from the faults. About 10 Gt storage resource of the lower Tuscaloosa Group is concentrated mainly in the western part of the DeSoto Canyon Salt Basin. Along with the existence of thick, resistant seal rocks with a proper headroom for injection (~9.4 MPa in the reference well), lower Tuscaloosa sandstone is a better option than the Paluxy sandstone for long-term commercial carbon storage in the western DeSoto Canyon Salt Basin. Paleocene-Miocene sandstone has ~120 Gt potential for storage (Pashin et al, 2018), due to the shallow depth of the reservoir, cost of drilling may favor the Paleocene-Miocene section. Although the reservoir and seal intervals have low UCS value due to weak consolidation of these strata, which may limit allowable injection pressure (~4.1 MPa in the reference well) into the Paleocene-Miocene objectives.

Geomechanical analysis demonstrates that the carbonate caprocks have the highest rock strength, followed by sandstone and shale. The UCS of Selma chalk varies greatly, and the histogram indicates a bimodal distribution (Figure 4.9c). A possible reason for this is the interbedded layering character of the chalk and limestone. A porous chalk interval normally contains low UCS, whereas a low-porosity limestone interval will form a tight zone with high UCS. UCS correlations used in this research were simulated from lab test on samples of sandstone and shale units in the Gulf of Mexico (Change et al., 2016) and carbonate rocks worldwide (Hadi and Nygaard, 2018). No experimental data exists regarding to the geomechanical properties of the cores from the three candidate reservoir unites in the study area. Therefore, laboratory tri-axial tests are recommended in the future to confirm the accuracy of the UCS correlations for

the DeSoto Canyon Salt Basin. It is also very important to understand the wellbore-related risks, geomechanical simulation, as well as conduct monitoring programs during and after CO_2 injection in future development.

4.7 Conclusion

Recent studies indicate that Gt-scale storage capacity exists in Cretaceous and Paleocene-Miocene sandstones in the DeSoto Canyon Salt Basin, eastern Gulf of Mexico. Each offshore block of the study area can potentially store CO_2 emissions from 13 major coal-fired power plants annually. Understanding the geomechanical properties of the potential storage units is essential in guiding the selection of sequestration sites and reduce the risk of leakage caused by injection. The purpose of this study is to evaluate the geomechanical integrity of reservoirs and seals, therefore facilitate effective long-term storage of CO_2.

Rock mechanical properties and stress information were calculated from geophysical well logs of three potential reservoir units, including the Paluxy Formation, the lower Tuscaloosa Group, and Paleocene-Miocene sand and sandstone. Geomechanical analysis indicate that Washita-Fredericksburg limestone and the Chalk caprock of the Selma Group have a higher failure strength than the reservoir sandstone and the shale caprock, preventing fracture propagation during injection.

Results of the reservoir and seal integrity analyses show that all three reservoir objectives and the associated seals are under stable stress conditions. Shear fracturing is unlikely to occur during the injection due to the high rock strength of the reservoir and seal. Tensile hydraulic fracturing can be prevented by limiting the injection pressure below the minimum effective horizontal stress. Combined with structural framework and reservoir property studies, Paluxy sandstone has the most allowable injection headroom and considerable storage capacity, but significant caution is needed when considering injecting near the Destin Fault System. Paleocene-Miocene sandstone has the greatest potential for commercial storage, but with limited allowable injection pressure. Lower Tuscaloosa sandstone reservoir is a sound option for long-term carbon storage due to its large storage potential, considerable allowable injection pressure, and stable structural styles around the reservoir.

Future work should focus on wellbore-related risks, geomechanical simulation, as well as monitoring programs during and after CO_2 injection to further ensure safe carbon storage. Laboratory tri-axial tests are recommended in the future to confirm the accuracy of the UCS correlations for the DeSoto Canyon Salt Basin.

Reference

Asquith, G. B., Krygowski, D., and Gibson, C. R., 2004, Basic well log analysis, American association of petroleum geologists Tulsa, 216 p.

Chandra, A., 2018, Geological Characterization and CO_2 Storage Potential of Cretaceous Sandstone in the DeSoto Canyon Salt Basin of the MAFLA Shelf [Master: Oklahoma State University, 76 p.

Chang, C., Zoback, M. D., and Khaksar, A., 2006, Empirical relations between rock strength and physical properties in sedimentary rocks: Journal of Petroleum Science and Engineering, v. 51, no. 3, 223-237.

Charbonneau, P., 2018, Geologic framework for the assessment of offshore CO_2 storage resources: West Florida Platform: Stillwater, Oklahoma State University, unpublished Master's thesis, 69 p.

Edimann, K., Somerville, J., Smart, B., Hamilton, S., and Crawford, B., Predicting rock mechanical properties from wireline porosities, *in* Proceedings SPE/ISRM Rock Mechanics in Petroleum Engineering1998, Society of Petroleum Engineers.

Esposito, R. A., Pashin, J. C., Hills, D. J., and Walsh, P. M., 2010, Geologic assessment and injection design for a pilot CO_2-enhanced oil recovery and sequestration demonstration in a heterogeneous oil reservoir: Citronelle Field, Alabama, USA: Environmental Earth Sciences, v. 60, no. 2, 431-444.

Folaranmi, A. T., 2015, Geologic characterization of a saline reservoir for carbon sequestration: The Paluxy Formation, Citronelle Dome, Gulf of Mexico Basin, Alabama: Oklahoma State University, 110p.

Hareland, G., and Nygaard, R., 2007, Calculating unconfined rock strength from drilling data, *in* Proceedings 1st Canada-US Rock Mechanics Symposium, American Rock Mechanics Association, 1-7.

Haug, K., Nygaard, R., and Keith, D., 2007, Evaluation of stress and geomechanical characteristics of a potential site for CO_2 geological storage in central Alberta, Canada, in Proceedings 60th Canadian Geotechnical Conference and 8th Joint CGS/IAH-CNC Groundwater Conference, 21-24.

Hawkes, C., McLellan, P., Zimmer, U., and Bachu, S., 2004, Geomechanical Factors Affecting Geological Storage of CO in Depleted Oil and Gas Reservoirs, *in* Proceedings Canadian International Petroleum Conference, Petroleum Society of Canada, 52-61.

Hawkes, C. D., Bachu, S., Haug, K., and Thompson, A., 2005, Analysis of in-situ stress regime in the Alberta Basin, Canada, for performance assessment of CO_2 geological sequestration sites, *in* Proceedings Fourth Annual Conference on Carbon Capture and Sequestration, p. 2-5.

Koperna, G., Riestenberg, D., Kuuskraa, V., Rhudy, R., Trautz, R., Hill, G. R., and Esposito, R., 2012, The SECARB Anthropogenic Test: A US Integrated CO_2 Capture, Transportation and Storage Test: International Journal of Clean Coal and Energy, v. 1, no. 2, 13-26.

Koperna, G. J., Riestenberg, D. E., Petrusak, R. L., Esposito, R. A., and Rhudy, R., Lessons, 2009, Learned While Conducting Drilling and CO_2 Injection Operations at the

Victor J. Daniel Power Plant, *in* Proceedings SPE Annual Technical Conference and Exhibition, Society of Petroleum Engineers, 1-26.

Lal, M., Shale stability: drilling fluid interaction and shale strength, 1999, *in* Proceedings SPE Asia Pacific Oil and Gas Conference and Exhibition, Society of Petroleum Engineers, 1-10.

Meng, J., Pashin, J. C., and Clark, P. E., 2017, Structural architecture of the Farnsworth oil unit: Implications for geologic storage of carbon dioxide: Environmental Geosciences, v. 24, no. 2, 73-94.

Onyia, E., 1988, Relationships between formation strength, drilling strength, and electric log properties, *in* Proceedings SPE Annual Technical Conference and Exhibition, Society of Petroleum Engineers, 605-618.

Pashin, J., McIntyre, M., Grace, R., and Hills, D., 2008, Southeastern Regional Carbon Sequestration Partnership (SECARB) Phase III, Final Report: Report to Advanced Resources International by Geological Survey of Alabama, Tuscaloosa, 1-75.

Pashin, J. C., Jin, G., and Hills, D. J., Mesozoic Structure and Petroleum Systems in the DeSoto Canyon Salt Basin in the Mobile, Pensacola, Destin Dome, and Viosca Knoll Areas of the MAFLA Shelf, *in* Proceedings 35th Annual Gulf Coast Section SEPM (GCSSEPM) Foundation Bob F Perkins Research Conference, Houston, Texas, 2016, 315-340.

Pashin, J. C., Meng, J., Hills, D. J., and Riestenberg, D., 2018, Eastern Gulf of Mexico, in Southern States Energy Board, eds., Southeast Offshore Storage Resource

Assessment, Prospective Storage Resource Assessment Results, U.S. Department of Energy Contract DE-FE0026086, 4-66.

Pashin, J. C., Raymond, D. E., Alabi, G. G., Groshong, R. H., Jr., and Guohai Jin, 2000, Revitalizing Gilbertown oil field: Characterization of fractured chalk and glauconitic sandstone reservoirs in an extensional fault system: Alabama Geological Survey Bulletin 168, 81 p.

Petrusak, R. L., Riestenberg, D. E., Goad, P. L., Schepers, K. C., Pashin, J., Esposito, R. A., and Trautz, R. C., 2009, World class CO_2 sequestration potential in saline formations, oil and gas fields, coal, and shale: the US southeast regional carbon sequestration partnership has it all, *in* Proceedings SPE International Conference on CO_2 Capture, Storage, and Utilization, Society of Petroleum Engineers. 1-18.

Southern States Energy Board, 2013, Preliminary Evaluation of Offshore Transport and Geologic Storage of Carbon Dioxide, 1-110.

Weingarten, J., and Perkins, T., 1995, Prediction of sand production in gas wells: methods and Gulf of Mexico case studies: Journal of Petroleum Technology, v. 47, no. 07, 596-600.

VITA

JINGYAO MENG

Candidate for the Degree of

Doctor of Philosophy

Dissertation: GEOLOGICAL AND GEOMECHANICAL CHARACTERISTICS OF THE DESOTO CANYON SALT BASIN, EAST-CENTRAL GULF OF MEXICO

Major Field: GEOLOGY

Biographical:

Education:

Completed the requirements for the Doctor of Philosophy in Geology at Oklahoma State University, Stillwater, Oklahoma in May, 2019.

Completed the requirements for the Master of Science in Geology at Oklahoma State University, Stillwater, Oklahoma in August, 2015.

Completed the requirements for the Bachelor of Engineering in Resource Exploration Engineering (Oil & Gas) at Jilin University, Changchun, China in 2012.

Professional Memberships:

American Association of Petroleum Geologists (AAPG), Geological Society of America (GSA), Society of Exploration Geophysicists (SEG), Society of Petroleum Engineers (SPE), American Institute of Professional Geologists (AIPG), Association for Women Geoscientists (AWG), Tulsa Geological Society (TGS), Houston Geological Society (HGS),